

Analysis and Resolution of RF Interference to Radars Operating in the Band 2700–2900 MHz from Broadband Communication Transmitters

**Frank H. Sanders
Robert L. Sole
John E. Carroll
Glenn S. Secrest
T. Lynn Allmon**



report series

Analysis and Resolution of RF Interference to Radars Operating in the Band 2700–2900 MHz from Broadband Communication Transmitters

**Frank H. Sanders
Robert L. Sole
John E. Carroll
Glenn S. Secrest
T. Lynn Allmon**



U.S. DEPARTMENT OF COMMERCE

October 2012

DISCLAIMER

This report identifies certain commercial equipment and materials to adequately specify technical aspects of the reported results. In no case does such identification imply recommendation or endorsement by the National Telecommunications and Information Administration (NTIA), nor does it imply that the material or equipment identified is the best available for this purpose.

CONTENTS

	Page
List of Figures	viii
List of Tables	xv
Abbreviations/Acronyms	xvi
Executive Summary	xviii
1 ELECTROMAGNETIC COMPATIBILITY Concerns Between 2700–2900 MHz	
Radar Systems and Terrestrial Communication Systems	2
1.1 Background	2
1.2 Preliminary Examination of Electromagnetic Compatibility (EMC) Issues Between WiMAX Transmitters and NEXRAD Receivers	2
1.3 Initial Joint Agency Work at Grand Rapids, Michigan, and Jacksonville, Florida	5
1.4 Objectives of Initial Field Work	5
2 NEXRAD Technical Characteristics	7
2.1 NEXRAD Radars Operating in the Band 2700–3000 MHz	7
2.2 NEXRAD Receiver Design	9
2.3 Frequency-Response Measurements of NEXRAD Receiver Stages	9
2.4 NEXRAD RF Gain Compression Measurement	13
2.5 Summary of NEXRAD Receiver EMC Characteristics	13
3 2.6-2.7 GHz WiMAX Technical Characteristics	14
3.1 Technical Characteristics of BRS/EBS WiMAX Base Stations	14
3.2 BRS/EBS Spectrum Channel Plan in the United States	16
3.3 WiMAX Base Station Antenna Characteristics and Frequency Response	18
3.4 Measured Technical Characteristics of Radiated WiMAX Signals	20
3.5 Radiated BRS WiMAX Power as a Function of Measurement Detection Mode and Bandwidth	24
3.6 Unfiltered Hardline Coupled Measurements of BRS WiMAX Emission Spectra	26
3.6.1 NTIA Hardline-Coupled BRS WiMAX Measurement System Set-Up	27
3.6.2 BRS WiMAX Base Station Emission Spectra Without Output Filtering	28
3.7 Summary of BRS/EBS Base Station Emission Characteristics	30
4 Interference Measurements at NEXRAD Field Locations	32
4.1 NEXRAD Configuration for Measurement and Characterization of Interference Signals	32
4.2 Interference Azimuth-Scan Results	33
4.3 Elevation-Scan Results for the Interference Signals	35
4.4 Measurements of the Interference Time Domain Envelopes	38
4.5 Spectrum Measurements of the Interference through the NEXRAD Antennas	39
4.6 Identification of the Interference Mechanism	43
4.6.1 Front-End Overload Condition	43
4.6.2 Appearance of Front-End Overload Responses in the Time Domain	43

4.6.3 Appearance of OOB Emissions in the Time Domain (Rabbit Ears)	43
4.6.4 Additional Proposed Tests for Front-End Overload.....	44
4.7 WiMAX Turn-Off Test in Jacksonville.....	46
4.8 Vector Signal Analyzer Recordings of the Interference Signal.....	47
5 Identification Of BRS/EBS Towers where Interference Originates	48
5.1 Identification of the Interference Source Locations	48
5.2 Verification of Grand Rapids BRS/EBS Emissions on Identified Towers.....	48
6 Development of aN Output Filter	52
6.1 Interference-to-Noise (<i>I/N</i>) Signal Strength on Each Azimuth	52
6.2 Approach for Developing EMC Curves	52
6.2.1 Development of a Filtering Option for BRS/EBS WiMAX Base Station Transmitters	53
6.3 Testing of WiMAX Output Filtering at Two NEXRAD Field Locations	58
6.4 Calculation of Minimum Separation Distances With and Without Filters.....	58
6.5 Summary of WiMAX Filter Development and Effectiveness.....	59
7 Interference Mitigation Options.....	60
7.1 Down-Tilting of WiMAX Base Station Transmitter Antennas	60
7.2 Off-tuning BRS/EBS Base Station Transmitters from Upper BRS/EBS Band Edge.....	61
7.3 Installation of Filters on BRS/EBS Base Station Transmitters.....	61
7.4 Establishing Larger Physical Separation Distances Between WiMAX Transmitters and Radar Receivers When Frequency Separations are Small.....	62
7.5 Reduction in the Heights of WiMAX Base Station Transmitter Antennas	62
7.6 Retuning NEXRAD Frequencies Enough to Mitigate Interference	62
8 Summary and Conclusions	64
8.1 Summary.....	64
8.2 Conclusions.....	64
9 Acknowledgements.....	66
10 References.....	67
Appendix A : Procedures for Measuring Interference at NEXRAD Stations	69
A.1 Introduction.....	69
A.2 Recommended Measurement Hardware	69
A.3 Procedures for Observing Interference Energy in the NEXRAD IF Stage	69
A.4 Procedures for Observing Interference Energy in the NEXRAD RF Stage	72
Appendix B : Interference Time Waveforms on Twelve Azimuths of the Jacksonville NEXRAD Receiver.....	74
Appendix C : ASR Technical Characteristics.....	80
C.1 ATC Radars Operating in the Band 2700-2900 MHz.....	80
C.2 Objectives.....	83
C.3 Measurement Procedures	83

C.4 LNA and Bandpass Filter Frequency-Response Measurements	83
C.5 LNA Gain Compression Measurements	83
C.6 IF Stage Frequency Response Measurement	84
C.7 Measurement Results for ASR Receivers	84
C.7.1 ASR-8 Receiver Measurement Results.....	84
C.7.2 ASR-9 Receiver Measurement Results.....	89
C.7.3 ASR-11 Receiver Measurement Results.....	93
C.8 ASR Receiver Characteristics Data Summary	98
C.9 Future Work on ASR Receiver Characteristics and Interference Responses	98
Appendix D : FDR Curves for WIMAX-to-Radar EMC Analysis.....	99
D.1 Objectives of EMC-Curve Development Effort	99
D.2 Calculation of Frequency Dependent Rejection (FDR).....	99
D.3 FDR for NEXRAD Radar	99
D.4 FDR for ASR-8 Radar	101
D.5 FDR for ASR-9 Radar	103
D.6 FDR for ASR-11 Radar	104
D.7 Calculation of Protection Distances.....	106
D.7.1 Calculated Separation Distances for 0 Degrees of WiMAX Antenna Down-Tilt.....	108
D.7.2 Calculated Separation Distances for 5 Degrees of WiMAX Antenna Down-Tilt.....	112
D.8 Summary of EMC Frequency-Separation Distance Curves	115
Appendix E : Procedures for Measuring Interference at ASR Stations.....	117
E.1 Introduction	117
E.2 Recommended Measurement Hardware	117
E.3 Procedures for Observing Interference Energy	117
E.4 Selecting an Optimal LNA for EMC/EMI Measurements.....	121
E.4.1 Procedure for Determining the Best Combination of Gain and Noise Figure for a Supplemental LNA.....	121
E.4.2 Example	122
E.4.3 Testing/Verifying the LNA Performance with the Spectrum Analyzer	122

LIST OF FIGURES

	Page
Figure 1. Baseline clear-air Grand Rapids NEXRAD reflectivity display with no interference. Baseline velocity and spectrum width displays look similar when no interference is present. The multi-colored area near the radar is a normal, interference-free condition called clutter; it is caused by radar echoes from objects and atmospheric particles in the radar’s vicinity.....	3
Figure 2. Strokes (three radial blue-and-green lines, compare to Figure 1) caused by interference in the Grand Rapids NEXRAD reflectivity data.	4
Figure 3. Strokes (two radial purple lines) in the Grand Rapids NEXRAD velocity data.	4
Figure 4. Strokes (two radial purple lines) in the Grand Rapids NEXRAD spectrum width data.	5
Figure 5. A typical NEXRAD radar tower, here at Grand Rapids, Michigan. The antenna center is 24 m (80 ft) above ground level (AGL). Transmitter and receiver are located in small shelter at tower base with low-loss waveguide running the tower length. Photo by author Sanders.....	7
Figure 6. Simplified block diagram of the NEXRAD receiver system.	9
Figure 7. Schematic block diagram of NEXRAD receiver-component frequency-response characterization measurements. Measurement hardware is shown in red.	10
Figure 8. Measured broadband frequency response of the NEXRAD front-end LNA.	10
Figure 9. Measured broadband PDL insertion loss. The loss was about 1.5 dB.	11
Figure 10. Measured broadband frequency response of the combination of the RF bandpass filter, PDL and LNA in the NEXRAD RF front end. This is essentially the frequency response of the RF filter, as it is the limiting component in the series.	11
Figure 11. Detail of the passband region of Figure 9.	12
Figure 12. Frequency response of the bandpass filter that follows the LNA. Its response is essentially identical to that of the front-end filter installed ahead of the LNA.....	12
Figure 13. Power-compression behavior of the NEXRAD front-end LNA.	13
Figure 14. Example of a WiMAX base station transmitter (photo by Groupe Aménagement Numérique des Territoires, licensed under Creative Commons Attribution 2.0 Generic license).	14

Figure 15. An example of a tower on which are mounted antennas for a variety of communication systems, including BRS, at Broomfield, Colorado. Photo by author Sanders.	15
Figure 16. A 2.6 GHz WiMAX base station sector-coverage antenna with +16 dBi gain and 90-degree azimuth coverage. Note mechanical down-tilt feature.	18
Figure 17. Antenna pattern of a typical WiMAX/LTE base station antenna, as measured by the manufacturer.	19
Figure 18. Measured frequency response of a typical WiMAX/LTE base station antenna.	20
Figure 19. NTIA RSMS during in situ BRS WiMAX measurements at Broomfield, Colorado. Photo by author Sanders.	21
Figure 20. A BRS WiMAX base station emission spectrum measured in situ at a field location. Transmissions occur on paired BRS/EBS channels E1-E2 (strongest signal, aimed toward measurement location) and E3-F1 and F2-F3 (directed away from the measurement system).	22
Figure 21. Measured time-domain characteristics of an operational BRS WiMAX base station signal. Preamble power is fixed while frame power levels vary.	22
Figure 22. Example of time variation in amplitudes of operational BRS WiMAX base station frames. Preamble power is fixed while frame power levels vary.	23
Figure 23. Peak-detected BRS WiMAX emissions in four measurement bandwidths.	25
Figure 24. Average-detected BRS WiMAX emissions in four measurement bandwidths.	25
Figure 25. Relative on-frequency measured BRS WiMAX peak and average power levels, with variation in measurement bandwidth. Data points taken at 2650 MHz from the curves in Figures 23–24.	26
Figure 26. NTIA/ITS hardline-coupled BRS WiMAX spectrum measurement block diagram.	27
Figure 27. Peak-detected emission spectrum of WiMAX Radio 1.	28
Figure 28. Peak-detected emission spectrum of WiMAX Radio 2.	29
Figure 29. Peak-detected emission spectrum of WiMAX Radio 3.	29
Figure 30. Comparative peak and average emission spectra of WiMAX Radio 2.	30
Figure 31. Schematic block diagram for NEXRAD interference-documentation measurements at Grand Rapids; at Jacksonville the measurements were only performed at J3 and J15.	33

Figure 32. 360-degree interference scan through the Grand Rapids NEXRAD antenna. The same 360-degree scan procedure was performed at Jacksonville.	34
Figure 33. Detailed azimuth scan on interference lobes. The noise floor is that of the radar, peak-detected. (The radar average noise floor limit is 10 dB lower.) The middle lobe between 289.4° and 304.8° has a complex structure described in Figure 34.....	34
Figure 34. Detailed azimuth scan on the central interference lobe of Figure 33. At this scale, the central lobe resolves into two interference azimuths, at 294.6° and 296.0°.	35
Figure 35. Elevation scan at 289.4° azimuth. The interference is measurable up to +2°.	36
Figure 36. Elevation scan at 294.6° azimuth. The interference is measurable up to +1.5°.	36
Figure 37. Elevation scan at 296.0° azimuth. The interference is measurable up to +2°.	37
Figure 38. Elevation scan at 304.8° azimuth. The interference is measurable up to +1.5°.	37
Figure 39. Example of the interference time-domain envelope that was observed in the Grand Rapids NEXRAD receiver on all four interference azimuths. Note intentional time-dependent variation in frame power. Irregular envelopes are explained in Section 4.6.3.....	38
Figure 40. Example of interference signal at Jacksonville at 84.5° azimuth. Eleven other azimuths at Jacksonville showed the same BRS/EBS WiMAX signature (see Appendix B).....	39
Figure 41. BRS/EBS WiMAX interference signal at Grand Rapids measured through the NEXRAD antenna on an azimuth of 289.4°.....	40
Figure 42. BRS/EBS WiMAX interference signal at Grand Rapids measured through the NEXRAD antenna on an azimuth of 294.6°.....	40
Figure 43. BRS/EBS WiMAX interference signal at Grand Rapids measured through the NEXRAD antenna on an azimuth of 296.0°.....	41
Figure 44. BRS/EBS WiMAX interference signal at Grand Rapids measured through the NEXRAD antenna on an azimuth of 289.4°.....	41
Figure 45. BRS/EBS WiMAX interference signals at Jacksonville measured through the NEXRAD antenna on an azimuth of 84.5°.....	42
Emissions from a BRS/EBS WiMAX base station transmitter at Jacksonville at 84.5°, measured across NEXRAD frequency of 2705 MHz. Measurement was performed in 300 kHz to show additional spectrum details. Channels G3-H1 are directed toward the measurement location; the next-higher channels H2-H3 are also occupied but are not aimed at the measurement location.....	42

Figure 47. Top: Measured time-domain responses of an LNA in various amounts of overload, from [18]. Bottom: Data from Figure 40 as they <i>would have</i> appeared if the NEXRAD LNA had been compressed by front-end overload, with overload added graphically in red.	45
Figure 48. Turn-off test observation in the Jacksonville NEXRAD for two BRS WiMAX signals at 2673.5 and 2561.5 MHz transmitted from a single base station.....	47
Figure 49. In situ measurement of tower emissions at 289.4°, Breton Rd. and 29 th St. SE, Grand Rapids, Michigan.	49
Figure 50. In situ measurement of tower emissions at 294.6°, Calvin Ave SE and Kalamazoo Ave SE, Grand Rapids, Michigan.....	49
Figure 51. In situ measurement of tower emissions at 296.0°, water tank at Shaffer Ave. SE and 29 th St. SE, Grand Rapids, Michigan.....	50
Figure 52. In situ measurement of tower emissions at 304.8°, Boston SE and Plymouth SE, Grand Rapids, Michigan.	50
Figure 53. Images of four Grand Rapids BRS/EBS towers where the signals shown in Figures 41–44 were transmitted. Azimuths are as measured from the Grand Rapids NEXRAD station location. Photos by author Sanders.....	51
Figure 54. Filter response that would provide compatibility between a WiMAX signal tuned to 2685 MHz (Figure 44) and a NEXRAD receiver 5 km away tuned to 2710 MHz.	54
Figure 55. Filter response that would provide compatibility between a WiMAX signal tuned to 2685 MHz and a NEXRAD receiver 5 km away tuned to 2705 MHz.	54
Figure 56. WiMAX output bandpass filter response as measured by the manufacturer, Commercial Microwave Technology (CMT), Inc.	55
Figure 57. WiMAX Radio 1 base station emission spectra with and without supplemental output filtering.	56
Figure 58. WiMAX Radio 2 emission spectra with and without output filtering.	57
Figure 59. WiMAX Radio 3 emission spectra with and without output filtering.	57
Figure 60. All emission spectra for WiMAX Radios 1-3, filtered and unfiltered, center frequency normalized to zero.....	58
Figure 61. Detail of Figure 17, showing amount of down-tilt needed to achieve 12 dB of decoupling in the antenna pattern.	60
Figure B-1. WiMAX interference, Jacksonville NEXRAD, 75.5° azimuth.....	74

Figure B-2. WiMAX interference, Jacksonville NEXRAD, 84.5° azimuth.....	74
Figure B-3. WiMAX interference, Jacksonville NEXRAD, 101.0° azimuth.....	75
Figure B-4. WiMAX interference, Jacksonville NEXRAD, 116.0° azimuth.....	75
Figure B-5. WiMAX interference, Jacksonville NEXRAD, 135.5° azimuth.....	76
Figure B-6. WiMAX interference, Jacksonville NEXRAD, 143.5° azimuth.....	76
Figure B-7. WiMAX interference, Jacksonville NEXRAD, 148.5° azimuth.....	77
Figure B-8. WiMAX interference, Jacksonville NEXRAD, 151.0° azimuth.....	77
Figure B-9. WiMAX interference, Jacksonville NEXRAD, 157.0° azimuth.....	78
Figure B-10. WiMAX interference, Jacksonville NEXRAD, 160.7° azimuth.....	78
Figure B-11. WiMAX interference, Jacksonville NEXRAD, 192.0° azimuth.....	79
Figure B-12. WiMAX interference, Jacksonville NEXRAD, 200.3° azimuth.....	79
Figure C-1. An airport surveillance radar antenna (here an ASR-11) as typically deployed on a tower. The beacon antenna is part of an electronically separate system.....	81
Figure C-2. Schematic measurement block diagram for characterization of the RF and IF stages in ASR receivers. The signal generator was programmed to step in small increments across the frequency bands of interest, and the data were recorded on a computer connected to a spectrum analyzer.	84
Figure C-3. Simplified block diagram of the ASR-8 receiver.....	85
Figure C-4. ASR-8 receiver LNA frequency response.....	86
Figure C-5. ASR-8 receiver LNA compression-response curve.	87
Figure C-6. ASR-8 receiver RF filter response.	88
Figure C-7. ASR-8 receiver RF filter plus IF frequency response.	88
Figure C-8. ASR-8 total receiver selectivity.....	89
Figure C-9. Simplified block diagram of the ASR-9 receiver.....	90
Figure C-10. ASR-9 receiver LNA frequency response.....	90
Figure C-11. ASR-9 receiver LNA gain compression response.....	91
Figure C-12. ASR-9 receiver RF filter response.	92

Figure C-13. ASR-9 receiver RF filter plus LNA response.....	92
Figure C-14. Overall frequency response of the ASR-9 receiver. This is also the effective frequency response of the ASR-9 IF stage, as that stage provides the limiting bandwidth of the system.	93
Figure C-15. ASR-11 receiver simplified block diagram.	94
Figure C-16. ASR-11 LNA frequency response.....	94
Figure C-17. ASR-11 LNA gain-compression response.	95
Figure C-18. ASR-11 RF filter frequency response.	96
Figure C-19. ASR-11 receiver IF-stage frequency response.	97
Figure C-20. ASR-11 total receiver frequency response.	97
Figure D-1. Measured NEXRAD IF frequency-response curve.....	100
Figure D-2. FDR plot for NEXRAD receiver versus WiMAX transmitters.	101
Figure D-3. ASR-8 IF plot.	102
Figure D-4. FDR plot for ASR-8 receiver versus WiMAX transmitters.....	102
Figure D-5. ASR-9 IF response plot.	103
Figure D-6. FDR plot for ASR-9 receiver versus WiMAX transmitters.....	104
Figure D-7. ASR-11 IF plot.	105
Figure D-8. FDR plot for ASR-11 receiver versus WiMAX transmitters.....	105
Figure D-9. Distance-frequency separation distance curves for NEXRAD and WiMAX, with WiMAX down-tilt angle = 0 degrees.	108
Figure D-10. Distance-frequency separation curves for ASR-8 and WiMAX, with WiMAX down-tilt angle = 0 degrees.	109
Figure D-11. Frequency-separation distance curves ASR-9 and WiMAX, with WiMAX down-tilt angle = 0 degrees.....	110
Figure D-12. Frequency-distance separation curves for ASR-11 and WiMAX, with WiMAX down-tilt angle = 0 degrees.	111
Figure D-13. Frequency-distance separation curves for NEXRAD and WiMAX, with WiMAX down-tilt angle = 5 degrees.	112

Figure D-14. Frequency-distance separation curves for ASR-8 and WiMAX, with WiMAX down-tilt angle = 5 degrees.	113
Figure D-15. Frequency-distance separation curves for ASR-9 and WiMAX, with WiMAX down-tilt angle = 5 degrees.	114
Figure D-16. Frequency-distance separation curves for ASR-11 and WiMAX, with WiMAX down-tilt angle = -5 degrees.	115

LIST OF TABLES

	Page
Table 1. Summary of NEXRAD (WSR-88D) technical characteristics (as provided by NWS).	8
Table 2. NEXRAD base data products and derivative processed outputs (see [13]).	8
Table 3. Channel frequencies for domestic BRS/EBS stations, from 47 CFR §27.5.	16
Table 4. Typical WiMAX base station transmitter characteristics.	17
Table 5. Typical 2.6 GHz WiMAX base station antenna characteristics.	18
Table 6. Grand Rapids towers identified as origination points of WiMAX interference to the Grand Rapids NEXRAD.	48
Table 7. I/N levels of the Grand Rapids (GR) and Jacksonville (JAX) NEXRAD interference on each azimuth.	52
Table 8. Summary of calculated separation distances (km) for $\Delta F = 22$ MHz.	59
Table C-1. Summary of ASR technical characteristics (as provided by FAA).	82
Table C-2. Summary data table of measured ASR receiver characteristics.	98
Table D-1. ITM model settings for WiMAX-to-radar EMC analysis.	106
Table D-2. Radar parameters for EMC analysis.	107
Table D-3. WiMAX antenna gain reduction as a function of down-tilt angle.	115
Table D-4. Summary separation distances (km) for $\Delta F = 22$ MHz.	116

ABBREVIATIONS/ACRONYMS

AGL	above ground level
ASR	airport surveillance radar
ATC	air traffic control
CTS	Cobham Technical Services
CFR	Code of Federal Regulations
CW	continuous wave
BRS	Broadband Radio Service
DOD	Department of Defense
EBS	Educational Broadband Service
EIRP	effective isotropic radiated power
EMC	electromagnetic compatibility
FAA	Federal Aviation Administration
FCC	Federal Communications Commission
FDR	frequency-dependent rejection
GMF	Government Master File
GPN	Ground Radar Navigation (DOD ATC radar)
IF	intermediate frequency (of a heterodyne receiver)
I/N	interference-to-noise ratio
IEEE	Institute of Electrical and Electronics Engineers
ITS	Institute for Telecommunication Sciences (NTIA)
ITU-R	International Telecommunications Union, Radiocommunication Sector
LBS	Lower Band Segment of BRS/EBS
LNA	low noise amplifier
LOS	line-of-sight (distance) on a smooth round Earth
LTE	Long Term Evolution
MBS	Middle Band Segment of BRS/EBS
NAS	National Airspace System
NEXRAD	Next Generation Weather Radar also designated WSR-88D
NOAA	National Oceanic and Atmospheric Administration
NTIA	National Telecommunications and Information Administration
NWS	National Weather Service
Ofcom	independent regulator and competition authority for the UK communications industries
OFDM	orthogonal frequency division multiplexing (modulation)
OOB	out of band (radio emissions)
PDL	passive diode limiter
PPI	plan position indicator (azimuth-range radar data display)
QAM	quadrature (four level states) amplitude modulation
QPSK	quadrature (four phase states) phase shift keyed modulation
RF	radio frequency
ROC	Radar Operations Center (of NOAA/NWS)
RSEC	United States Radar Spectrum Engineering Criteria
S Band	United States band designation for frequencies between 2700 and 3700 MHz
TDWR	Terminal Doppler Weather Radar

UBS	Upper Band Segment of BRS/EBS
VSA	vector signal analyzer
VSG	vector signal generator
WFO	Weather Forecasting Office of NOAA/NWS
WiMAX	Worldwide Interoperability for Microwave Access (trademark of the WiMAX forum)
WSR-88D	NEXRAD weather surveillance radar, type accepted 1988, Doppler-capable

This page intentionally left blank.

EXECUTIVE SUMMARY

This report describes an investigation into, and solutions for, radio frequency interference to radars from communication systems operating in another band, specifically interference from licensed radio communications stations in the Broadband Radio Service (BRS) and the Educational Broadband Service (EBS) into Federal radar receivers above 2700 MHz. The report describes the methodology for determining the interference source, its mechanism, and effective technical solutions to mitigate the interference. It shows that a careful and methodical technical approach to mitigating interference between systems that operate in different bands can yield effective and affordable engineering solutions.

National Weather Service (NWS) Next Generation Weather Radars (NEXRADs) that operate in the band 2700–3000 MHz have received interference from stations in the BRS and EBS bands; that interference is analyzed in this report. Airport surveillance radars (ASRs) operated by the Federal Aviation Administration (FAA), and their equivalent navigation radars (GPNs) operated by the Department of Defense (DOD), that operate in the band 2700–2900 MHz are analyzed as well because they use the same spectrum as NEXRADs and have similar receiver characteristics.

The report documents that the interference to the NEXRAD radars results from BRS/EBS base stations operating in the BRS/EBS Upper Band Segment (UBS) of 2614–2690 MHz and emitting orthogonal frequency division multiplexed (OFDM) WiMAX signals. The problem is *not* a function of WiMAX emissions per se. Due to the lower antenna gains and heights of those radars however, the potential for interference from BRS/EBS stations to ASRs is found to be relatively low; no ASR interference incidents due to BRS/EBS have been reported or documented.

The report documents that out-of-band (OOB) emissions from BRS/EBS base station transmitters can cause interference to NEXRAD receivers. The report quantifies the power levels that result in interference to the NEXRAD receivers and the amount of de-coupling required to mitigate the interference based on a combination of frequency separation and/or spatial separation with and without antenna down-tilt. The report also provides a procedure to measure the interference power levels. Analysis techniques and interference mitigation solutions that are described here should be applicable in other scenarios where communication systems and radar systems operate in nearby bands.

The report lists various solutions to mitigate the interference, with their pros and cons. The solutions include: careful frequency planning to maximize the frequency differences between BRS/EBS transmitters and radar receivers, using down-tilt of the BRS/EBS antennae along with careful placement and height adjustment, and installing filters on the outputs of BRS/EBS transmitters to reduce their OOB emission levels. The report shows that, because the BRS/EBS OOB emissions are on the radars' assigned frequencies, adding filtering to NEXRAD radar receivers will not mitigate the interference. The report describes the trade-offs between costs, effectiveness, and coordination efforts for each solution and concludes that careful network planning and effective communication between radar operators and BRS/EBS licensees can significantly reduce the likelihood of interference occurring. A number of the report's interference mitigation options have already been implemented in several United States cities served by a BRS/EBS licensee, at licensee WiMAX stations where NEXRAD radar operations

are located nearby. As of the date of this report's release, interference from the licensee's WiMAX links to NEXRAD receivers in those markets has been successfully mitigated using the techniques described herein.

ANALYSIS AND RESOLUTION OF RF INTERFERENCE TO RADARS OPERATING IN THE BAND 2700–2900 MHZ FROM BROADBAND COMMUNICATION TRANSMITTERS

Frank H. Sanders,¹ Robert L. Sole,² John E. Carroll,¹ Glenn S. Secrest,³ T. Lynn Allmon³

This report describes the methodology and results of an investigation into the source, mechanism, and solutions for radiofrequency (RF) interference to WSR-88D Next-Generation Weather Radars (NEXRADs). It shows that the interference source is nearby base station transmitters in the Broadband Radio Service (BRS) and the Educational Broadband Service (EBS) and that their out-of-band (OOB) emissions can cause interference on NEXRAD receiver frequencies. The methodology for determining interference power levels and mitigation solutions is described. Several technical solutions that can mitigate the problem are shown to be effective. Trade-offs between effectiveness, difficulty, and costs of various solutions are described, but it is shown that there is always at least one effective technical solution. The report shows that careful planning and coordination between communication system service providers and Federal agencies operating nearby radars is important in the implementation of these interference-mitigation techniques. A number of the report's interference mitigation options have already been implemented in several United States cities served by a BRS/EBS licensee, at licensee WiMAX stations where NEXRAD radar operations are located nearby. As of the date of this report's release, interference from the licensee's WiMAX links to NEXRAD receivers in those markets has been successfully mitigated using the techniques described herein.

Key words: airport surveillance radar (ASR); electromagnetic compatibility (EMC); interference-to-noise (I/N) ratio; NEXRAD; out-of-band (OOB) emissions; radar interference; radio frequency (RF) interference; WiMAX; WSR-88D

¹ The authors are with the Institute for Telecommunication Sciences, National Telecommunications and Information Administration, U.S. Department of Commerce, Boulder, Colorado 80305.

² The author is with the Office of Spectrum Management, National Telecommunications and Information Administration, U.S. Department of Commerce, Washington, DC 20230.

³ The authors are with the National Oceanic and Atmospheric Administration's National Weather Service Radar Operations Center, Norman, Oklahoma 73069.

1 ELECTROMAGNETIC COMPATIBILITY CONCERNS BETWEEN 2700–2900 MHZ RADAR SYSTEMS AND TERRESTRIAL COMMUNICATION SYSTEMS

1.1 Background

In 2007 the United Kingdom (UK) Office of Communications (Ofcom) examined the issue of electromagnetic compatibility between UK air traffic control (ATC) radar transmissions (2700–2900 MHz) and the receivers of next generation mobile broadband wireless systems using frequencies just below 2700 MHz [1]. In 2008 and 2009 Ofcom examined the reverse issue of compatibility between such services' transmissions and ATC radar receivers [2]–[7]. In these studies Ofcom indicated awareness of possible interference between future mobile broadband services operating just below 2700 MHz and UK Watchman ATC radars that operate above that frequency. The overall results of the Ofcom studies were summarized [8] at the end of 2009. By 2011, Ofcom had applied the results of the earlier work to move forward with use of spectrum below the ATC band [9], [10]. The current technical and administrative situation regarding use of this spectrum in the UK, including current knowledge regarding compatibility between the new wireless services and maritime radars, is described in [11]. The Electronic Communications Committee (ECC) of the European Conference of Postal and Telecommunications Administrations (CEPT) recently released its own report on compatibility in Europe between the mobile service in 2500–2690 MHz band and the radiodetermination (radar) service in the 2700–2900 MHz band [12].

In the United States, and similarly in the UK, government ATC radars (called airport surveillance radars, or ASRs, models 7, 8, 9, and 11) operate between 2700 and 2900 MHz. These and electronically equivalent monitoring radars designated GPNs are operated by the Federal Aviation Administration (FAA) and the Department of Defense (DOD), respectively. In addition, the National Weather Service (NWS) operates meteorological (weather) radars (Next Generation Weather Radars (NEXRADs, also known as WSR-88Ds)) between 2700 and 3000 MHz. Similarly to spectrum use in the UK, the United States Federal Communications Commission (FCC) has authorized wireless broadband systems to operate between 2496–2690 MHz, just below the 2700–2900 MHz band.

1.2 Preliminary Examination of Electromagnetic Compatibility (EMC) Issues Between WiMAX Transmitters and NEXRAD Receivers

In May 2010, a brief preliminary investigation of operational weather radar products by NTIA engineers indicated that interference might already have been occurring in the United States from BRS/EBS base station transmitters to some weather radars in the 2700–3000 MHz band. This investigation employed a methodology that used combined data observations of weather-reporting and earth-satellite observation web sites. NEXRAD weather products at several locations across the United States showed strobes⁴ that aligned on azimuths of local BRS/EBS base stations within line-of-sight of the radar stations. Although this circumstance could have

⁴ Strobes are interference artifacts; they are radially oriented, blanked-out coverage zones on radar displays. Desired targets and weather data are suppressed where strobes occur on radar displays.

been coincidental, NTIA believed that further investigation was needed to characterize radio frequency (RF) environments so as to positively identify any sources of interference. On 15 September 2010 the National Weather Service (NWS) notified NTIA that their NEXRAD in Grand Rapids, Michigan, was experiencing interference.

Figure 1 shows a Grand Rapids NEXRAD display when no interference was present; the multi-colored zone near the radar is a normal, clear-air, interference-free baseline condition. In contrast, Figures 2–4 show examples of Grand Rapids radar displays when interference was present, as observed by NWS and NTIA engineers in October 2010. As seen in Figures 2–4, the strobes contaminated all three of the radar’s base moments: reflectivity, velocity, and spectrum width data. (The NEXRAD is described more fully in Section 2 of this report. Meteorological data products such as reflectivity, velocity and spectrum width are described in [13]. General effects of radio interference on radar receivers, including strobes, are described in [13] and [14].)

Preliminary data gathered by the NWS indicated that the source of this interference could be BRS/EBS base station transmitters located within a few kilometers of the radar’s location. The initial evidence consisted of correlations between BRS/EBS tower azimuths and the azimuths of the strobes. Emission spectra of the interference sources that were collected within the Grand Rapids NEXRAD receiver (as described in Section 3) were consistent with known emission spectra of WiMAX transmitters. The Grand Rapids interference had begun shortly after BRS/EBS service was inaugurated in that area.

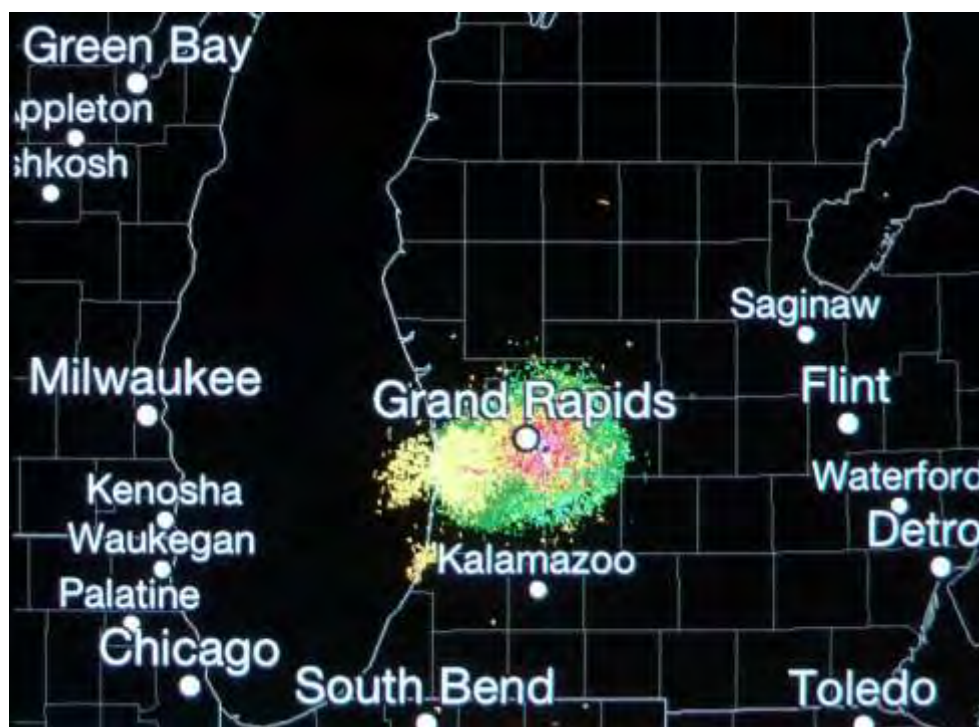


Figure 1. Baseline clear-air Grand Rapids NEXRAD reflectivity display with no interference. Baseline velocity and spectrum width displays look similar when no interference is present. The multi-colored area near the radar is a normal, interference-free condition called clutter; it is caused by radar echoes from objects and atmospheric particles in the radar’s vicinity.

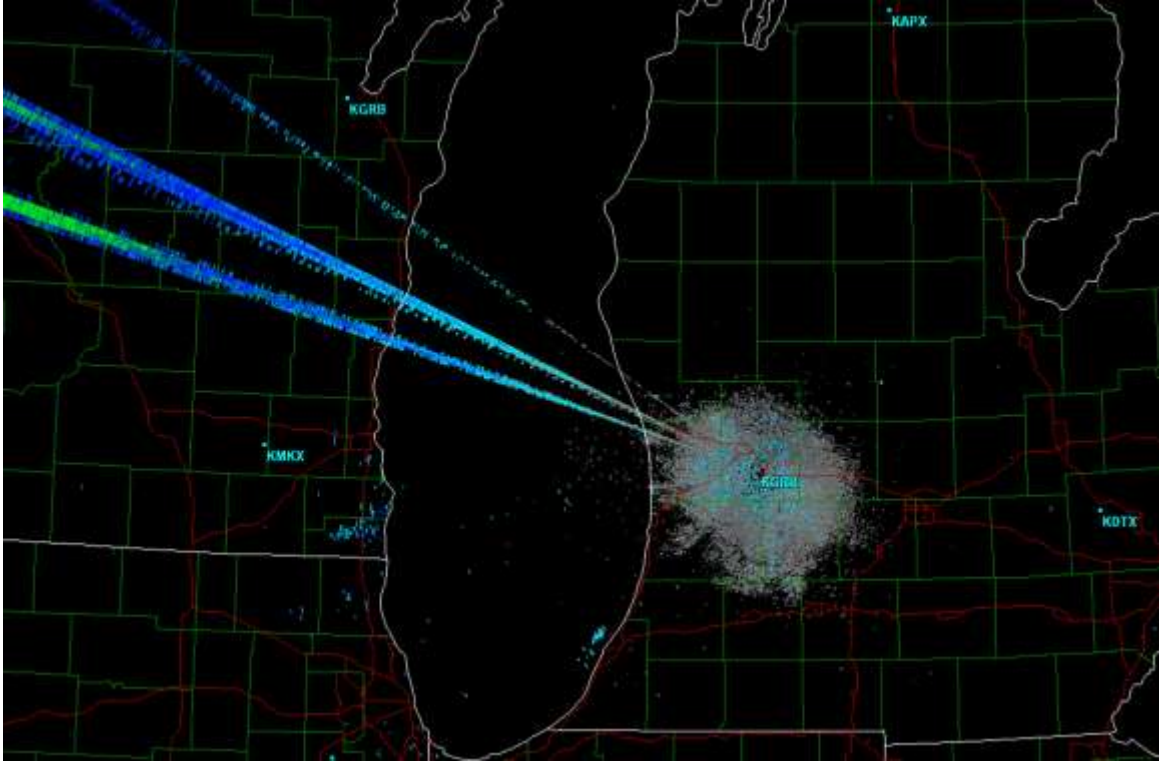


Figure 2. Strokes (three radial blue-and-green lines, compare to Figure 1) caused by interference in the Grand Rapids NEXRAD reflectivity data.

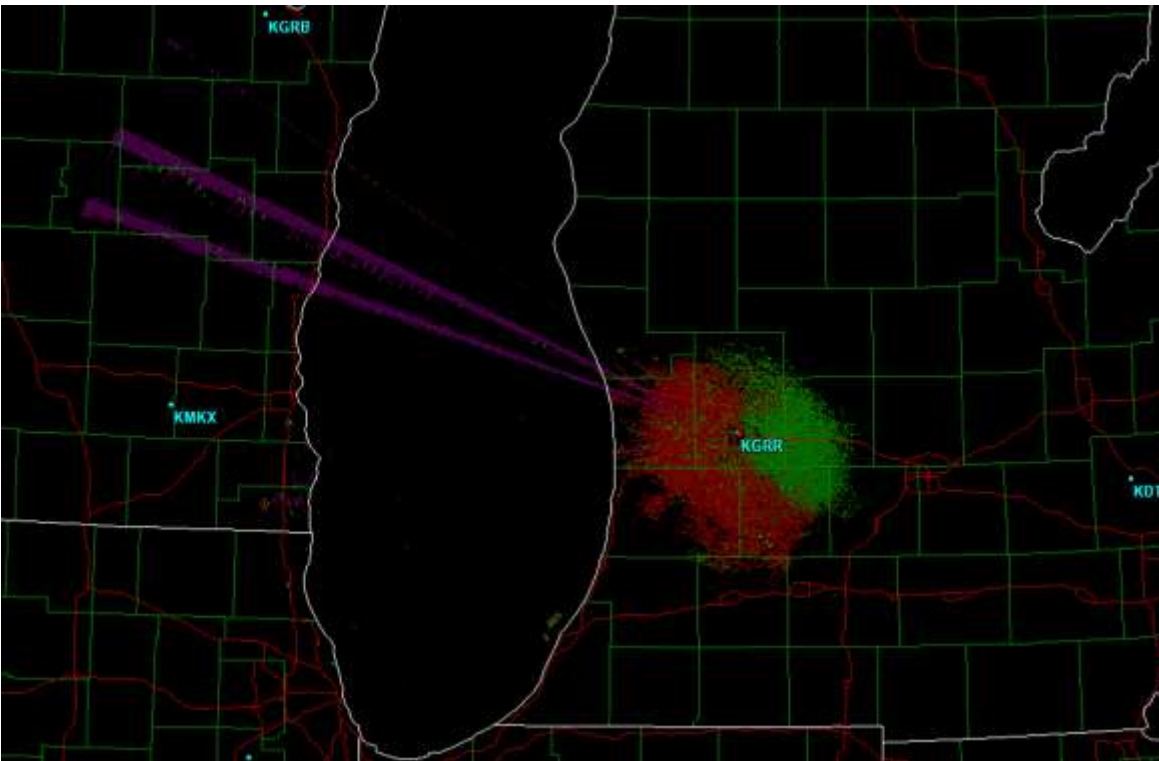


Figure 3. Strokes (two radial purple lines) in the Grand Rapids NEXRAD velocity data.

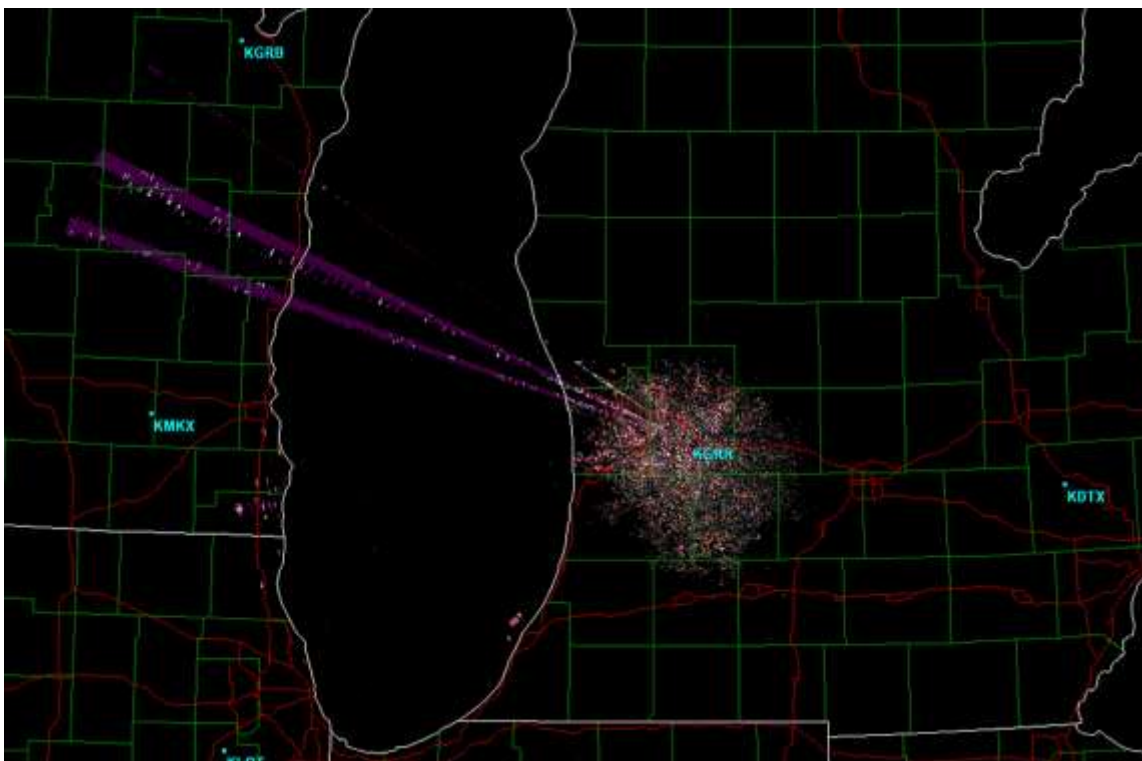


Figure 4. Strobos (two radial purple lines) in the Grand Rapids NEXRAD spectrum width data.

1.3 Initial Joint Agency Work at Grand Rapids, Michigan, and Jacksonville, Florida

The Department of Commerce (DOC) requested that NTIA investigate this interference to their important weather radar using resources from NTIA's Office of Spectrum Management (OSM) in Washington, DC, and NTIA's Institute for Telecommunication Sciences (ITS) laboratory in Boulder, Colorado. After a review of preliminary NWS data from Grand Rapids and discussion with NWS engineers, NTIA and NWS engineers traveled to Grand Rapids and, during 4–5 October 2010 and performed the detailed interference investigation described in this report. Similar interference was later reported at a NEXRAD station at Jacksonville, Florida. A joint team of personnel from NWS, NTIA, FCC and FAA investigated this on-site during 14–17 February 2011. NTIA and NWS personnel subsequently analyzed the Grand Rapids and Jacksonville data; this report presents the results of that analysis and the follow-up work that identified solutions for the problem.

1.4 Objectives of Initial Field Work

The overall goal of initial field work was to identify and document the source of the interference, identify the interference mechanism (i.e., to distinguish between the mechanism of RF front-end overload in the radar receivers versus interference directly on the radar operational frequencies), and determine the power level of the interference relative to the internal receiver noise floor of the radar receiver. With these data in hand, EMC analyses could indicate technical solutions for the interference problem. Specific tasks to accomplish were:

1. Measure and record the RF and intermediate frequency (IF) response (frequency selectivity) of the NEXRAD receiver's RF front-end filter.
2. Measure and record the NEXRAD front-end low noise amplifier (LNA) gain-response curve as a function of frequency and determine its power-output compression behavior.
3. Measure and record the RF frequency-domain response of the entire NEXRAD RF front end, comprising its RF bandpass filter, passive diode limiter (PDL), and LNA.
4. Measure and record the frequency response of the entire NEXRAD receiver from the input of the RF front-end filter to the output of the IF stage.
5. Formally document the RF configuration of the NEXRAD receiver front end and IF downconversion hardware stages.
6. Formally document the interference by measuring and recording the interference in both the frequency domain and the time domain at the following points in the NEXRAD receiver: a) the antenna output (which is the same as the front end RF bandpass filter input); b) the LNA output; and c) the IF stage output.
7. Observe and record the overall interference environment by scanning 360 degrees of horizon around the NEXRADs at a low elevation angle while the radar was operated in a receive-only mode and the IF stage output was monitored and recorded in the time domain for the duration of the scan. Any interfering signals that were being received at or above -6 dB below the radar receiver's internal noise floor would appear as bumps that would be 1 dB or more higher than the receiver's noise floor. The interference signal at each bump was observed in the time domain to ascertain its modulation and hence its likely source. This observation would identify interference signals that could cause possible degradation of the NEXRADs' performance but which were too low-powered to produce overtly visible strobes on the radar's plan position indicator (PPI) output display.

2 NEXRAD TECHNICAL CHARACTERISTICS

2.1 NEXRAD Radars Operating Between 2700–3000 MHz

NEXRAD weather radars (Figure 5) operate within the United States and Possessions at frequencies between 2700–3000 MHz. As summarized in Table 1, they use klystrons to generate high-power pulses approximately 1 μ s long, transmitting and receiving with high gain parabolic antennas that generate pencil beams that are repetitively conically scanned through space around each radar station. The lowest tuned frequency for any NEXRAD is 2705 MHz.

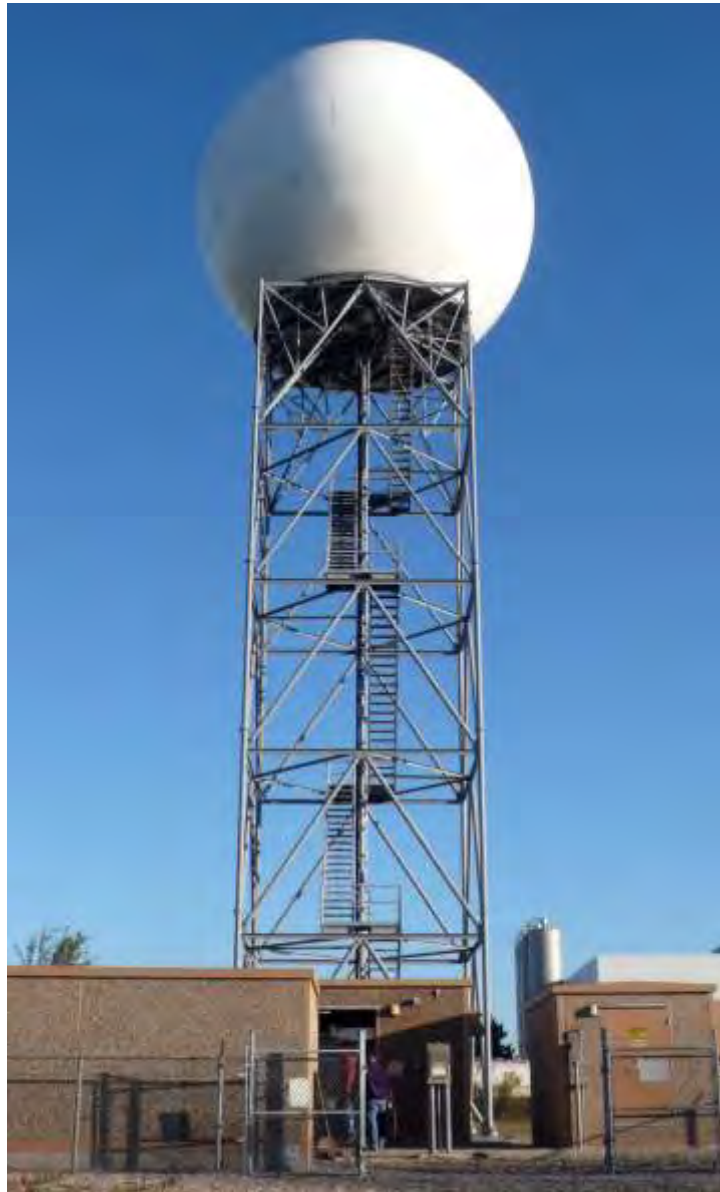


Figure 5. A typical NEXRAD radar tower, here at Grand Rapids, Michigan. The antenna center is 24 m (80 ft) above ground level (AGL). Transmitter and receiver are located in a small shelter at the tower base with low-loss waveguide running the tower length. Photo by author Sanders.

Table 1. Summary of NEXRAD (WSR-88D) technical characteristics (as provided by NWS).

Parameter	Description
Peak transmitter power	750 kW
Transmitter type	klystron tube
Operational frequency range	2700-3000 MHz
Antenna type	9 m (28 ft) diameter parabolic reflector with microwave feed horn at power center
Antenna gain	45.5 dBi
Antenna height above ground	24 m (80 ft)
Antenna beam type	Pencil
Antenna beam width	0.95° (3 dB width) 0.15° (boresight accuracy)
Antenna polarization	linear horizontal
Antenna sidelobe levels	At least 27 dB below main-beam gain
Antenna beam scanning protocol	conical scan, +0.5° to +20° elevation
Antenna beam scanning rate	6 rpm (10 sec/scan revolution interval)
Transmitted pulse widths	short pulse: 1.6 μ s long Pulse: 4.5 μ s
Transmitted pulse modulation	P0N (unmodulated CW pulses)
Transmitted pulse repetition rates	short pulse: 318 to 1304 pulses/sec long pulse: 318 to 452 pulses/sec
Receiver bandwidth	0.795 MHz
Receiver channels	linear output, I/Q, and log output
Nominal receiver noise figure	1.5 dB
Receiver thermal noise level in 0.795 MHz bandwidth	-113.5 dBm (computed)
Base moments (data products)	reflectivity, velocity and spectrum width
Maximum operational distances	reflectivity: 460 km (248 nm) velocity: 230 km (124 nm)

NWS NEXRAD operations have safety-of-life status in the United States spectrum Table of Allocations [15]. General technical and operational aspects of meteorological radars are described in [13]. As summarized in Table 2, NEXRADs observe and track severe weather including precipitation, hail, tornado and wind shears. NEXRAD data generate watches and warnings for severe weather, including emergency National Oceanic and Atmospheric Administration (NOAA) Weather Radio broadcasts.

Table 2. NEXRAD base data products and derivative processed outputs (see [13]).

Base Moment Output	Processed Outputs
Reflectivity	Precipitation monitoring and tracking, hail structures, echo tops, vertically integrated liquid, severe weather probability and forecasting
Velocity	Mesocyclone observations, tornado vortex signatures, velocity azimuth displays, shear-structure observations
Spectrum width	Turbulence observations

2.2 NEXRAD Receiver Design

NEXRAD receivers incorporate the following stages, in the order that meteorological echo energy passes through them: the antenna (parabolic reflector and feed); an RF front-end channel bandpass filter; a PDL; an LNA; a length of low-loss RF cable running from the top of the tower to the receiver shelter; another RF bandpass channel filter; a frequency mixer-downconverter which converts the RF energy to an IF passband centered at 57.56 MHz; and an analog-to-digital converter. Base data products of reflectivity, velocity, and spectrum width are derived from the digital data stream. Figure 6 shows the receiver design in a simplified block diagram schematic.

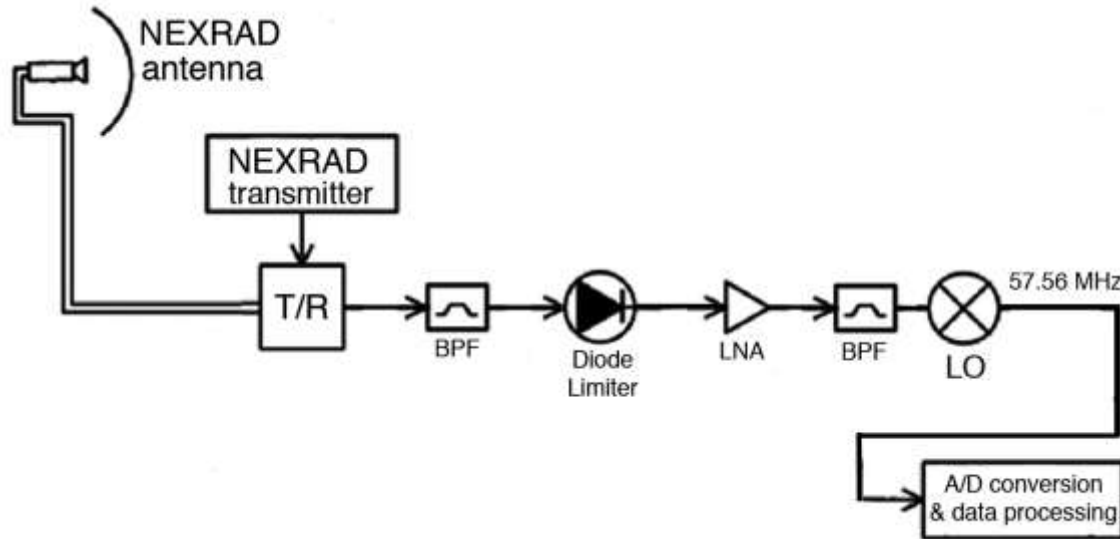


Figure 6. Simplified block diagram of the NEXRAD receiver system.

2.3 Frequency-Response Measurements of NEXRAD Receiver Stages

As shown in Figure 7, various combinations of NEXRAD receiver components were swept with a carrier wave from a vector signal generator (VSG) to characterize their frequency responses.

The results of the front-end component characterization measurements are shown in Figures 8–12. Figure 8 shows the LNA frequency response; Figure 9 shows the insertion loss of the PDL, which is constant with frequency. Figure 10 shows the frequency response of the front-end RF filter, the PDL and the LNA; this figure demonstrates the significant extent to which the front-end filter limits the coupling of the LNA to energy that is off-frequency from the radar receiver's desired range of operation. Figure 11 shows a detailed view of the radar receiver's front-end bandpass filtering; it is centered on the radar's frequency of 2710 MHz and is 13 MHz wide at the 3 dB points. Figure 12 shows the bandpass response of the RF filter that follows the LNA, and which is intended to filter out unwanted LNA response products. Its response is essentially identical to that of the front-end filter.

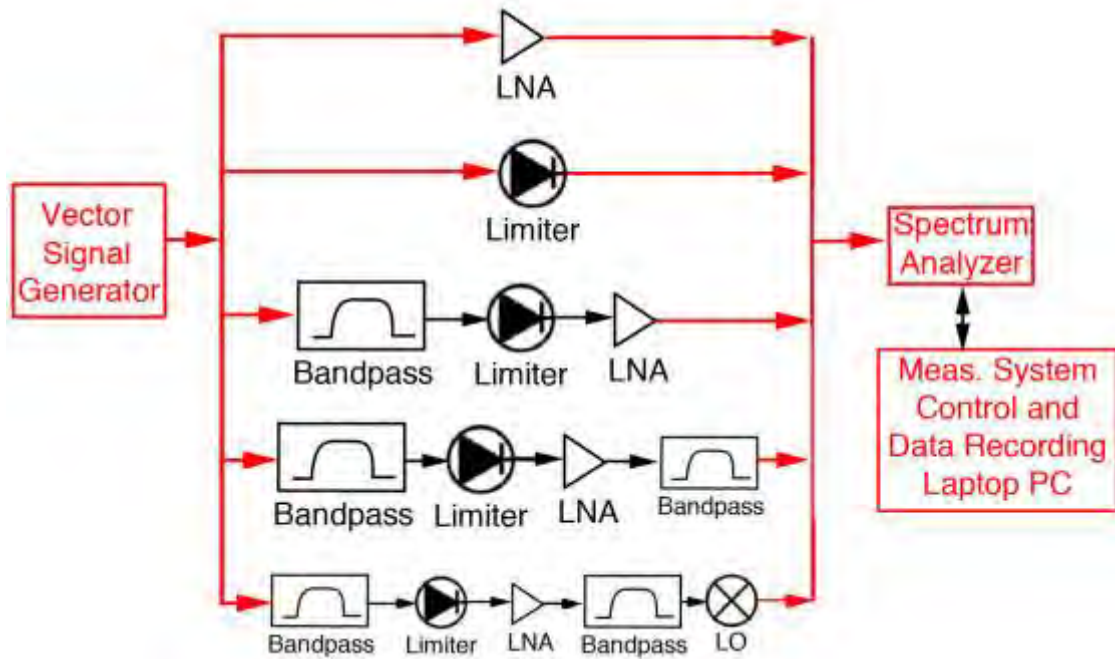


Figure 7. Schematic block diagram of NEXRAD receiver-component frequency-response characterization measurements. Measurement hardware is shown in red.

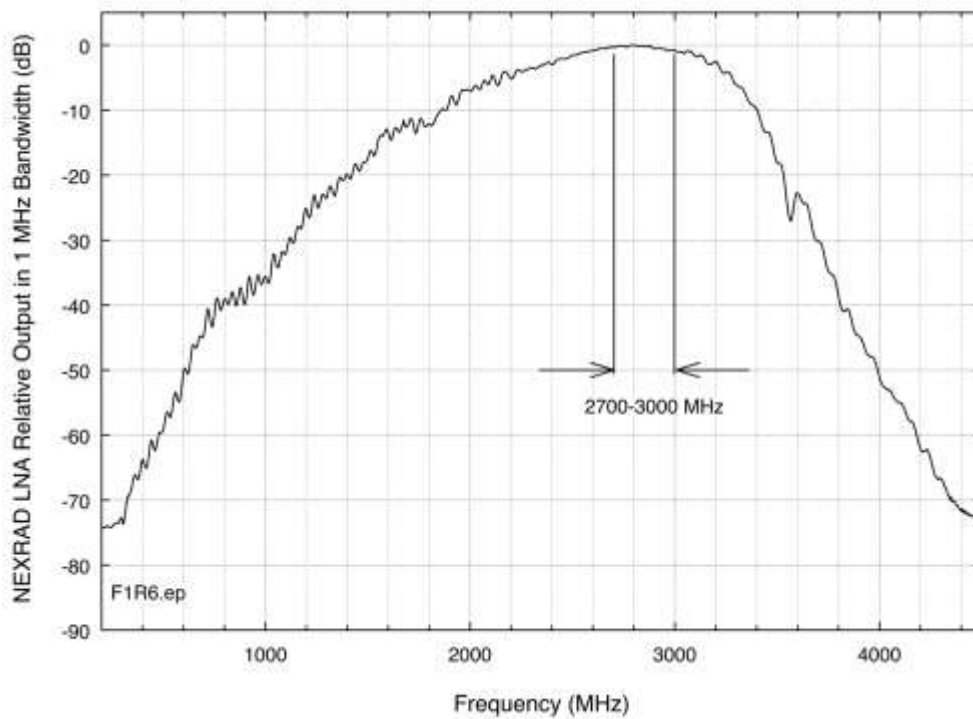


Figure 8. Measured broadband frequency response of the NEXRAD front-end LNA.

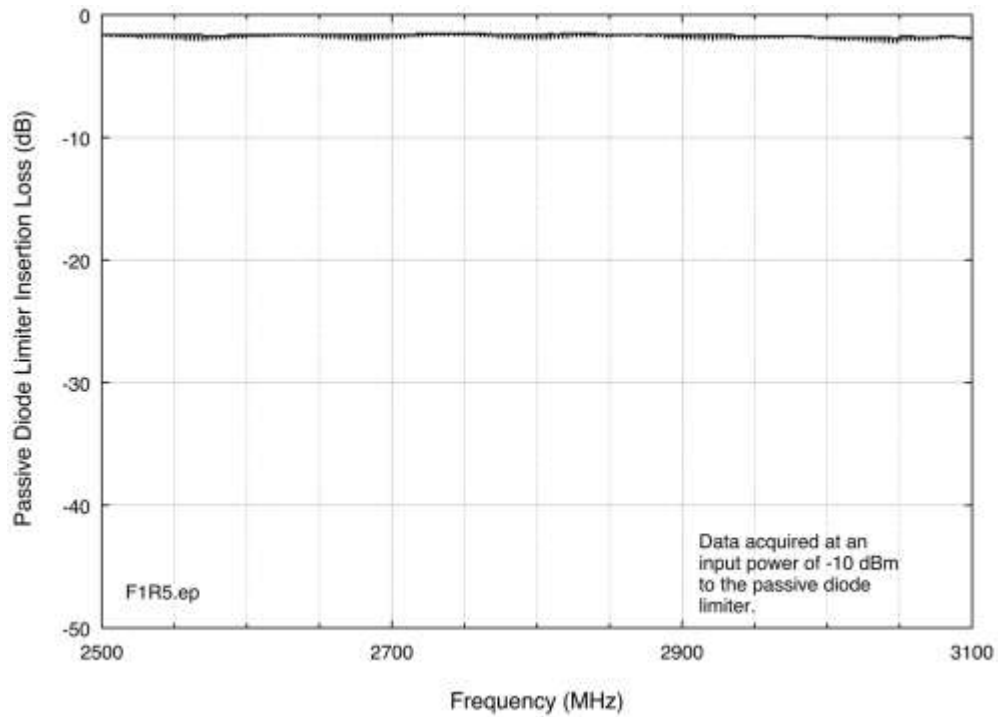


Figure 9. Measured broadband PDL insertion loss. The loss was about 1.5 dB.

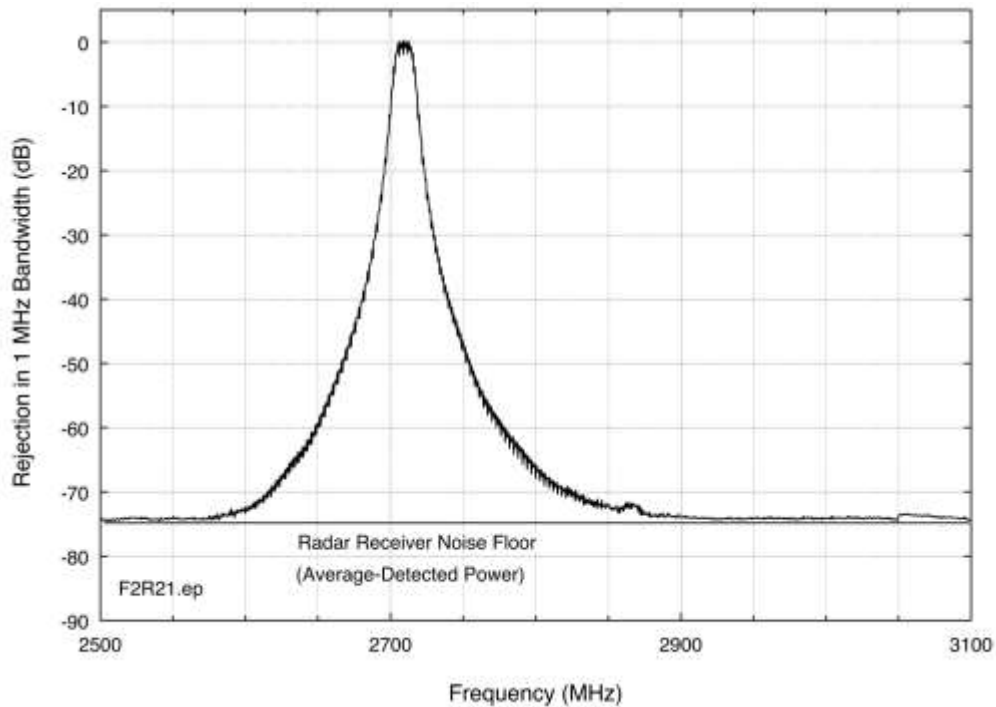


Figure 10. Measured broadband frequency response of the combination of the RF bandpass filter, PDL and LNA in the NEXRAD RF front end. This is essentially the frequency response of the RF filter, as it is the limiting component in the series.

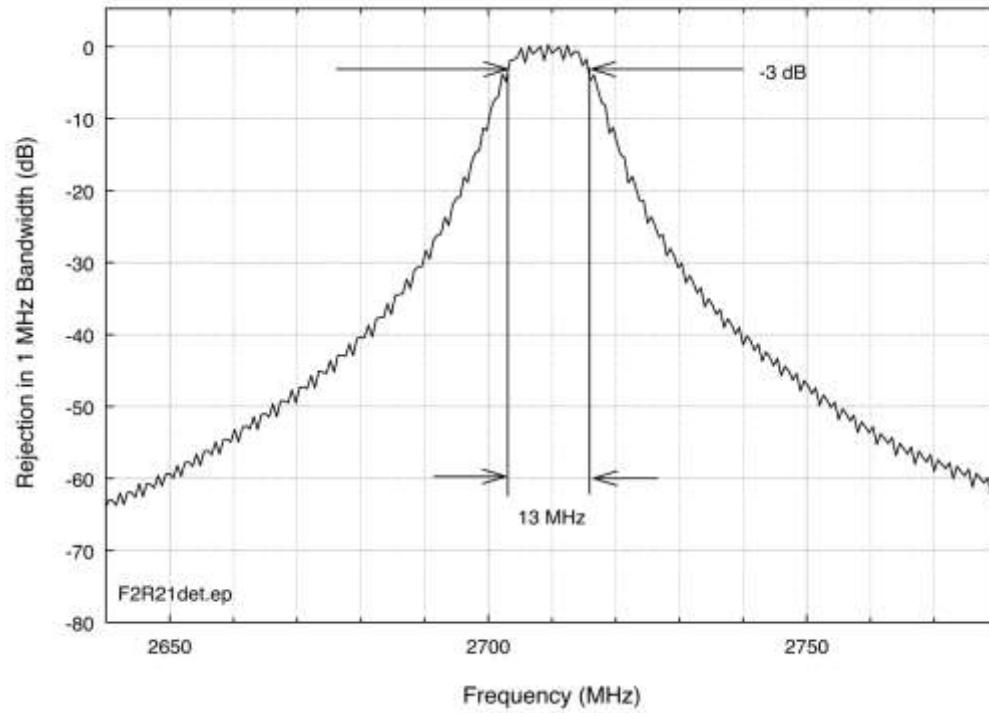


Figure 11. Detail of the passband region of Figure 9.

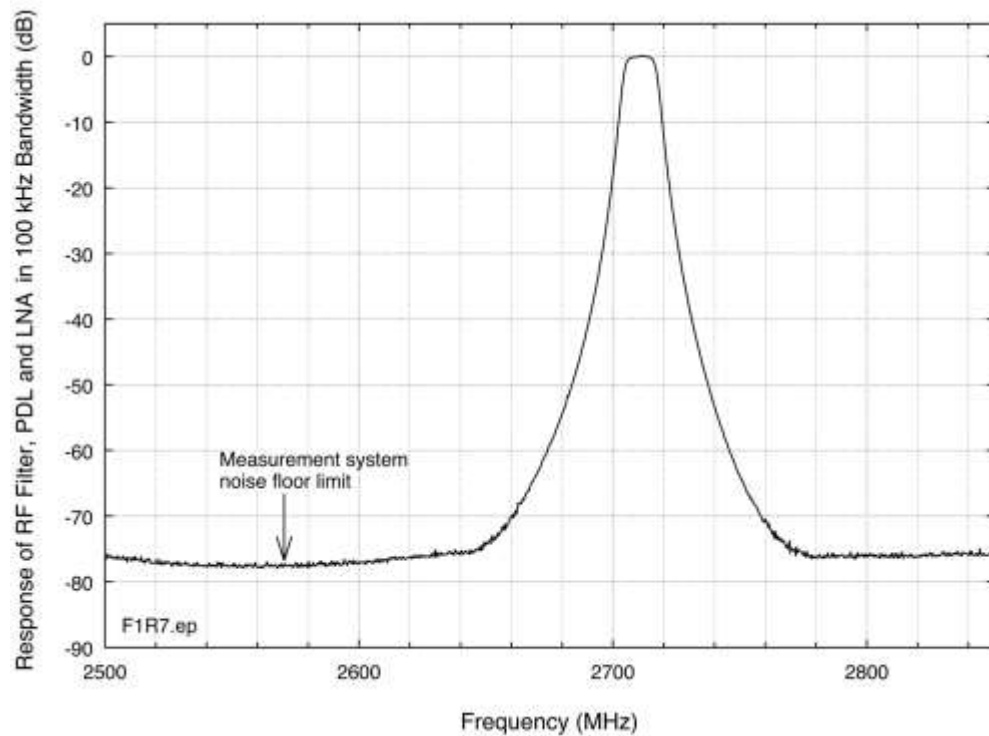


Figure 12. Frequency response of the bandpass filter that follows the LNA. Its response is essentially identical to that of the front-end filter installed ahead of the LNA.

2.4 NEXRAD RF Gain Compression Measurement

The VSG was also used to measure the power-compression behavior of the NEXRAD LNA. For this measurement, the VSG was fixed-tuned to the radar's operational frequency and its input power to the LNA was increased in 1 dB increments as the output power of the LNA was measured. The resulting data are shown in Figure 13. The 1 dB compression level occurs at an input power of -7.5 dBm to the LNA

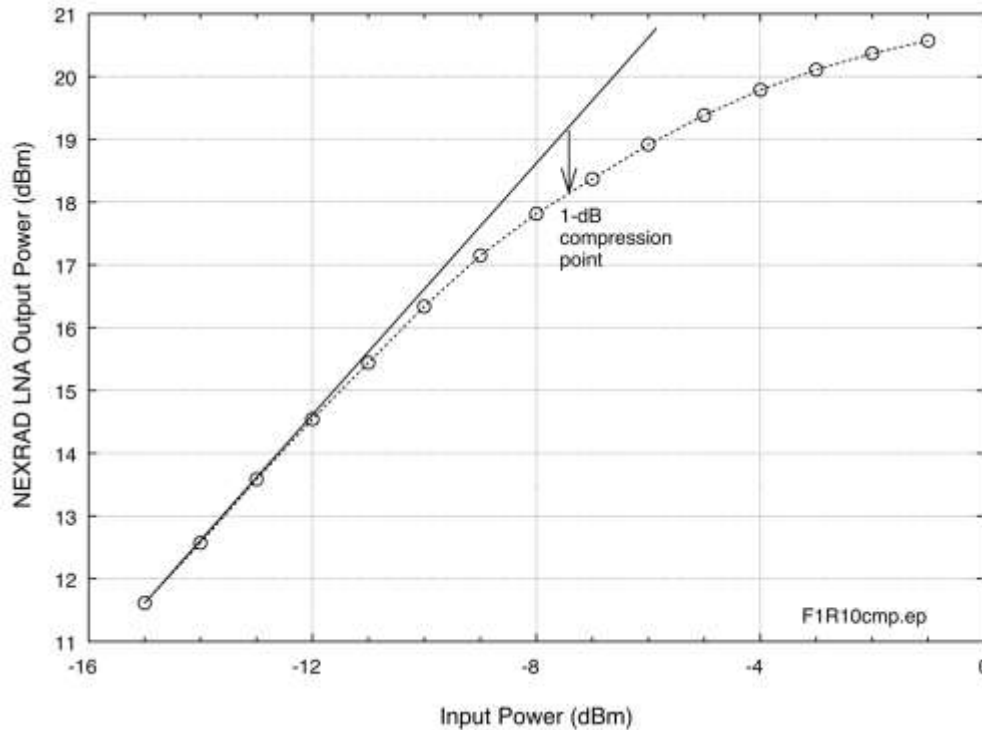


Figure 13. Power-compression behavior of the NEXRAD front-end LNA.

2.5 Summary of NEXRAD Receiver EMC Characteristics

The data presented here show that the NEXRAD receiver design conforms to well-recognized practices for robust EMC performance in the presence of high-power out-of-band signals. The radar receiver's wideband, highly sensitive front-end LNA input is protected from high-power out-of-band energy by a diode limiter to protect against catastrophically high input power that could damage electronic circuitry and a narrowband channel bandpass filter to eliminate overload effects. Another, identical filter is installed at its output to eliminate possible intermodulation products.

However, no receiver front-end design, including that of NEXRADs, can mitigate interference from co-channel interference energy. Furthermore, NEXRADs cannot be significantly re-tuned unless their front-end filter assemblies and klystrons are replaced.

3 2.6-2.7 GHZ WIMAX TECHNICAL CHARACTERISTICS

3.1 Technical Characteristics of BRS/EBS WiMAX Base Stations

WiMAX (IEEE 802.16-2009)⁵ is a relatively new technology that is used for high speed data transfer for fixed and mobile terminals with licensed stations in the BRS/EBS radio band 2496–2690 MHz.⁶ BRS/EBS services utilizing WiMAX technology began to be offered in selected United States cities in 2008. WiMAX service competes with that of carriers that are using 3G, EDGE and LTE technology.⁷ EMC concerns are not exclusive to WiMAX; any technology can potentially cause EMC problems between systems operating in different bands.

WiMAX system architecture is similar to cellular telephone systems, comprising base stations (Figure 14) and tower-mounted antennas (Figure 15) and servicing fixed or mobile terminals. In the course of this study the authors observed that WiMAX base station transmitter power levels and antenna gains were typically 20 W and +16 dBi, respectively, giving these stations a typical EIRP of 790 W.



Figure 14. Example of a WiMAX base station transmitter (photo by Groupe Aménagement Numérique des Territoires, licensed under [Creative Commons Attribution 2.0 Generic](#) license).

⁵ See <http://resources.wimaxforum.org/resources/documents/technical/release>

⁶ For more information about WiMAX systems, see <http://www.WiMAXforum.org/>. See also 47 CFR Part 27, Subpart M (Broadband Radio Service and Educational Broadband Service) and Sec. 27.5(i).

⁷ See http://hraunfoss.fcc.gov/edocs_public/attachmatch/FCC-11-103A1.pdf



Figure 15. An example of a tower on which are mounted antennas for a variety of communication systems, including BRS, at Broomfield, Colorado. Photo by author Sanders.

3.2 BRS/EBS Spectrum Channel Plan in the United States

The Lower, Middle and Upper Band Segments (LBS, MBS and UBS, respectively) channels and frequencies of BRS/EBS base station transmitters are shown in Table 3. Transmitter and antenna characteristics are provided in Table 4. Domestic BRS/EBS licensees are authorized to merge contiguous channel authorizations into other channel bandwidths, with an emission bandwidth of 10 MHz being most commonly used.

Table 3. Channel frequencies for domestic BRS/EBS stations, from 47 CFR §27.5.

Band Segment	Broadcast Radio Service (BRS) Channel	Channel Frequency Range
LBS	BRS Channel 1	2496–2502 MHz or 2150–2156
LBS	EBS Channel A1	2502–2507.5 MHz
LBS	EBS Channel A2	2507.5–2513 MHz
LBS	EBS Channel A3	2513–2518.5 MHz
LBS	EBS Channel B1	2518.5–2524 MHz
LBS	EBS Channel B2	2524–2529.5 MHz
LBS	EBS Channel B3	2529.5–2535 MHz
LBS	EBS Channel C1	2535–2540.5 MHz
LBS	EBS Channel C2	2540.5–2546 MHz
LBS	EBS Channel C3	2546–2551.5 MHz
LBS	EBS Channel D1	2551.5–2557 MHz
LBS	EBS Channel D2	2557–2562.5 MHz
LBS	EBS Channel D3	2562.5–2568 MHz
LBS	EBS Channel JA1	2568.00000–2568.33333 MHz
LBS	EBS Channel JA2	2568.33333–2568.66666 MHz
LBS	EBS Channel JA3	2568.66666–2569.00000 MHz
LBS	EBS Channel JB1	2569.00000–2569.33333 MHz
LBS	EBS Channel JB2	2569.33333–2569.66666 MHz
LBS	EBS Channel JB3	2569.66666–2570.00000 MHz
LBS	EBS Channel JC1	2570.00000–2570.33333 MHz
LBS	EBS Channel JC2	2570.33333–2570.66666 MHz
LBS	EBS Channel JC3	2570.66666–2571.00000 MHz
LBS	EBS Channel JD1	2571.00000–2571.33333 MHz
LBS	EBS Channel JD2	2571.33333–2571.66666 MHz
LBS	EBS Channel JD3	2571.66666–2572.00000 MHz
MBS	EBS Channel A4	2572–2578 MHz
MBS	EBS Channel B4	2578–2584 MHz
MBS	EBS Channel C4	2584–2590 MHz
MBS	EBS Channel D4	2590–2596 MHz
MBS	EBS Channel G4	2596–2602 MHz
MBS	EBS Channel F4	2602–2608 MHz
MBS	EBS Channel E4	2608–2614 MHz

Band Segment	Broadcast Radio Service (BRS) Channel	Channel Frequency Range
UBS	BRS Channel KH1	2614.00000–2614.33333 MHz
UBS	BRS Channel KH2	2614.33333–2614.66666 MHz
UBS	BRS Channel KH3	2614.66666–2615.00000 MHz
UBS	BRS Channel KG1	2615.00000–2615.33333 MHz
UBS	BRS Channel KG2	2615.33333–2615.66666 MHz
UBS	BRS Channel KG3	2615.66666–2616.00000 MHz
UBS	BRS Channel KF1	2616.00000–2616.33333 MHz
UBS	BRS Channel KF2	2616.33333–2616.66666 MHz
UBS	BRS Channel KF3	2616.66666–2617.00000 MHz
UBS	BRS Channel KE1	2617.00000–2617.33333 MHz
UBS	BRS Channel KE2	2617.33333–2617.66666 MHz
UBS	BRS Channel KE3	2617.66666–2618.00000 MHz
UBS	BRS Channel 2	2618–2624 MHz or 2156–2162 MHz
UBS	BRS Channel 2A	2618–2624 MHz or 2156–2160 MHz
UBS	BRS/EBS Channel E1	2624–2629.5 MHz
UBS	BRS/EBS Channel E2	2629.5–2635 MHz
UBS	BRS/EBS Channel E3	2635–2640.5 MHz
UBS	BRS/EBS Channel F1	2640.5–2646 MHz
UBS	BRS/EBS Channel F2	2646–2651.5 MHz
UBS	BRS/EBS Channel F3	2651.5–2657 MHz
UBS	BRS Channel H1	2657–2662.5 MHz
UBS	BRS Channel H2	2662.5–2668 MHz
UBS	BRS Channel H3	2668–2673.5 MHz
UBS	EBS Channel G1	2673.5–2679 MHz
UBS	EBS Channel G2	2679–2684.5 MHz
UBS	EBS Channel G3	2684.5–2690 MHz

Table 4. Typical WiMAX base station transmitter characteristics.⁸

WiMAX Base Station Parameter	Value
Emission bandwidth	5 and 10 MHz
Modulation	Adaptable range from QPSK to 64 QAM
Typical channel transmission power	20 watts = +43 dBm
Typical channel EIRP	790 watts = +59 dBm
Computed unfiltered spurious emissions	-70 dB below fundamental power

⁸ These characteristics were observed by the authors while working with a BRS/EBS licensee in the course of this study.

3.3 WiMAX Base Station Antenna Characteristics and Frequency Response

The authors observed, in the course of this study, that WiMAX base station antennas (Figure 16) are typically mounted on high towers, water tanks, and rooftops to provide sector coverage. As noted by the authors at BRS/EBS WiMAX field sites, groups of sectors provide 360-degree coverage around each site. The antennas form fan-shaped beams with wide azimuth (sector) width but with a narrow elevation-angle dimension. Elevation beam angles are usually tilted slightly downward to maximize coverage for customers located at or near ground level.



Figure 16. A 2.6 GHz WiMAX base station sector-coverage antenna with +16 dBi gain and 90-degree azimuth coverage. Note mechanical down-tilt feature.

Table 5 lists characteristics of typical WiMAX base station antennas. Most base stations employ sets of dual element, slant-polarized⁹ 90° or 65° coverage antennas to illuminate a 120° sector for each 10 MHz channel; three such sectors provide 360° coverage at a typical base station tower, with three 10 MHz channels being concomitantly used per tower.

Table 5. Typical 2.6 GHz WiMAX base station antenna characteristics.¹⁰

2.6 GHz UBS WiMAX Parameter	Value
Typical sector antenna gain	+16 dBi
Typical sector antenna azimuth coverage	120° (most common), also sometimes 90°
Polarization	Slant (+/- 45 degrees, most common), also sometimes vertical or horizontal
Typical antenna height above ground	30 m (100 ft)

⁹ Slant polarization supports the decorrelated multiple elements needed for Multiple Input Multiple Output (MIMO) operation.

¹⁰ As observed by the authors at multiple BRS/EBS WiMAX field sites and described in communication with a BRS/EBS licensee.

Antenna patterns for a model manufactured by the Argus company¹¹ and commonly used by WiMAX and LTE service providers for their WiMAX and LTE base stations are shown in Figure 17. The antenna's beam can be down-tilted by as much as -10 degrees below horizontal by mechanically adjusting the mount. Vertical tilt angles are adjusted with either a manual crank mechanism or else a remotely-controlled electric motor, depending on the site.

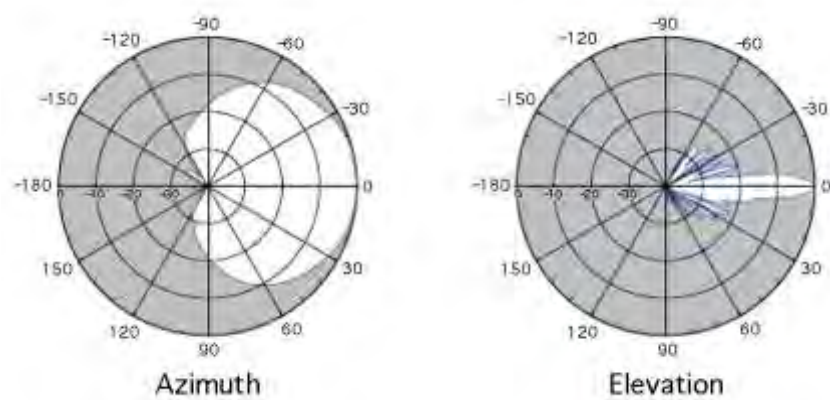


Figure 17. Antenna pattern of a typical WiMAX/LTE base station antenna, as measured by the manufacturer.

ITS engineers measured the antenna's frequency response at NTIA's Boulder, Colorado laboratory; the result is shown in Figure 18. The radiated-emission measurement was performed with the antenna's main beam boresighted on a suitcase measurement system. Figure 18 shows that across frequencies of 2500–2850 MHz the antenna's response is essentially flat, with just 3 dB of reduction occurring between 2850–3000 MHz. Thus the antenna's response across radar frequencies of 2700–3000 MHz will not significantly reduce the out-of-band (OOB) levels that would be coupled from WiMAX or LTE transmitters to radar receivers.

¹¹ Argus model number LLPX310R-V1, specified by the manufacturer as slant-polarized, +17 dBi gain, 65 degrees horizontal beamwidth, 7 degrees vertical beamwidth, front-to-back ratio in excess of 30 dB, rated for up to 250 watts input power.

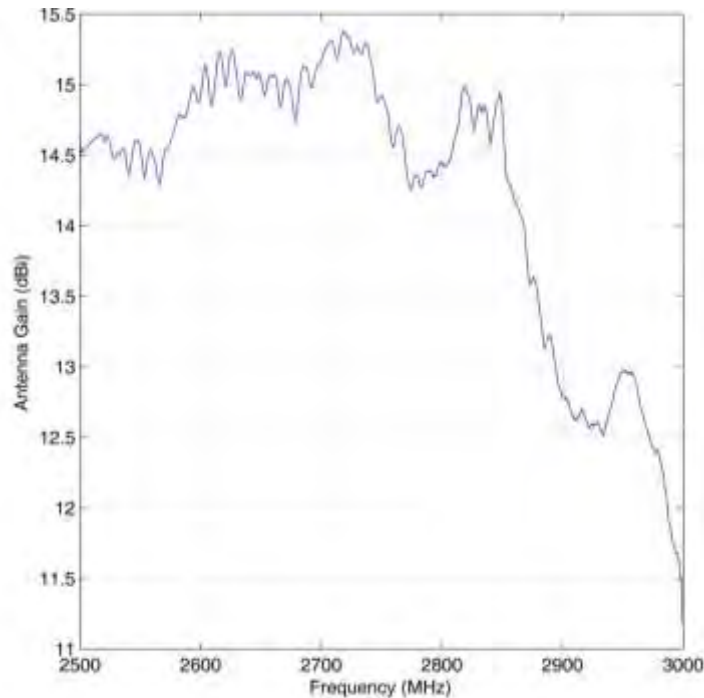


Figure 18. Measured frequency response of a typical WiMAX/LTE base station antenna.

3.4 Measured Technical Characteristics of Radiated WiMAX Signals

Prior to traveling to Grand Rapids and Jacksonville, and in order to obtain baseline technical characteristics of BRS/EBS base station transmitters against which the characteristics of interference signals from unidentified locations could later be compared for the purpose of signal identification, NTIA engineers performed detailed emission measurements on a BRS WiMAX system at Broomfield, Colorado. The measurements of radiated WiMAX emissions were performed with the 4th Generation NTIA Radio Spectrum Measurement System (RSMS-4G), as shown in Figure 19. The received signals were measured only for spectrum and time domain envelopes; they were not demodulated. The measured spectrum is shown in Figure 20; typical time domain envelopes are shown in Figures 21–22.

Figure 20 shows three signals, each 10 MHz wide,¹² that correspond to different azimuthal coverage sectors. The sector within which the measurement system was located shows the highest power level; the power levels for the other sectors appear lower because the measurement system was not located within the main-beam coverage sectors of those other two base station antennas. The spectrum shape is characterized by a rapid drop of about 45 dBc (from the desired emissions' power level to the beginning of the roll-off) to the beginning of the OOB

¹² Detailed examination of the nominal 10 MHz channel structure shows that each channel is actually composed of a pair of 5 MHz wide sub-channels. The orthogonal frequency division multiplexed (OFDM) WiMAX signal constellation consists of a large number of contiguous, narrow-band carriers, with a zero-amplitude carrier in the center; these render the appearance of two 5 MHz-wide sub-channels.

roll-off. On the low-frequency side, the OOB roll-off extends from -45 dBc to -67 dBc. Beyond that, the spurious emissions are suppressed to between approximately -67 dBc to -70 dBc. On the high-frequency side of the fundamental-frequency emissions, the OOB roll-off of the emission in the coverage sector of the measurement system is masked by the in-band, desired emissions of the other two coverage sectors. The spurious emissions of the lowest-frequency transmitter emerge, however, from the desired emissions of the other two sectors at 2655 MHz and, like those on the low-frequency side of the spectrum, remain at a plateau of about -68 dBc up to a frequency of 2700 MHz. The spurious emissions roll off above 2700 MHz but are still measurable above the measurement system noise floor at frequencies up to 2720 MHz.



Figure 19. NTIA RSMS during in situ BRS WiMAX measurements at Broomfield, Colorado.
Photo by author Sanders.

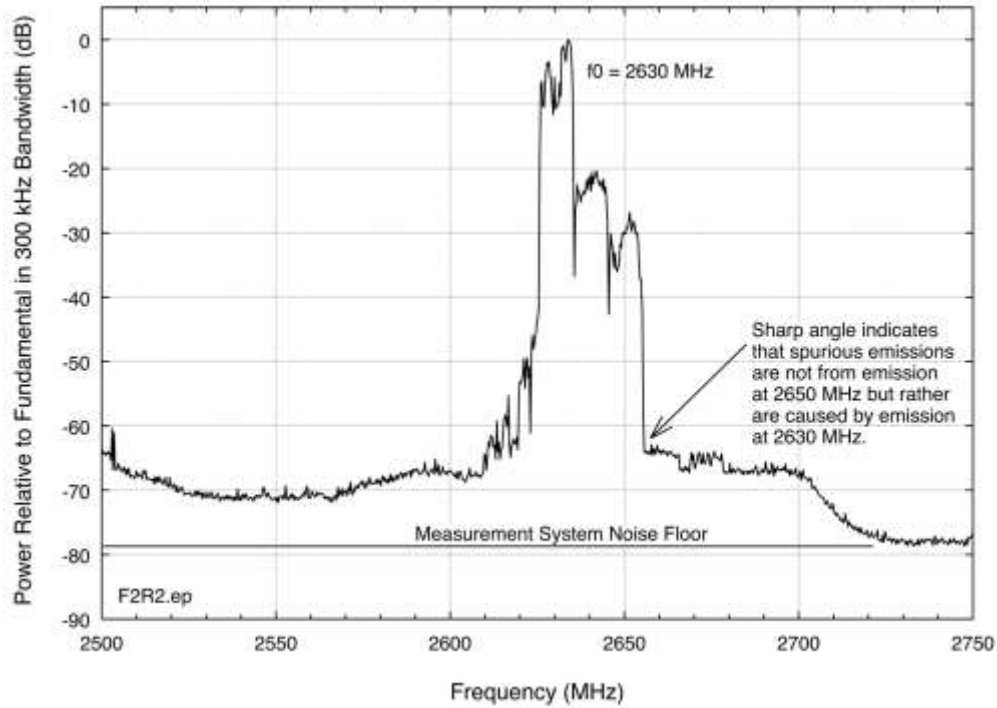


Figure 20. A BRS WiMAX base station emission spectrum measured in situ at a field location. Transmissions occur on paired BRS/EBS channels E1-E2 (strongest signal, aimed toward measurement location) and E3-F1 and F2-F3 (directed away from the measurement system).

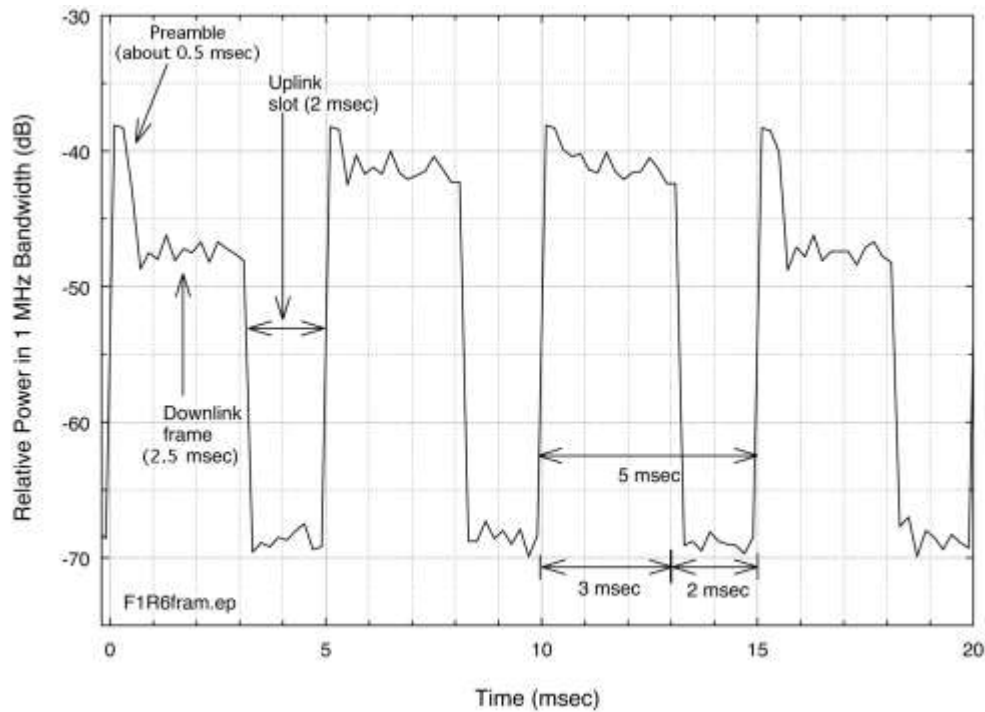


Figure 21. Measured time-domain characteristics of an operational BRS WiMAX base station signal. Preamble power is fixed while frame power levels vary.

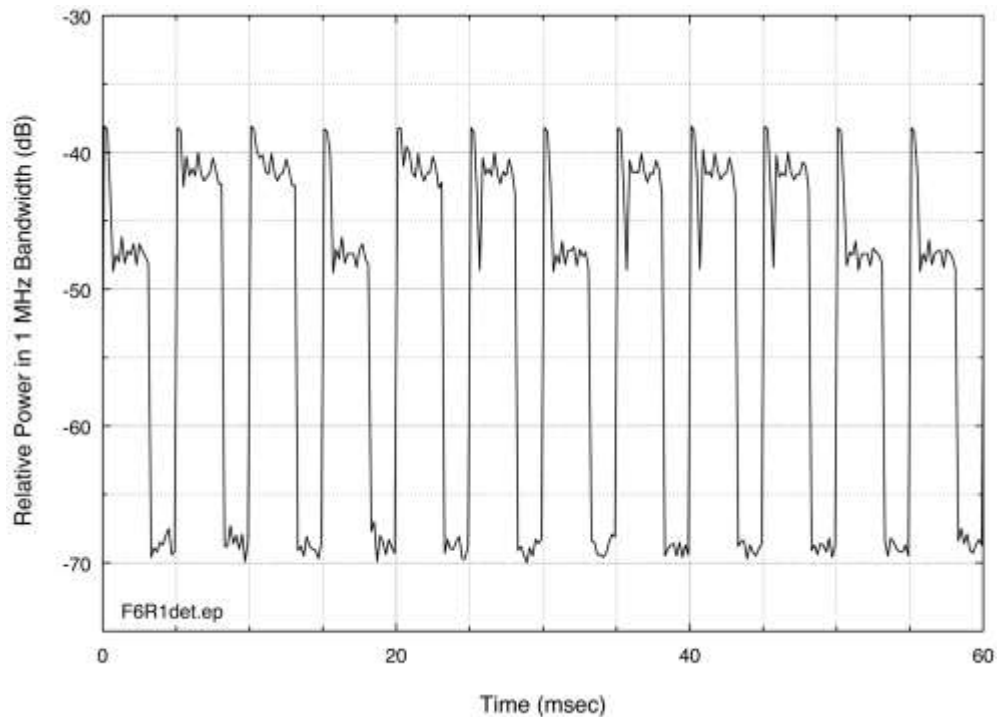


Figure 22. Example of time variation in amplitudes of operational BRS WiMAX base station frames. Preamble power is fixed while frame power levels vary.

In summary, the baseline emission spectrum data taken in Colorado show that a typical WiMAX emission consists of three contiguous fundamental-frequency emissions, each 10 MHz. These desired emissions will appear to vary in power from one to the next as result of the fact that a measurement system will always be located within the mainbeam coverage of one sector and will necessarily therefore be located within the sidelobe or backlobe coverage of the other sectors. The desired emissions drop rapidly to about -45 dBc at their edges, and then the spectrum roll-off will be more gradual from that point to a level where the emission levels plateau at -68 dBc, the spectrum width from the -45 dBc point to the -68 dBc point being on the order of 15–20 MHz.

In the time domain, the envelope emission measurements of Figures 21–22 show that the BRS WiMAX base station (downlink) signal is characterized by a periodic on-and-off sequence. The overall repetition interval is 5 ms, with the first 3 ms being occupied by the transmitted downlink signal and the following 2 ms being quiet (Figure 21) for reception of uplink signals from subscriber units. Each 3 ms downlink transmission interval consists of a preamble lasting approximately 0.5 ms followed by a data frame lasting 2.5 ms.

As shown in Figures 21–22, the amplitudes of the preambles are constant. But as shown in the same figures the amplitudes of the data frames can vary from one to the next by at least 8 dB. This observation has implications for the selection of optimal detection modes in measurements of radiated WiMAX emissions. Positive peak detection will yield consistent and repeatable power measurements of WiMAX signals since the constant-amplitude preambles will always be detected at a constant amplitude in this mode. In comparison, root-mean-square (RMS) average

detection results could vary somewhat depending on the extent to which the frame-data amplitudes might vary.

3.5 Radiated BRS WiMAX Power as a Function of Measurement Detection Mode and Bandwidth

When assessing interference effects in radar receivers, the incident power level, I , of interference signals needs to be compared to the average¹³ thermal noise level, N , of the receivers [14]. The gated¹⁴ average level of interference in the receivers is the relevant parameter for EMC studies for high duty cycle interference (above 1 percent, [14], pp. 85, 105–109, 132–137, and Appendices A and D), as found in WiMAX signals. Power received in WiMAX signals as a function of receiver bandwidth also needs to be known for such studies.

Since N is thermal noise with Gaussian characteristics, it has an approximately 10 dB difference between peak and average. Its power level varies in direct proportion to measurement bandwidth, resulting in a 10-log variation with bandwidth for decibel-unit measurements of N .

The levels of I as a function of detection mode and bandwidth were ascertained empirically for the operational, radiated BRS WiMAX signal at Broomfield, Colorado. The signal was measured with both peak and average detection in bandwidths of 100 kHz, 300 kHz, 1 MHz and 3 MHz; the results are shown in Figures 23 and 24.

The power levels measured for that signal at 2650 MHz in each detection mode and measurement bandwidth in Figures 23–24 are plotted in Figure 25. As read from Figure 23, both the peak and average power levels of BRS WiMAX signals vary in direct proportion to the measurement bandwidth, resulting in a 10-log rate of variation with bandwidth for decibel measurements. This happens to be identical to the rate of variation of thermal noise power with bandwidth (as occurs in radar receivers). The offset between the peak and average power levels of the WiMAX signal is observed to be 17 dB; it is independent of the measurement (and therefore receiver) bandwidth.

¹³ Unless otherwise noted, the term “average” in this report always refers to linear, root mean square (linear, or RMS) average power. For thermal noise RMS average power is 2 dB lower than log average.

¹⁴ “Gated” means average power *during* WiMAX preambles and frames, not the average across complete frame-to-frame cycles that would include about 40 percent down time.

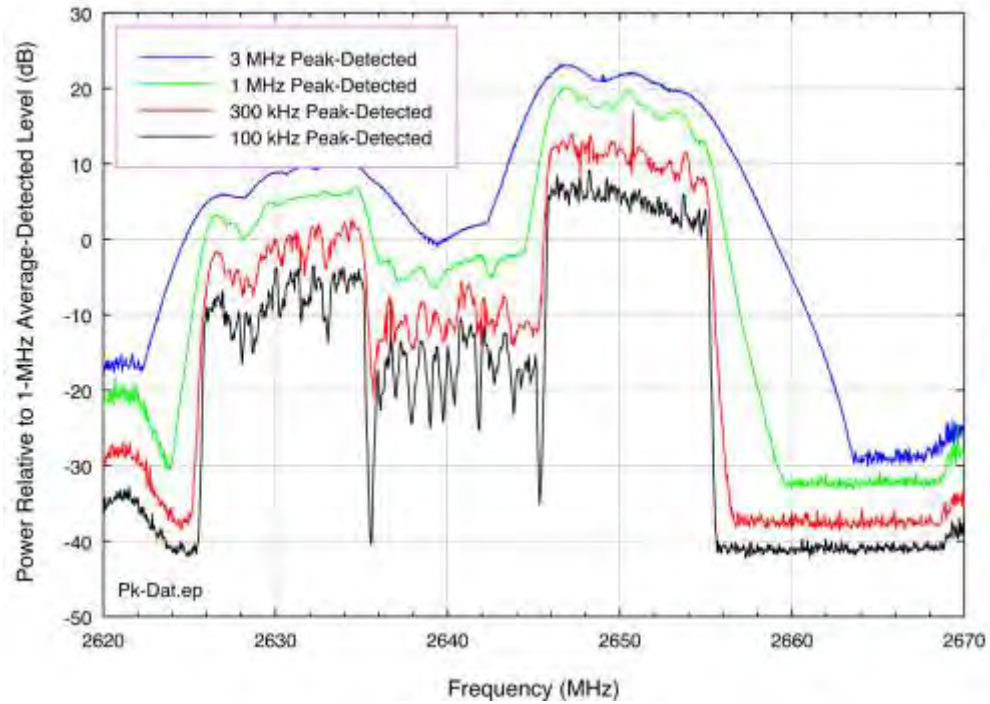


Figure 23. Peak-detected BRS WiMAX emissions in four measurement bandwidths.

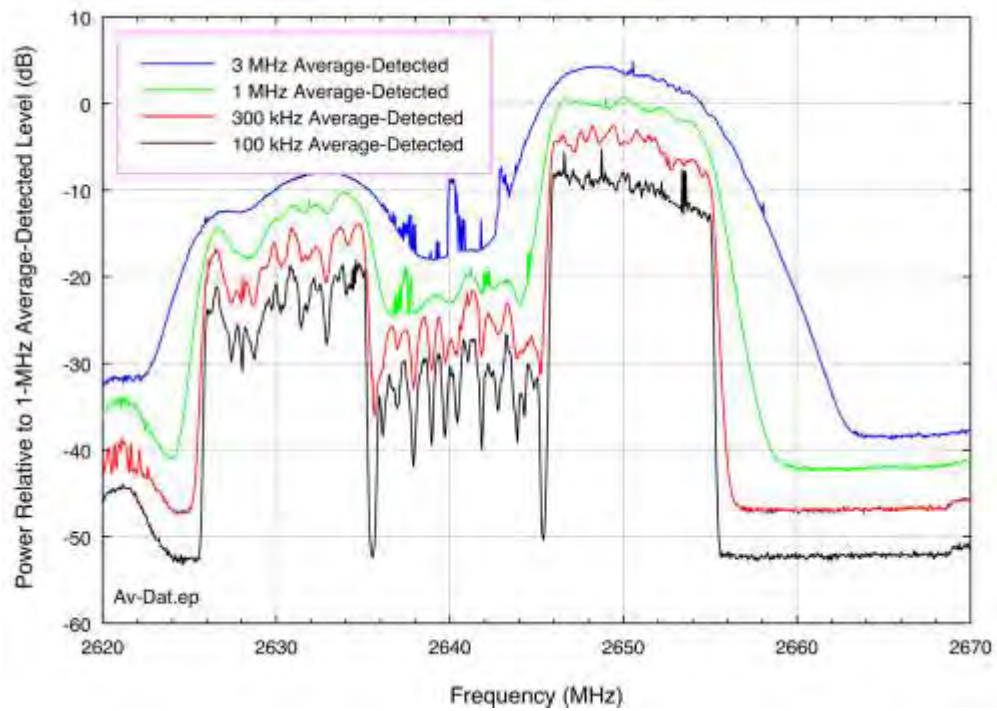


Figure 24. Average-detected BRS WiMAX emissions in four measurement bandwidths.

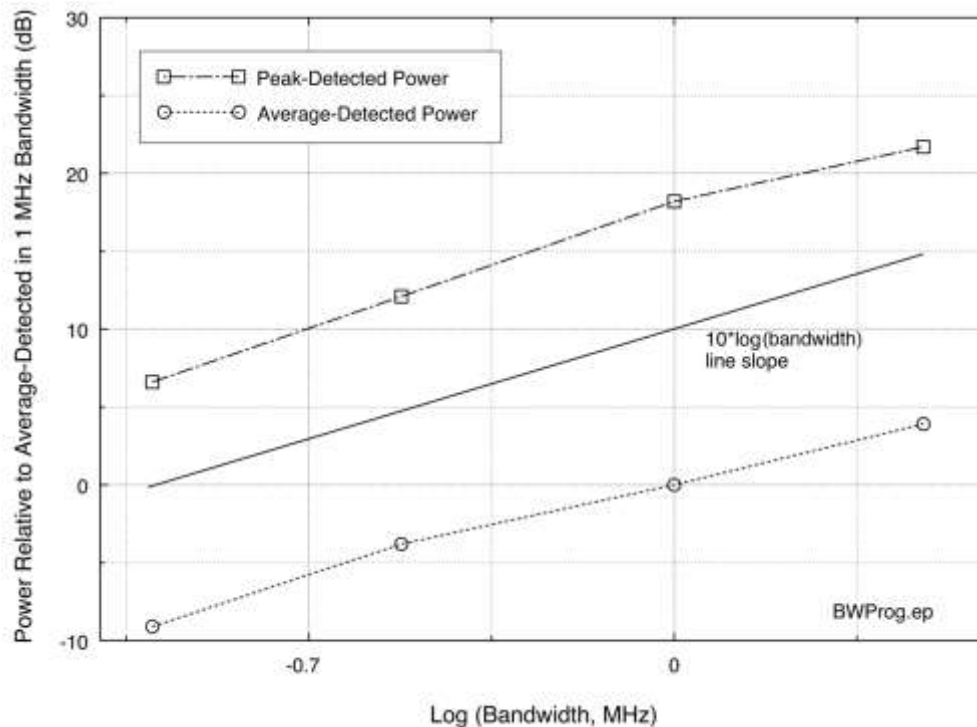


Figure 25. Relative on-frequency measured BRS WiMAX peak and average power levels, with variation in measurement bandwidth. Data points taken at 2650 MHz from the curves in Figures 23–24.

3.6 Unfiltered Hardline Coupled Measurements of BRS WiMAX Emission Spectra

BRS WiMAX OOB and spurious emission levels needed to be measured. Emission measurements can be obtained at field locations but may be best measured under controlled conditions in laboratory environments when possible. For this purpose, NTIA’s OSM staff contacted a BRS licensee in mid-2011 and requested assistance with the problem of measuring such radio emissions. The licensee responded by working with NTIA engineers from OSM and ITS on a series of emission spectrum measurements that were performed at the licensee’s facilities near Washington, DC, in August and October 2011. At the licensee’s facility, NTIA engineers set up a portable emission spectrum measurement system on a workbench inside an underground, shielded enclosure as shown in Figure 26.

NTIA performed an initial scan with the BRS WiMAX stations turned off, so as to observe and document the background spectrum environment inside the shielded room; no ambient signals were present in the band 2700–2900 MHz. Next, emission spectra were measured for three BRS WiMAX base station transmitters, each manufactured by a different company.

Each BRS WiMAX radio was operated by the service provider’s engineers in a typical field configuration at its normal output power level and with simulated communication traffic running on the highest-frequency channel in the band at 2683.5 MHz. A high-power attenuator in the shielded room (Figure 26) kept the WiMAX input power to the measurement system below

+10 dBm. Baseline measurements were performed with no supplemental filtering on the radio outputs as this unfiltered configuration is used by default by the service provider at field locations.

NTIA performed the spectrum measurements in 1 MHz and 100 kHz bandwidths with peak and average detection. NTIA engineers used a yttrium-iron-garnet (YIG) (Figure 26) off-tuning technique to minimize the effects of a dynamic range “coffin corner” effect that arises when the instantaneous dynamic range of a measurement system cannot overcome a rapid frequency-dependent change in spectrum power.

3.6.1 NTIA Hardline-Coupled BRS WiMAX Measurement System Set-Up

The NTIA measurement system consisted of an RF front end, a front-end controller, a spectrum analyzer, a vector signal analyzer (VSA), controller computers for the spectrum analyzer and the VSA, and associated miscellaneous RF cables and connectors (Figure 26). Although Figure 26 shows two possible WiMAX radios for schematic purposes, in fact any number of BRS/EBS WiMAX radio types could be measured at the facility.

The RF front end was a custom-built portable box containing a calibration noise diode, a tunable YIG microwave bandpass filter, and preamplifiers. A second box controlled this RF front-end box. All the units were operated under computer control as described in [16]; the stepped-frequency measurement technique described in [16] was used to obtain the data.

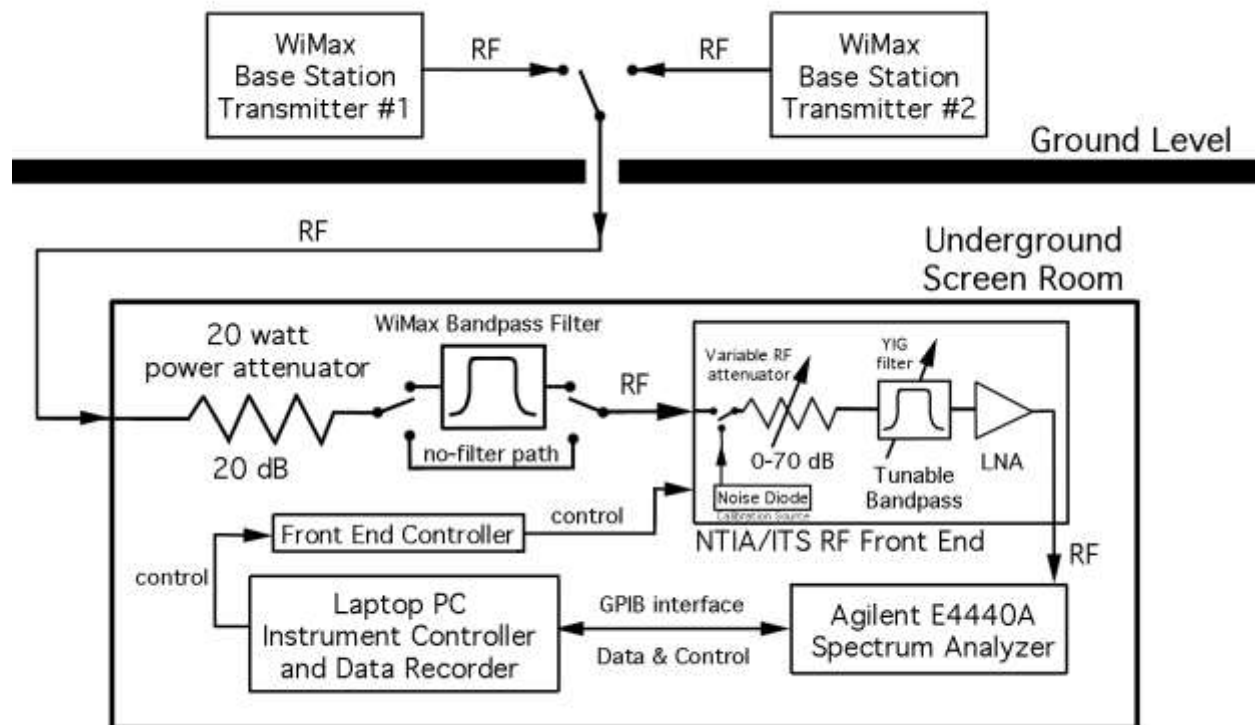


Figure 26. NTIA/ITS hardline-coupled BRS WiMAX spectrum measurement block diagram.

A goal of the spectrum measurements was to measure the unfiltered BRS WiMAX base station spectra with as much dynamic range as possible, and hence over the widest frequency range possible. The measurements ultimately achieved dynamic ranges of 91 to 96 dB.

3.6.2 BRS WiMAX Base Station Emission Spectra Without Output Filtering

As already noted, the baseline emission spectra of the BRS WiMAX base stations were measured without any output filtering installed, as the radios are normally deployed without supplemental filtering. Figures 28–30 show measured spectra for three types of WiMAX radio base stations produced by three separate manufacturers. In this report these are designated as WiMAX Radios 1, 2, and 3.

Each peak spectrum was measured in 1 MHz and 100 kHz bandwidths. This comparative measurement showed the extent to which the fundamental, OOB, and spurious WiMAX emissions vary as 10-log or 20-log of bandwidth as discussed in Appendix G of [14]. The data show that peak-detected WiMAX spectra vary as 10-log of bandwidth. Figure 30 shows the peak and average-detected spectra of Radio 2. The spectra of Radios 1 and 3 would look very similar. The offset between peak and average emissions is nearly constant across the fundamental, OOB, and spurious regions, running between 15 to 20 dB at all frequencies. This result is consistent with the radiated peak vs. average WiMAX data in Figures 23–25.

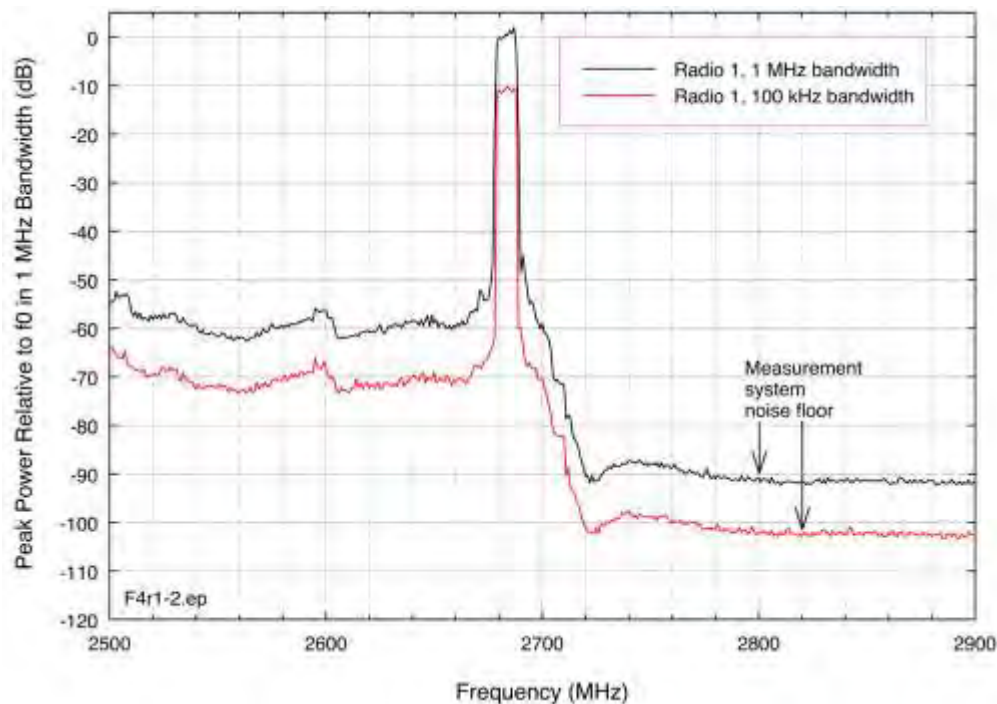


Figure 27. Peak-detected emission spectrum of WiMAX Radio 1.

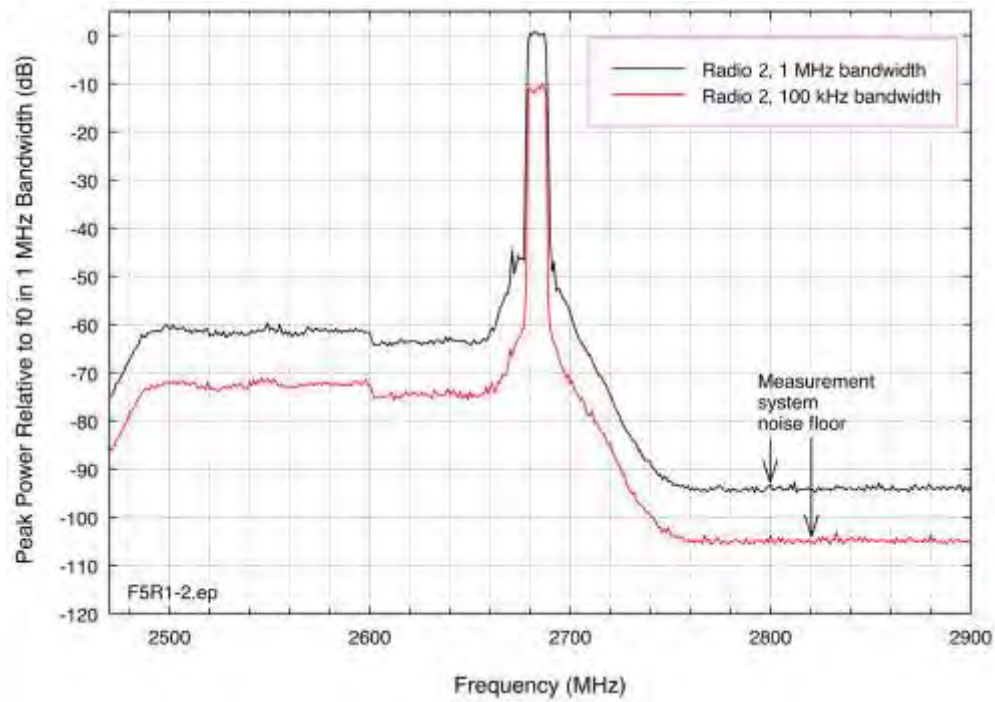


Figure 28. Peak-detected emission spectrum of WiMAX Radio 2.

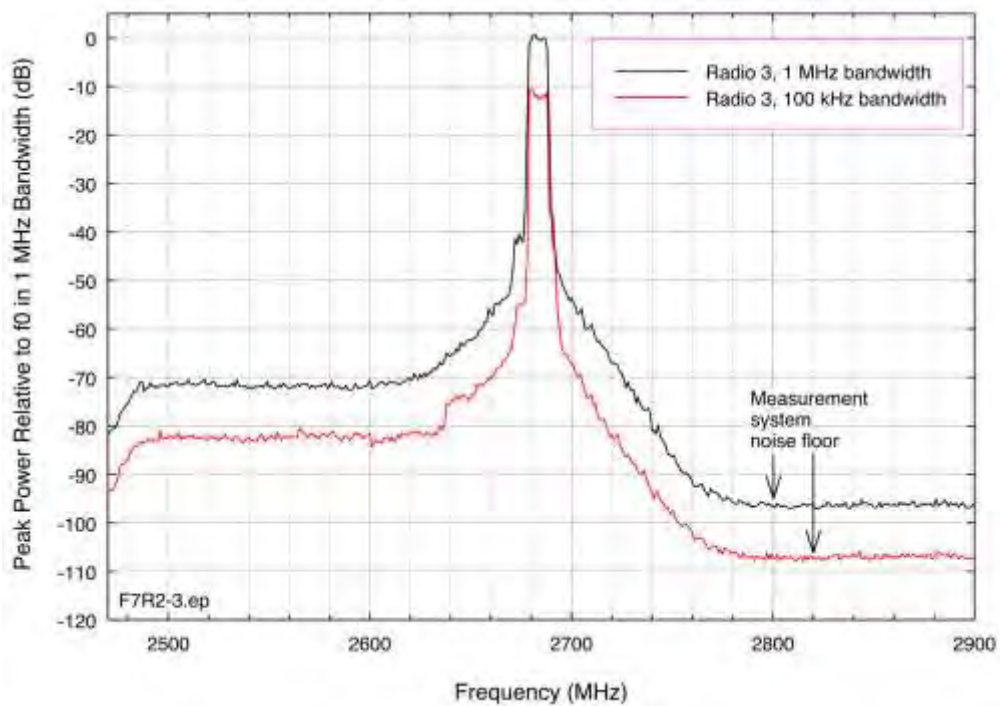


Figure 29. Peak-detected emission spectrum of WiMAX Radio 3.

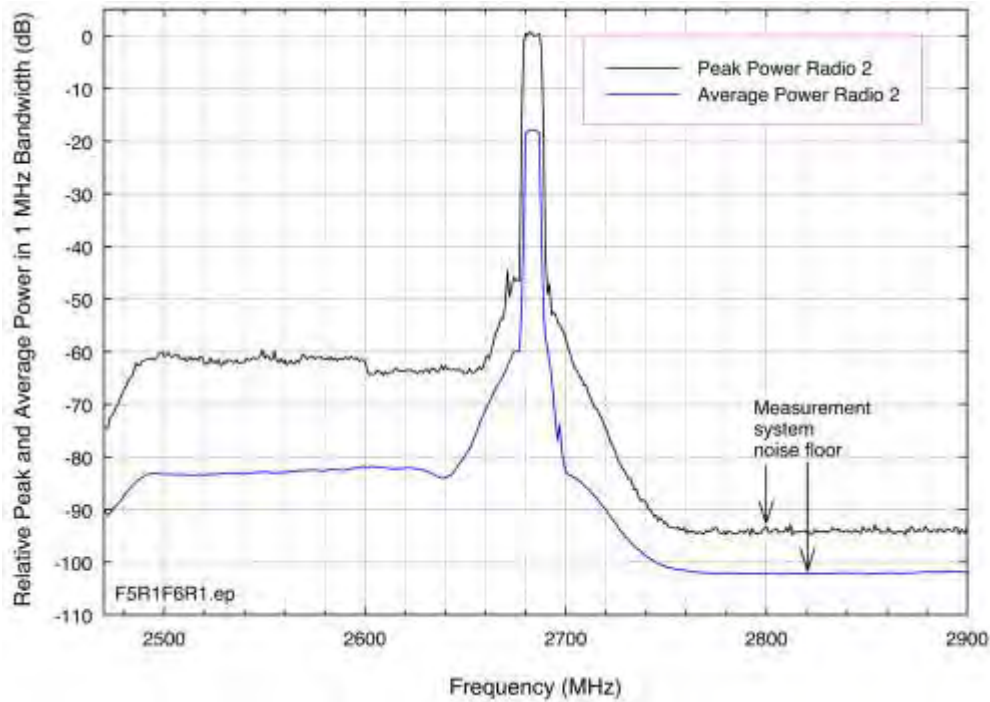


Figure 30. Comparative peak and average emission spectra of WiMAX Radio 2.

3.7 Summary of BRS/EBS Base Station Emission Characteristics

The BRS/EBS WiMAX base stations examined by the authors have used multi-sector sets of antennas on high towers, rooftops, and water tanks (typically 30 m AGL) to provide services to subscribers. BRS/EBS channel bandwidths are 5 MHz but operationally each azimuth sector typically occupies 10 MHz, made up of pairs of 5 MHz channels. Intentional radiation is transmitted on frequencies between 2496 MHz and 2690 MHz. In markets occupied by a BRS/EBS licensee who worked with the authors, frequency diversity is used at each station on a sector-dependent basis. Three frequencies are typically used per tower, one for each 120-degree coverage sector.

BRS/EBS WiMAX base station antennas have broad azimuthal patterns but narrow vertical patterns. Vertical antenna beam widths are on the order of 7 degrees and the vertical tilt angles of the antennas are adjustable; antenna tilt angles are usually set somewhat below horizontal to maximize coverage of subscribers. Antenna polarization is usually slanted at 45 degrees and antenna frequency response is nearly flat up to at least 3000 MHz, well above the lower radar band edge at 2700 MHz. Therefore antenna polarization and frequency response will probably not be useful for de-confliction of possible EMC problems from systems in other bands. Adjustment of antenna tilt angles, however, might be effective for this purpose.

BRS/EBS WiMAX base station downlink signals radiate with a 5 ms periodicity. In each 5 ms period the first 3 ms is used for a 0.5 ms preamble transmission followed immediately by a 2.5 ms data frame transmission. The last 2 ms is a quiet period for reception of subscriber uplink

data. The preamble amplitude is fixed but the data frame amplitudes vary by at least 8 dB on a frame-to-frame basis.

BRS/EBS WiMAX base station signal power varies as 10-log of measurement (or receiver) bandwidth across the fundamental, OOB, and spurious regions of emission spectra. Peak-detected spectrum measurements will yield consistent and repeatable results due to the fixed preamble amplitudes. Average-detected measurements of operational, radiated BRS/EBS WiMAX signals may be more problematic due to the variation in frame amplitudes. The offset between peak-detected and average-detected WiMAX emission spectra runs between 15 and 20 dB across the fundamental, OOB, and spurious regions. On the whole, 17 dB may be used as a best-fit number for the WiMAX peak-to-average offset.

The gated (not frame-to-frame) average level of interference in NEXRAD receivers is the relevant parameter for EMC studies for high duty cycle interference ([14], pp. 85, 105–109, 132–137, and Appendices A and D), as occurs in BRS/EBS WiMAX signals. NEXRAD receivers are designed to mitigate low duty cycle pulsed interference from other radars, not high duty cycle communication signals.

Unfiltered BRS/EBS WiMAX emission spectra measured with up to 96 dB of dynamic range show measurable OOB and spurious emissions at frequencies as high as 2760, 2780 and 2800 MHz for the three radio models that were measured for this report.

4 INTERFERENCE MEASUREMENTS AT NEXRAD FIELD LOCATIONS

4.1 NEXRAD Configuration for Measurement and Characterization of Interference Signals

In response to reported interference at NEXRAD field sites, NTIA, NWS Radar Operations Center (ROC), and FCC personnel performed an initial set of interference-assessment measurements at the Grand Rapids, Michigan, NEXRAD site. The purpose of the measurements was to identify the characteristics of the interference and to identify, if possible, the interference source(s).

The interference signals were measured and documented by performing measurements of their frequency domain and time domain characteristics at various points within the NEXRAD receiver, as shown schematically in Figure 31. An abbreviated set of these measurements (at one IF point and one RF point) was subsequently performed at the Jacksonville, Florida, NEXRAD station.¹⁵

Detailed procedures that were developed and followed during this study for interference assessments at NEXRAD stations are provided in Appendix A; they are summarized briefly here. Interference-assessment measurements were performed with the NEXRAD transmitter turned off; the radar was operated in a passive, receive-only mode. The radar antenna was initially scanned 360 degrees around the horizon to catalog and record all possible interference signals with both peak and average detection. The azimuthal catalog was created from spectrum analyzer data, the spectrum analyzer being operated in a zero-hertz span mode with a sweep time equal to the time required to rotate the NEXRAD antenna 360 degrees around the horizon. The spectrum analyzer bandwidth was adjusted to 1 MHz to replicate the processing bandwidth of the NEXRAD receiver. Peak detection showed impulsive activity, including signals from other radars in the area. Average detection eliminated impulsive, radar-like signals and showed only high duty signals such as produced by communication transmitters.

The NEXRAD antenna was then slewed to each individual azimuth where high duty cycle interference signals had been observed. The antenna elevation-tilt angle was adjusted to maximize the level of the interference at each azimuth. Interference was usually maximized at a 0.5-degree elevation angle, the lowest angle of the radar's regular conical scan.¹⁶

Detailed time-domain measurements of interference characteristics were then performed on each of those azimuths. Time domain measurements of the detected envelope of the interference signal were performed with a spectrum analyzer that was operated in a zero-hertz span mode. Data were recorded via a laptop PC connected to the spectrum analyzer.

¹⁵ Characterization of the NEXRAD receiver at Jacksonville would have been redundant to the work done previously at Grand Rapids.

¹⁶ NEXRAD antennas can be down-tilted to zero degrees and even to angles below horizontal, but such tilt angles are not commonly used operationally.

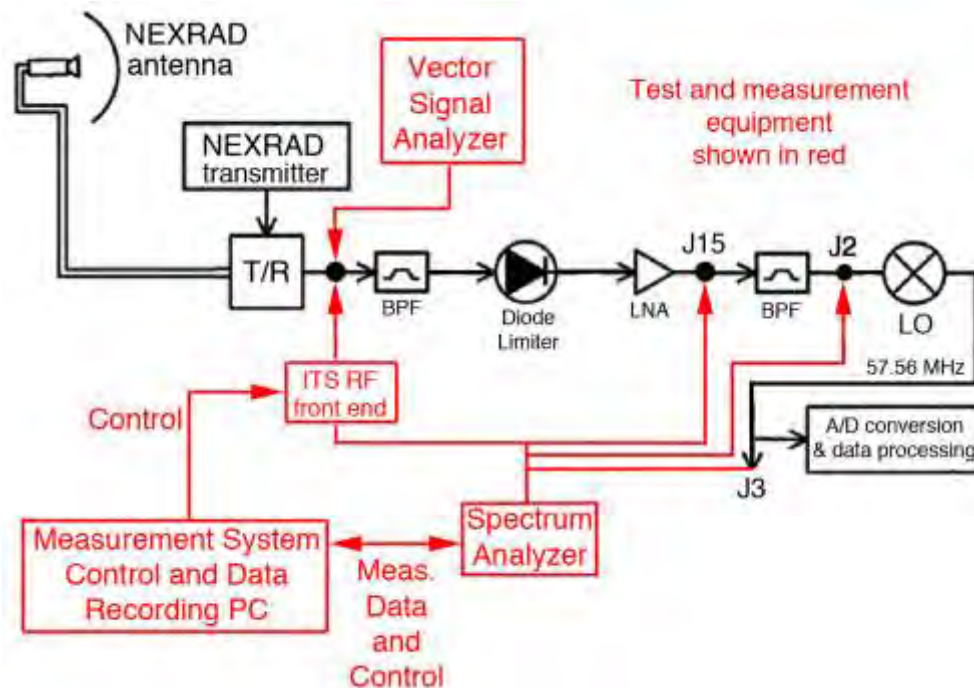


Figure 31. Schematic block diagram for NEXRAD interference-documentation measurements at Grand Rapids; at Jacksonville the measurements were only performed at J3 and J15.

4.2 Interference Azimuth-Scan Results

The results of the Grand Rapids 360° peak and average scanning are shown in Figure 32. Although some impulsive energy occurred on some azimuths (as evidenced by its appearance on the peak-detected scan but not on the average-detected scan), such emissions are unlikely to cause interference to the NEXRAD receiver due to their low duty cycle, as described and documented in [13]. Three azimuths (determined to be four after close examination) exhibited high levels on both the peak and average scans. These occurred on azimuths where interference strobos had been noted in the radar data (Figures 2–4). *It is important to note that the noise floors in Figure 32 are those of the radar receiver, not the measurement system.* Thus the interference-to-noise (I/N) ratios that are observed in this figure are the I/N ratios of the interference in the radar receiver.

A detailed azimuth-scan observation was performed on each of the interference azimuths that were identified in Figure 32. The result is shown in Figure 32. In this figure, the exact azimuths of two of the interference lobes are established as being at 289.4° and 304.8°. The central lobe, which showed some complexity in its structure, was examined more closely, with the result shown in Figure 34. It was resolved into two separate azimuths at 294.6° and 296.0°. Similarly detailed sets of individual azimuth scans were performed at Jacksonville.

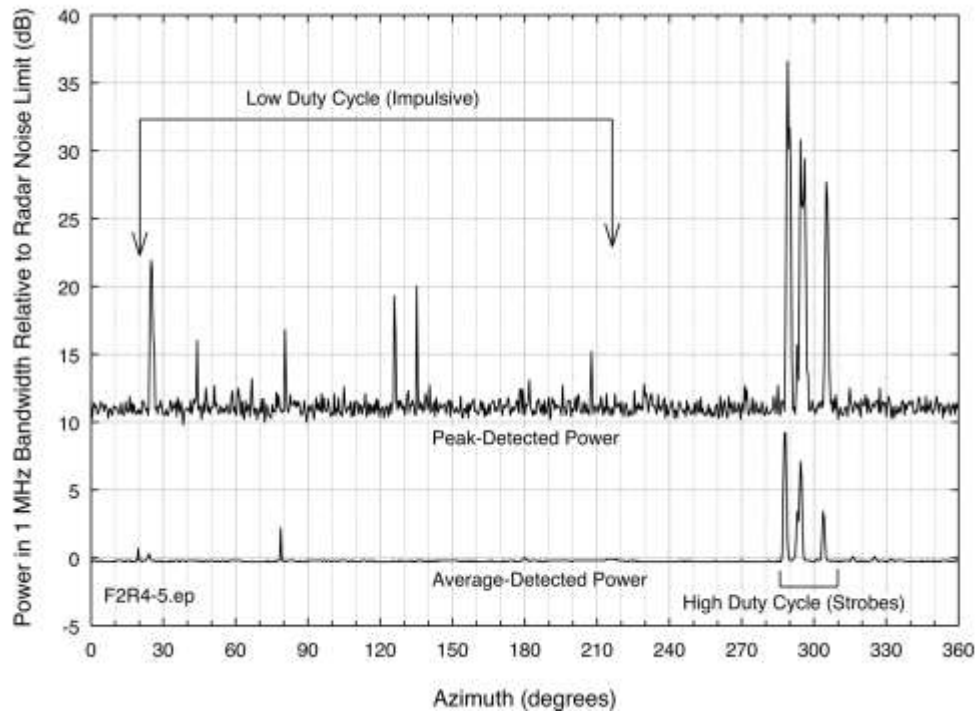


Figure 32. 360-degree interference scan through the Grand Rapids NEXRAD antenna. The same 360-degree scan procedure was performed at Jacksonville.

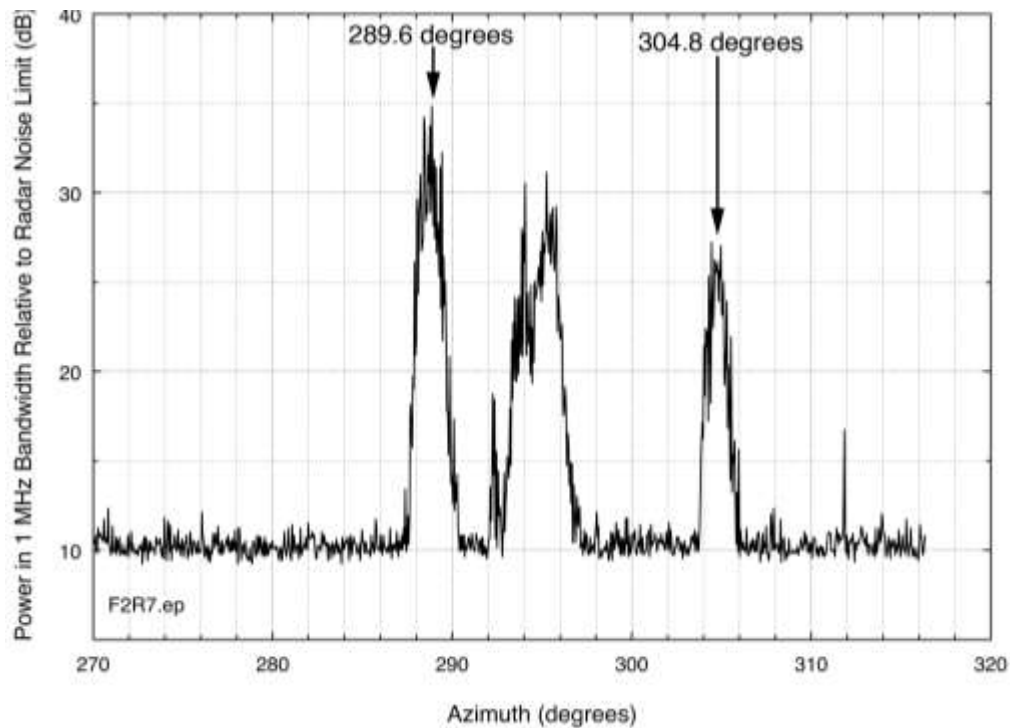


Figure 33. Detailed azimuth scan on interference lobes. The noise floor is that of the radar, peak-detected. (The radar average noise floor limit is 10 dB lower.) The middle lobe between 289.4° and 304.8° has a complex structure described in Figure 34.

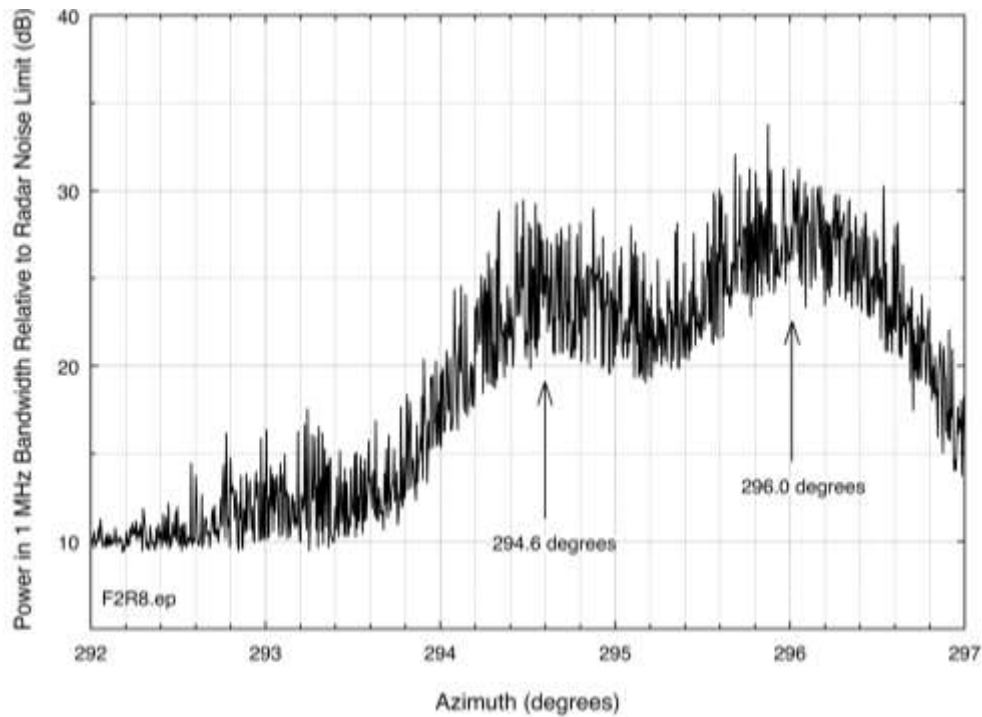


Figure 34. Detailed azimuth scan on the central interference lobe of Figure 33. At this scale, the central lobe resolves into two interference azimuths, at 294.6° and 296.0°.

4.3 Elevation-Scan Results for the Interference Signals

On each of the interference azimuths at Grand Rapids, the NEXRAD antenna was scanned in elevation from 0° to +20°, to ascertain the range of elevations through which the interference is occurring. The results are shown in Figures 35–38. At Jacksonville all measurements were performed at an elevation angle of +0.5°.

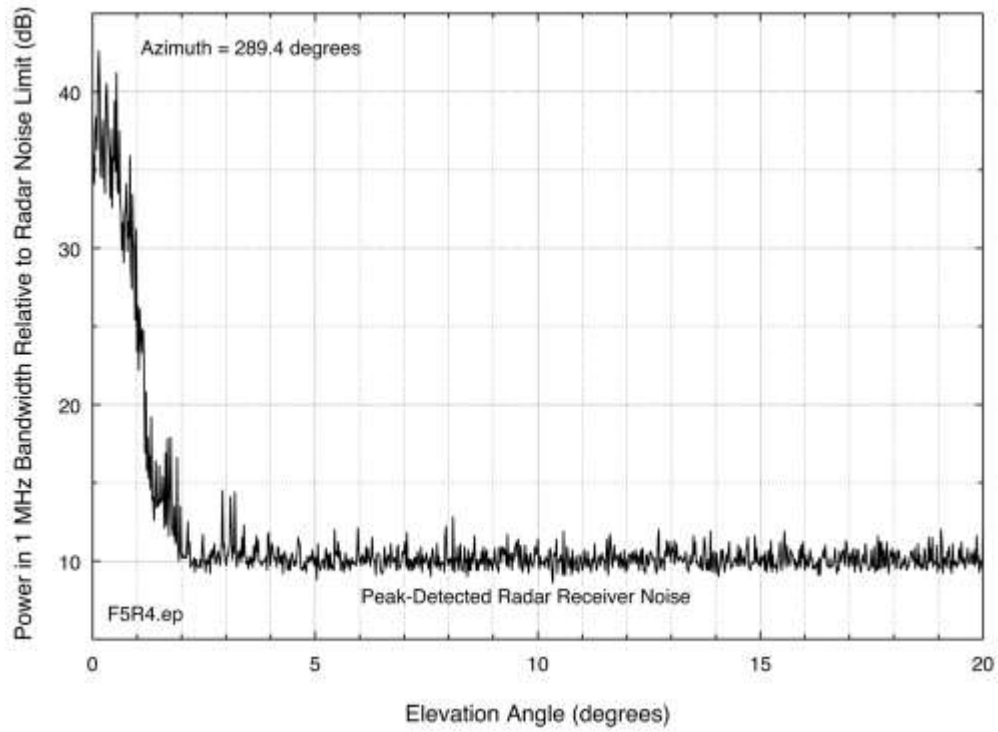


Figure 35. Elevation scan at 289.4° azimuth. The interference is measurable up to +2°.

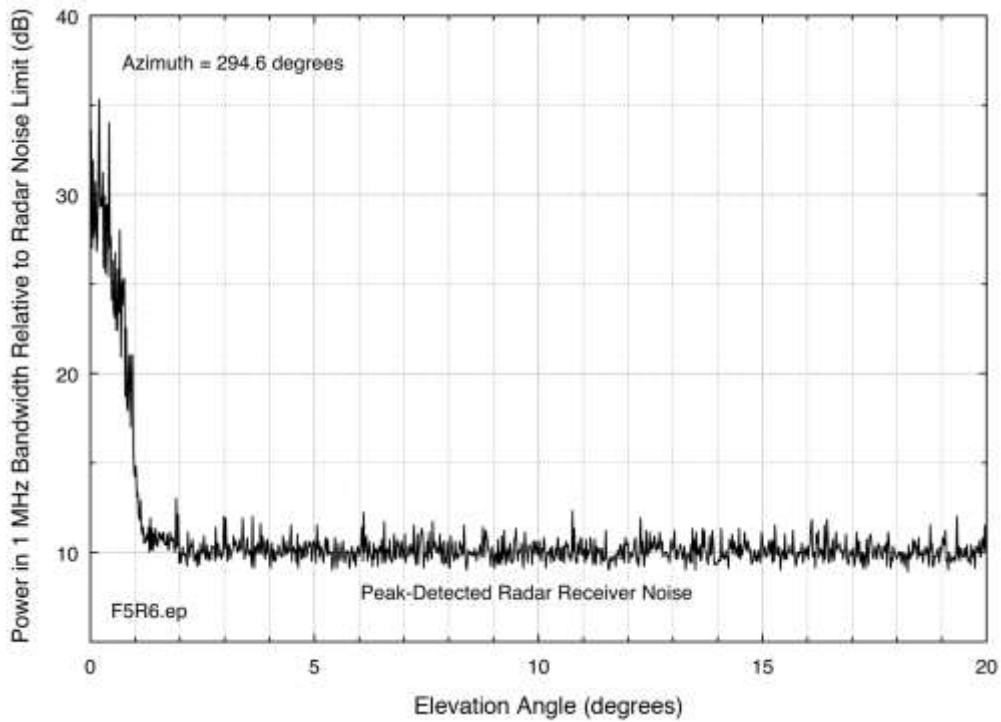


Figure 36. Elevation scan at 294.6° azimuth. The interference is measurable up to +1.5°.

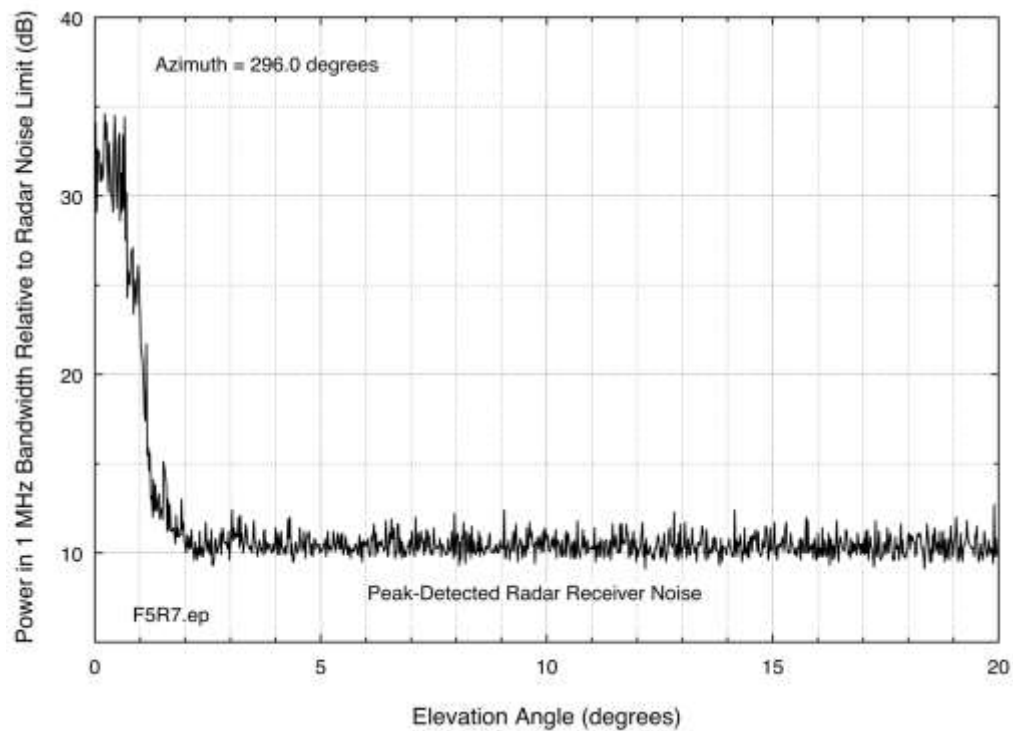


Figure 37. Elevation scan at 296.0° azimuth. The interference is measurable up to +2°.

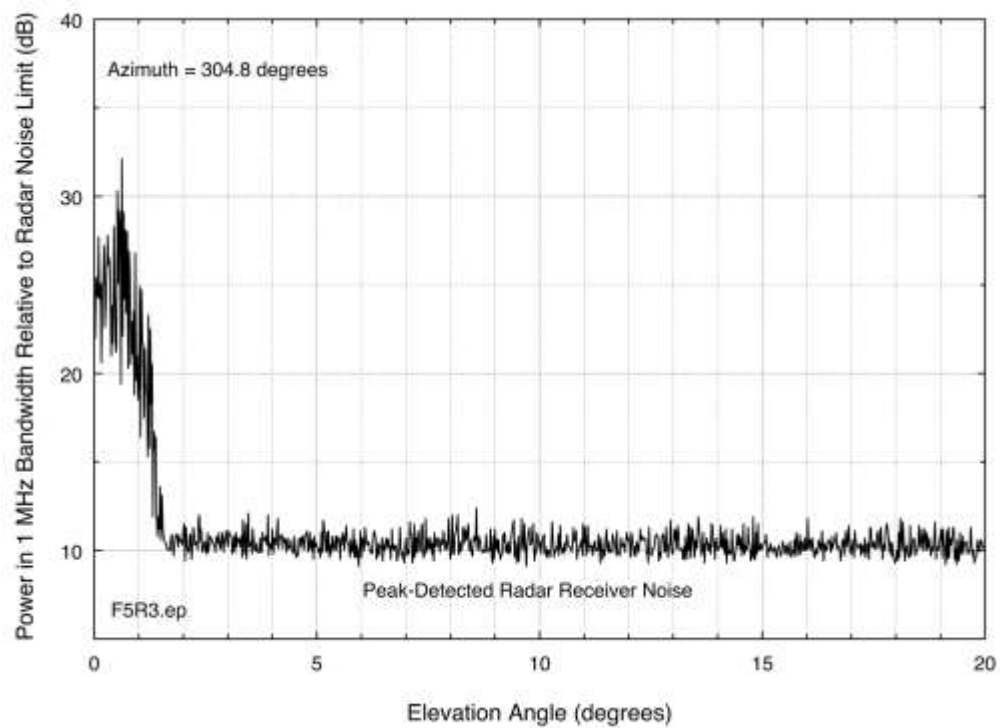


Figure 38. Elevation scan at 304.8° azimuth. The interference is measurable up to +1.5°.

4.4 Measurements of the Interference Time Domain Envelopes

Time domain scans were performed on each of the four interference azimuths (289.4° , 294.6° , 296.0° , and 304.8°) at Grand Rapids. The same signal modulation, that of WiMAX (as earlier baselined, Figures 21–22), was observed on all four azimuths. Figure 39 shows an example of the observed interference modulation on the strongest interference azimuth at 289.4° .

Comparing this to the baseline BRS/EBS WiMAX measurement data of Figures 21–22, this modulation, with an overall 5 ms periodicity consisting of 3 ms on and 2 ms off, is consistent with WiMAX signal modulation. All interference azimuths at Grand Rapids and Jacksonville showed the same WiMAX-consistent signal structure. Figure 40 and Appendix B show time-domain interference envelopes for signals at Jacksonville. In all cases the interference characteristics were consistent with BRS/EBS WiMAX signals.

The time-domain envelopes of Figures 39–40 and Appendix B generally lack the well-defined preambles and well-formed frames seen in Figures 21–22. This can be explained as being due to the fact that the interference signals were observed on NEXRAD frequencies, well above the center-tuned frequencies of the stations that were transmitting them. Due to an off-tuning effect called the rabbit ears phenomenon [17], pulses measured with systems that do not convolve the pulses' fundamental-frequency energy will show a different envelope than they do when measured on their fundamental frequencies, while leaving the observed the pulse widths unchanged. The data of Figures 39–40 and Appendix B are consistent with this off-tuning effect.

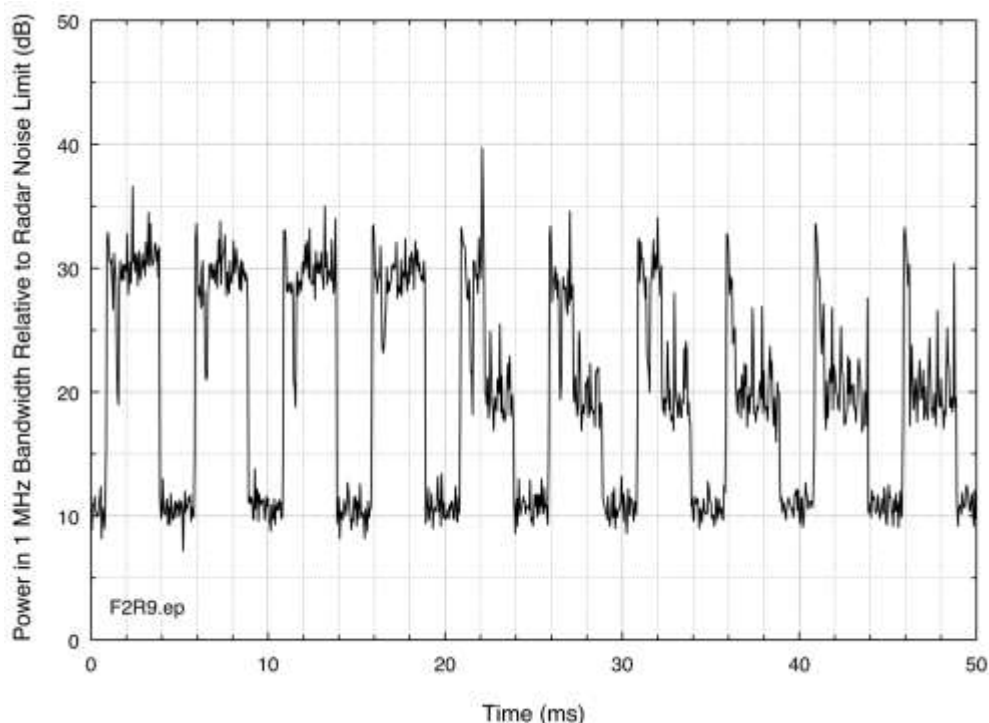


Figure 39. Example of the interference time-domain envelope that was observed in the Grand Rapids NEXRAD receiver on all four interference azimuths. Note intentional time-dependent variation in frame power. Irregular envelopes are explained in Section 4.6.3.

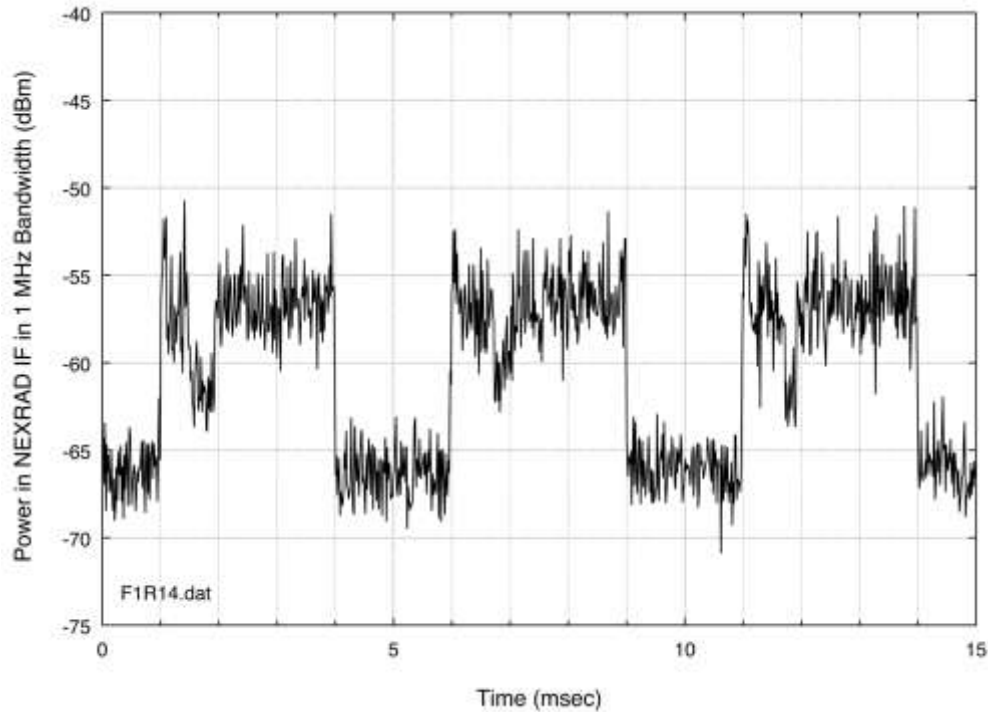


Figure 40. Example of interference signal at Jacksonville at 84.5° azimuth. Eleven other azimuths at Jacksonville showed the same BRS/EBS WiMAX signature (see Appendix B).

4.5 Spectrum Measurements of the Interference through the NEXRAD Antennas

On each of the interference azimuths at Grand Rapids and Jacksonville, the spectra of the interference signals were measured through the NEXRAD dish, ahead of its RF front-end bandpass filter. The results are shown in Figures 41–46.

In these figures, the observed interference signals have the spectrum characteristics of BRS/EBS WiMAX base stations (see the spectra of Section 3). OOB emissions of signals with WiMAX characteristics were observed on the frequencies of the Grand Rapids and Jacksonville NEXRADs (2710 and 2705 MHz, respectively). The spurious emission plateau that is characteristic of BRS/EBS WiMAX base station signals (see Section 3) is observed on the low-frequency side of the WiMAX emissions in Figures 41–46, but on the high-frequency side of those emissions the spectra at Grand Rapids extend to lower power levels.

Eventually all of the interference azimuths identified at Grand Rapids and Jacksonville were exactly correlated with operational BRS base stations, confirming that the interference was caused by BRS station operations. However, the interference mechanism remained to be determined.

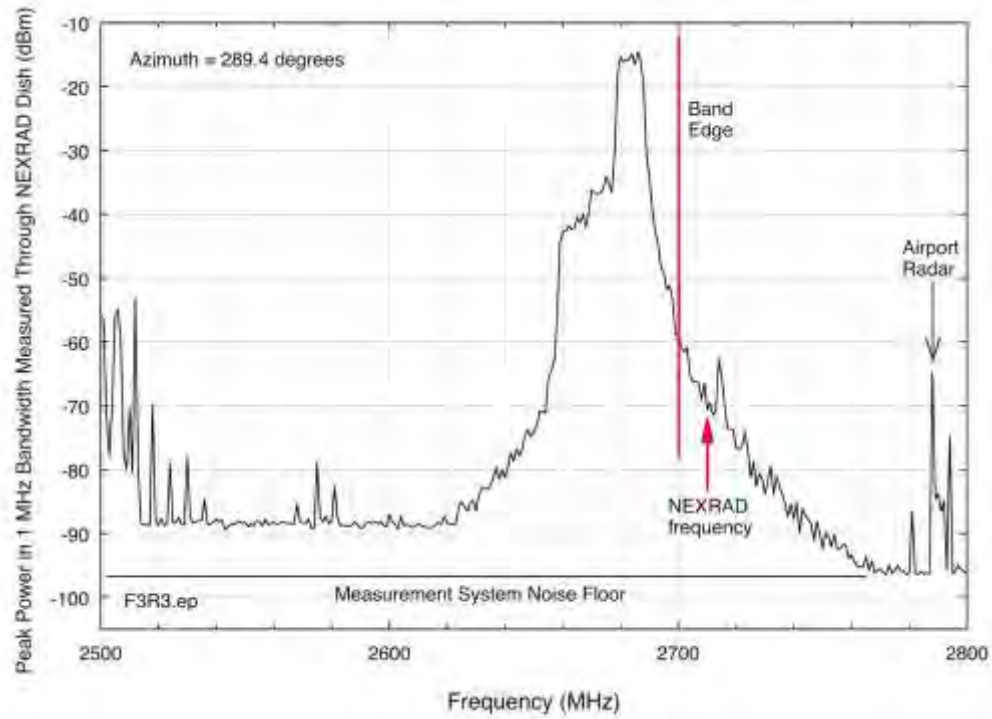


Figure 41. BRS/EBS WiMAX interference signal at Grand Rapids measured through the NEXRAD antenna on an azimuth of 289.4°.

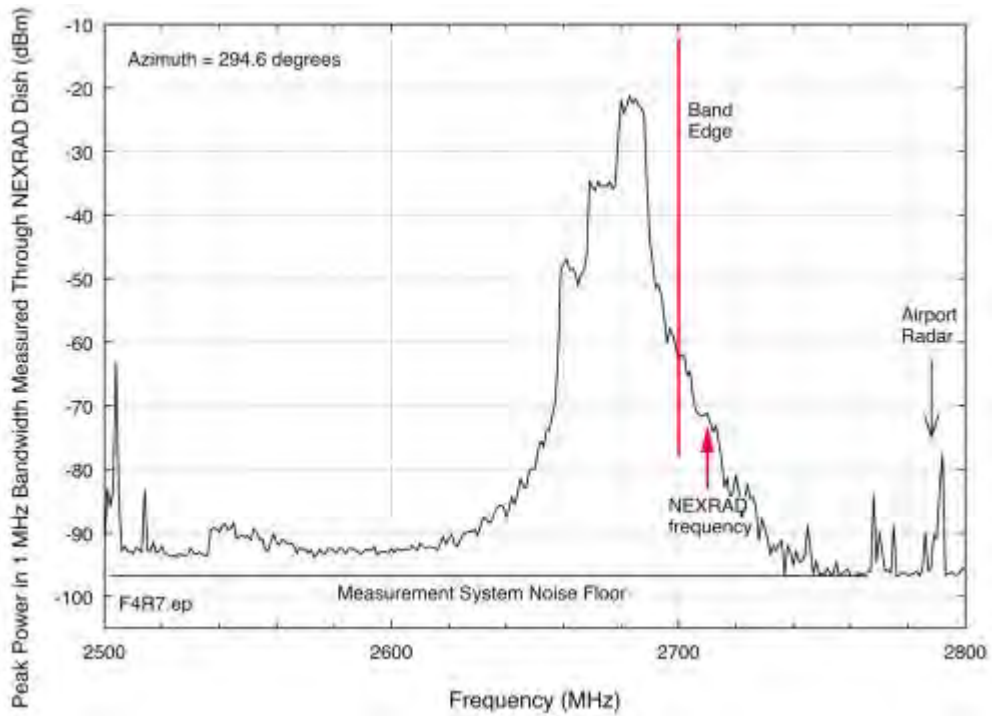


Figure 42. BRS/EBS WiMAX interference signal at Grand Rapids measured through the NEXRAD antenna on an azimuth of 294.6°.

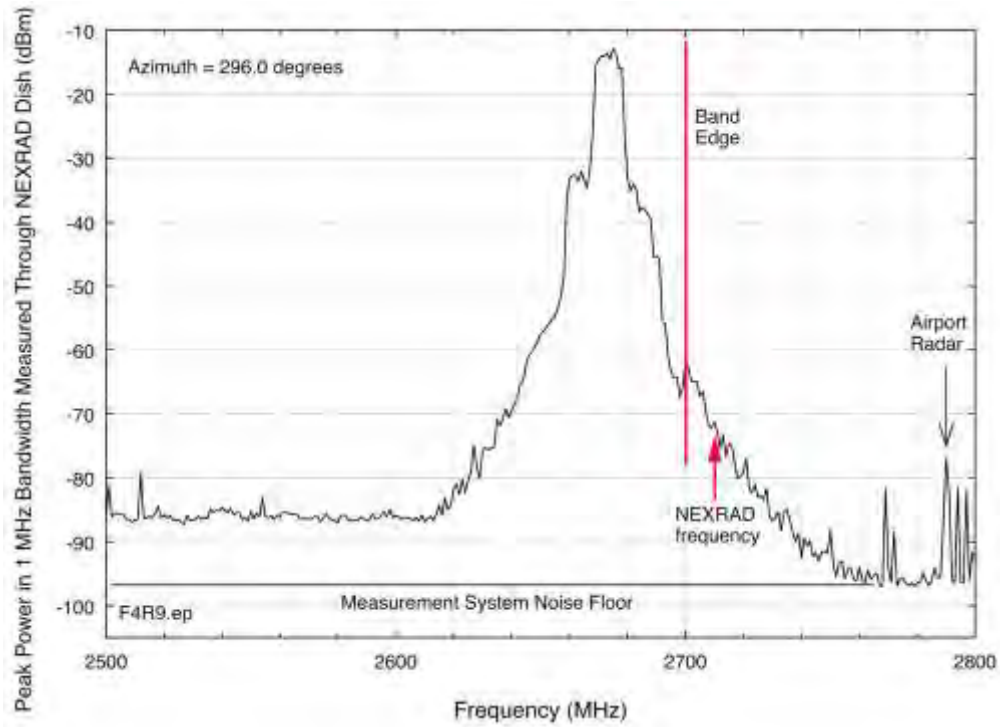


Figure 43. BRS/EBS WiMAX interference signal at Grand Rapids measured through the NEXRAD antenna on an azimuth of 296.0°.

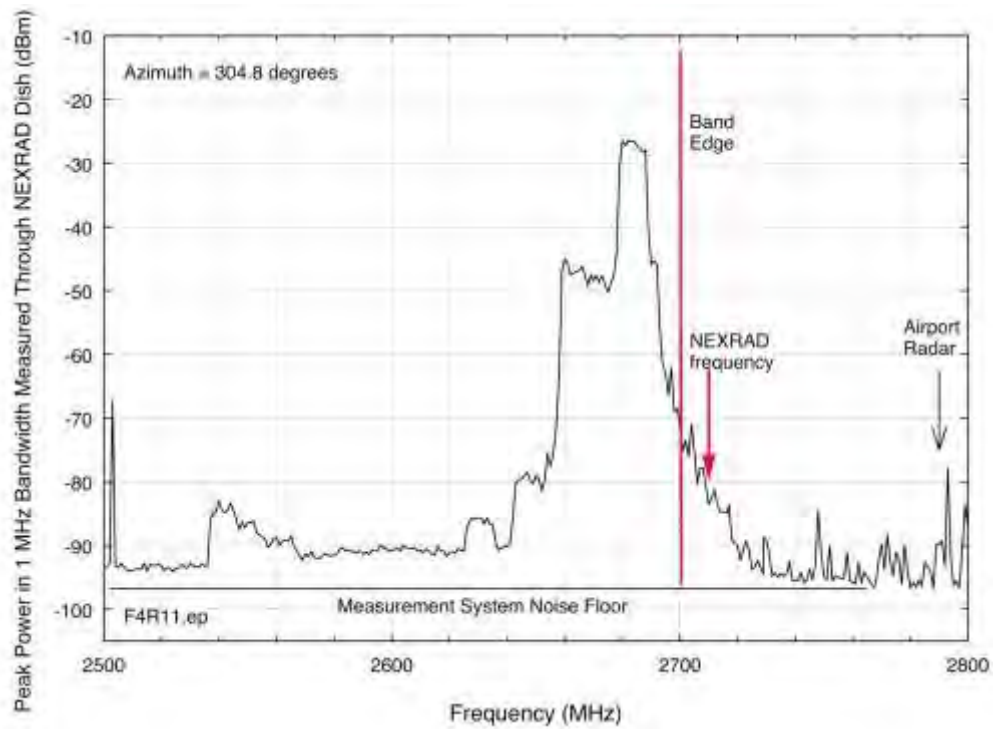


Figure 44. BRS/EBS WiMAX interference signal at Grand Rapids measured through the NEXRAD antenna on an azimuth of 289.4°.

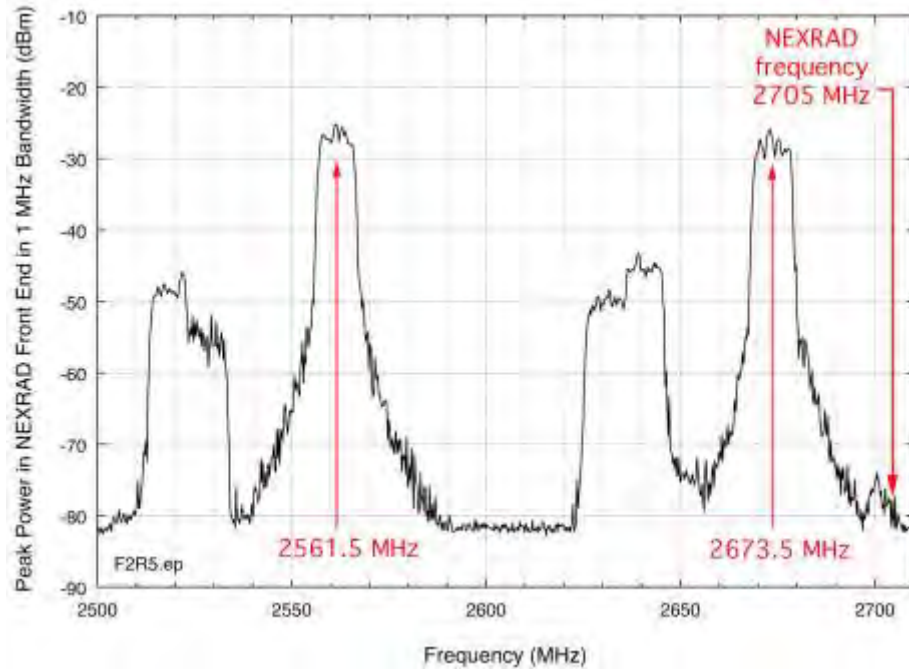
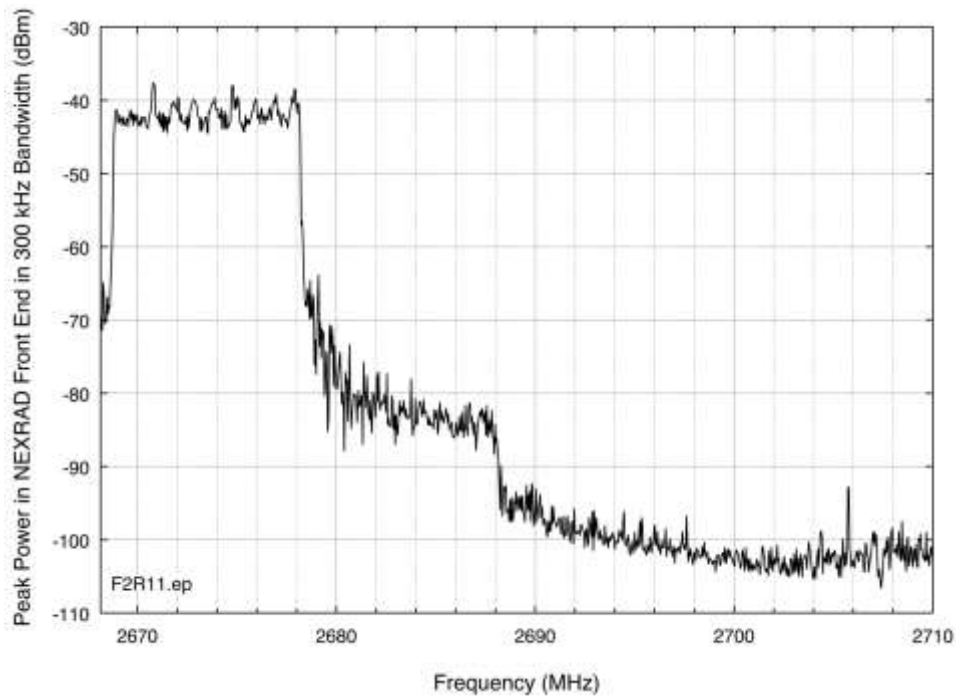


Figure 45. BRS/EBS WiMAX interference signals at Jacksonville measured through the NEXRAD antenna on an azimuth of 84.5°.



Emissions from a BRS/EBS WiMAX base station transmitter at Jacksonville at 84.5°, measured across NEXRAD frequency of 2705 MHz. Measurement was performed in 300 kHz to show additional spectrum details. Channels G3-H1 are directed toward the measurement location; the next-higher channels H2-H3 are also occupied but are not aimed at the measurement location.

4.6 Identification of the Interference Mechanism

Two possibilities existed for the interference mechanism: front-end RF overload of the radar front-end low-noise amplifier or out-of-band BRS/EBS WiMAX emissions that are co-channel with the radar frequency. These possibilities were not mutually exclusive; although typically only one or the other occurs for receivers in general, both can occur simultaneously. Therefore it was necessary to positively identify or exclude each of these interference mechanisms.

4.6.1 Front-End Overload Condition

Front-end overload occurs when the LNA in a receiver RF front end is not adequately protected (de-coupled) from high-power out-of-band energy by a front-end bandpass filter between the receiver antenna and the LNA's input. Conversely, the presence of a front-end bandpass filter in front of an LNA in a receiver should automatically prevent the possibility of front-end overload of a receiver's LNA [18]. This means that, based on the receiver-characteristics data that NTIA has collected for NEXRADs and ASRs (as described in Section 2 and Appendix C of this report) the NEXRAD and ASR-9 receivers should be immune to front-end overload from out-of-band (2496–2690 MHz) BRS/EBS fundamental-frequency energy. The ASR-8 and ASR-11 receivers could be vulnerable to this problem due to either their lack of front-end bandpass filtering (for the ASR-8) or very wide front-end bandpass filter bandwidth (for the ASR-11).

4.6.2 Appearance of Front-End Overload Responses in the Time Domain

It is possible to directly demonstrate from measurement data that front-end overload is or is not occurring, the approach being to carefully observe the characteristics of the victim receiver's noise floor in the time domain when an interference signal is present. Because front-end overload causes a decrease in the gain of the LNA whenever the interference signal is present, and because there is a non-zero interval required for the gain of the LNA to recover to its normal level after the interference signal (a pulse, in the case of WiMAX emissions) ceases, front-end overload will manifest itself in the time domain as a dip in the victim receiver noise floor in the time interval immediately after the end of each interference pulse. This overload response artifact is shown for an actual LNA output, measured under controlled conditions, at the top of Figure 47. For the WiMAX pulses that have been observed in the NEXRAD receivers at Grand Rapids and Jacksonville, the corresponding deep, sharp dip that would be expected to occur after each WiMAX pulse has been sketched schematically in red on the data from Figure 40, as reproduced at the bottom of Figure 47. The *lack* of such dips after each WiMAX pulse in the actual NEXRAD time domain receiver data (as in the data of Figures 39–40) provides a positive demonstration that the BRS/EBS WiMAX interference mechanism in NEXRAD receivers is *not* front-end overload.

4.6.3 Appearance of OOB Emissions in the Time Domain (Rabbit Ears)

As noted above, when pulsed energy is observed in the time domain on frequencies that do not include its fundamental frequency, the pulse shapes no longer look the same as at the fundamental [17]. Instead, on some OOB frequencies the centers of the pulses drop in amplitude

relative to the pulse edges. The occurrence of this so-called rabbit ears effect (which sometimes only shows prominent rising edges) is therefore an indication that OOB energy is being observed. Many of the BRS WiMAX measurements in Grand Rapids and Jacksonville show the rabbit ears effect, which is seen in Figures 39–40 and is exhibited most strongly in Figures B-4 and B-11. The occurrence of rabbit ears is another indication that the interference is due to OOB emissions from WiMAX transmitters.

4.6.4 Additional Proposed Tests for Front-End Overload

Two additional tests for front-end overload might be performed between NEXRAD receivers and BRS/ERBS base stations. One of these tests would be to observe the power level of interference in the NEXRAD receiver while the output power of the interfering BRS/EBS base station is reduced by some known amount of power. If the power reduction at the BRS/EBS base station is X dB, then a reduction of X dB in the observed interference level would indicate that front-end overload is *not* the cause, because front-end overload is a non-linear effect. Unfortunately, since the levels of OOB emissions produced by a power amplifier do not necessarily change linearly with total amplifier power output, a non-linear response could also be consistent with OOB emissions as the source of the interference. A power-reduction test of the base station transmitter would therefore tend to be inconclusive.

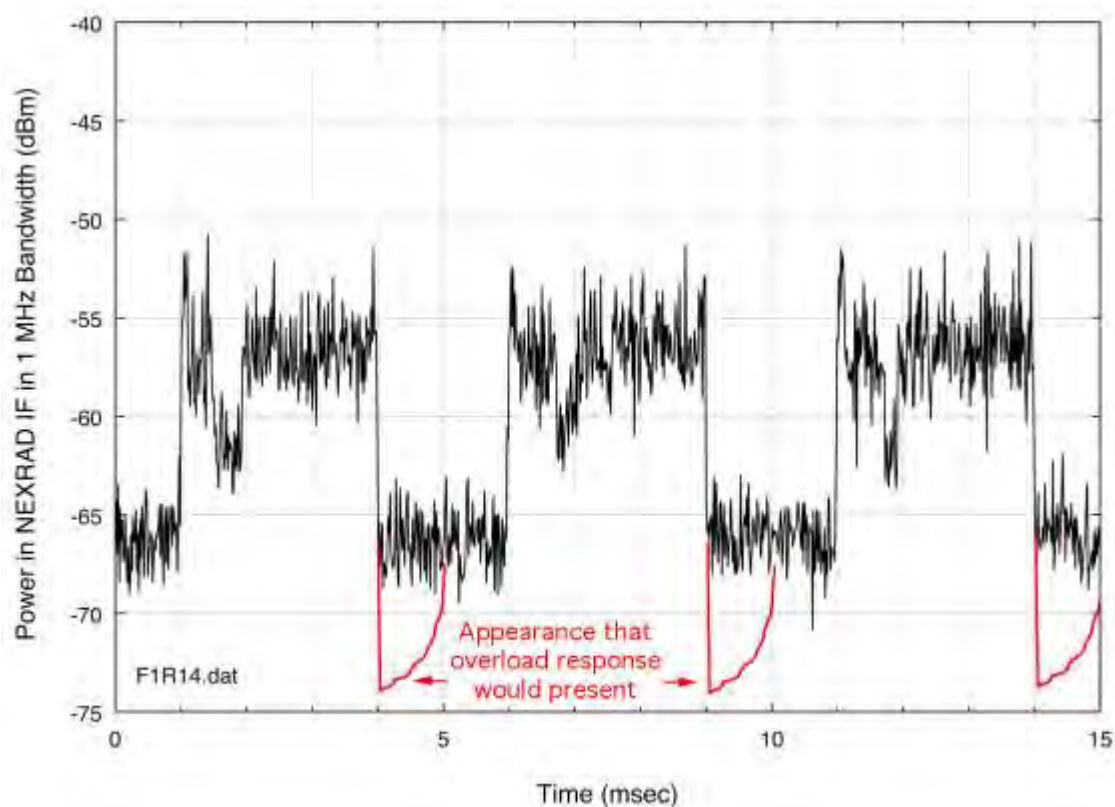
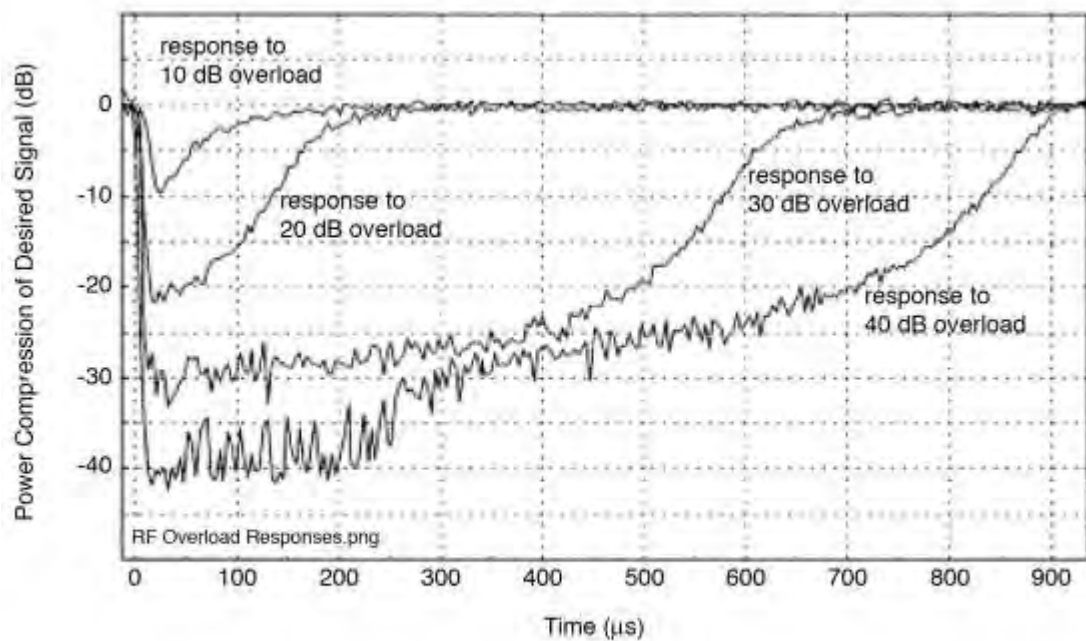


Figure 47. Top: Measured time-domain responses of an LNA in various amounts of overload, from [18]. Bottom: Data from Figure 40 as they *would have* appeared if the NEXRAD LNA had been compressed by front-end overload, with overload added graphically in red.

A different test for front-end overload, and one that would be conclusive, would be to install either a 2496–2690 MHz bandpass filter or a 2690 MHz lowpass filter on the output of a BRS/EBS base station that is causing interference. If the interference is eliminated by the filter installation, then front-end overload is eliminated as a causative mechanism, and OOB emissions are confirmed as the cause. Filter installation at some BRS/EBS transmitter sites in the United States has now provided this confirmation.

4.7 WiMAX Turn-Off Test in Jacksonville

FCC personnel from Tampa, Florida, coordinated a turn-off test of two BRS/EBS base station signals. The two frequencies, which were earlier observed in the interference data of Figure 45, originated from a single WiMAX base station and occurred on the single azimuth of 84.5° from the NEXRAD at frequencies of 2673.5 MHz (channel pair BRS/EBS H3–G1) and 2561.5 MHz (channel pair EBS D2–D3). (The power of the channels H3–G1 signal at 2673.5 MHz was much higher than that of the channels D2–D3 2561.5 MHz signal.) The test consisted of turning off first the stronger H3–G1 signal at 2673.5 MHz, and then the weaker D2–D3 signal at 2561.5 MHz, while the IF output of the NEXRAD was monitored at connector NEXRAD J3 (Figure 31). Then the weaker signal was turned back on, and finally the stronger signal was restored to operation. As with the earlier observations, the radar IF output was monitored with a spectrum analyzer that was tuned to the NEXRAD's IF frequency and which was running in a zero-hertz span mode so as to show the time response of the radar receiver to the interference energy.

The results of this turn-off test are shown in Figure 48. When the first, and stronger, signal was turned off, the interference power level in the radar IF dropped significantly. (The signals were observed with average detection to make them distinctly and cleanly visible; the peak-power levels of Figure 48 were therefore 10 dB higher than the average levels seen in Figure 40.) This drop-off is visible in Figure 48. When the second signal, tuned 143.5 MHz below the NEXRAD frequency, was turned off, Figure 48 shows a second drop-off of energy in the radar receiver.

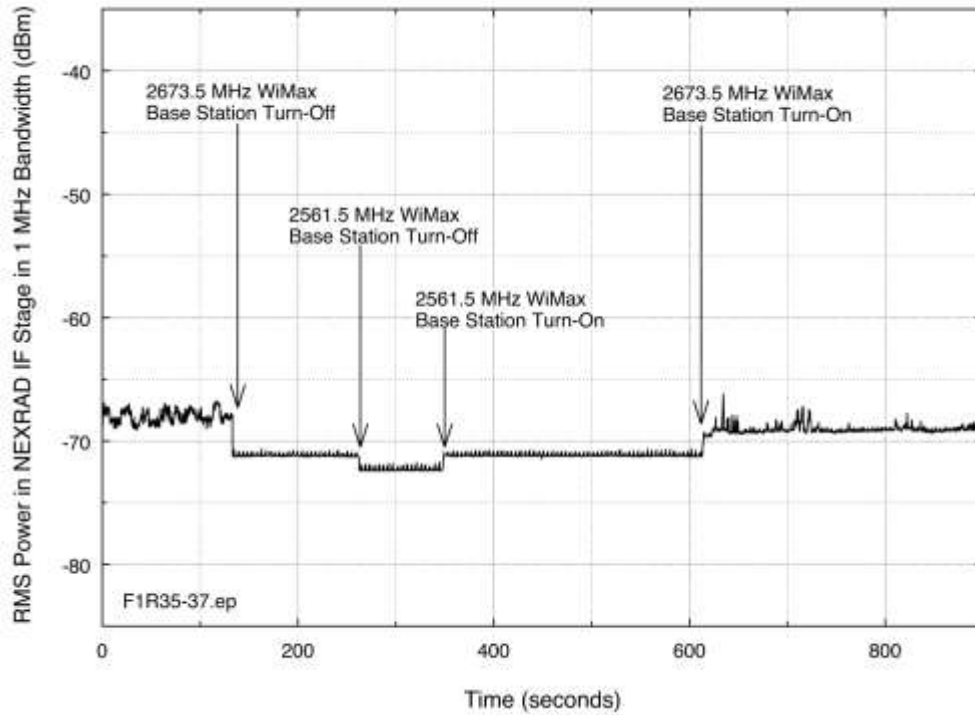


Figure 48. Turn-off test observation in the Jacksonville NEXRAD for two BRS WiMAX signals at 2673.5 and 2561.5 MHz transmitted from a single base station.

4.8 Vector Signal Analyzer Recordings of the Interference Signal

The interference signal was recorded at Grand Rapids as a complex waveform with a vector signal analyzer (VSA) at the NEXRAD antenna feed, ahead of the first bandpass filter, as shown in Figure 31. The strongest interference signal, at 289.4°, was measured. The VSA has a bandwidth of 36 MHz. In order to record the interference across both its intentional emission region and its out-of-band (OOB) and spurious emissions regions, the VSA was tuned initially to the intentional frequency of the interference source, the source's emissions were recorded, and then the VSA was gradually tuned to successively higher frequencies, 36 MHz at a time, with recordings made across the OOB and spurious regions. These VSA recordings may be used for play-back into a variety of radar receivers in subsequent interference-effects tests and measurements of NEXRADs, ATC radars (ASRs and GPNs), and possibly even eventually maritime surface search radars, using the interference-coupling techniques described in [14].

5 IDENTIFICATION OF BRS/EBS TOWERS WHERE INTERFERENCE ORIGINATES

5.1 Identification of the Interference Source Locations

The spectra and time-domain waveforms of the Grand Rapids and Jacksonville interference matched the baseline WiMAX spectra of Section 3. The spectrum measurements performed through the NEXRAD antennas at these two locations showed that WiMAX base station OOB emissions on NEXRAD operational frequencies caused the interference. An on-line search of the Grand Rapids licensee's WiMAX coverage resulted in the identification of four towers within 4–8 km of the NEXRAD that were thought to be strong candidates as source locations of the interference. The initial identifications were based on identical azimuths of the towers with the observed azimuths of the interference. Table 6 summarizes these tower locations.

Table 6. Grand Rapids towers identified as origination points of WiMAX interference to the Grand Rapids NEXRAD.

Az from Nexrad	Latitude (decimal)	Longitude (decimal)	Dist. (km)	Approx. height AGL ¹⁷ (m)	Description
289.4°	42.909803	-85.606453	5.38	33	Tower near RR tracks at Breton Rd SE and 29th St SE
294.6°	42.923983	-85.634836	8.07	30	Tower near RR tracks at Calvin Ave SE and Kalamazoo Ave SE
296.0°	42.909275	-85.588439	3.94	26	Water tank near Shaffer SE and 29th St SE
304.8°	42.935686	-85.626319	8.10	26	Water tank near Boston SE and Plymouth SE

5.2 Verification of Grand Rapids BRS/EBS Emissions on Identified Towers

At each of the four preliminarily identified towers at Grand Rapids, spectrum measurements were performed in situ to verify that they were sources of BRS/EBS emissions, and that the emissions matched those observed at the NEXRAD on each of the four interference azimuths. A portable spectrum analyzer and microwave horn antenna were transported to the vicinity of each tower and were used to measure the emissions from each tower. The measurements were performed whenever possible from the same direction relative to the tower as the NEXRAD. Because WiMAX base stations use frequency diversity for sector coverage, matching of in situ measurement azimuths to the NEXRAD azimuth at each tower caused the in situ data to match, as nearly as possible, the spectrum emissions observed at the NEXRAD (Figures 41–44). The results of the in situ measurements are shown in Figures 49–52; images of the four towers are shown in Figure 53. Individual BRS/EBS WiMAX towers were not visited at Jacksonville.

¹⁷ AGL is above-ground-level height; heights were determined by shadow lengths of the BRS/EBS towers observed in Google Earth™ imagery, as compared with the shadow length of the Grand Rapids NEXRAD tower of known height.

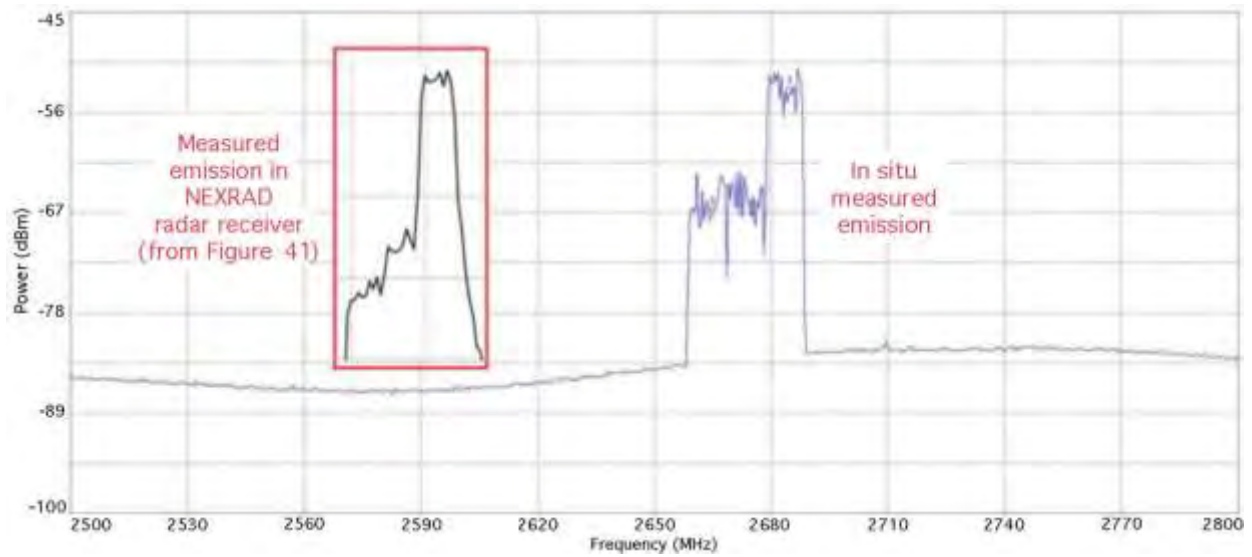


Figure 49. In situ measurement of tower emissions at 289.4°, Breton Rd. and 29th St. SE, Grand Rapids, Michigan.

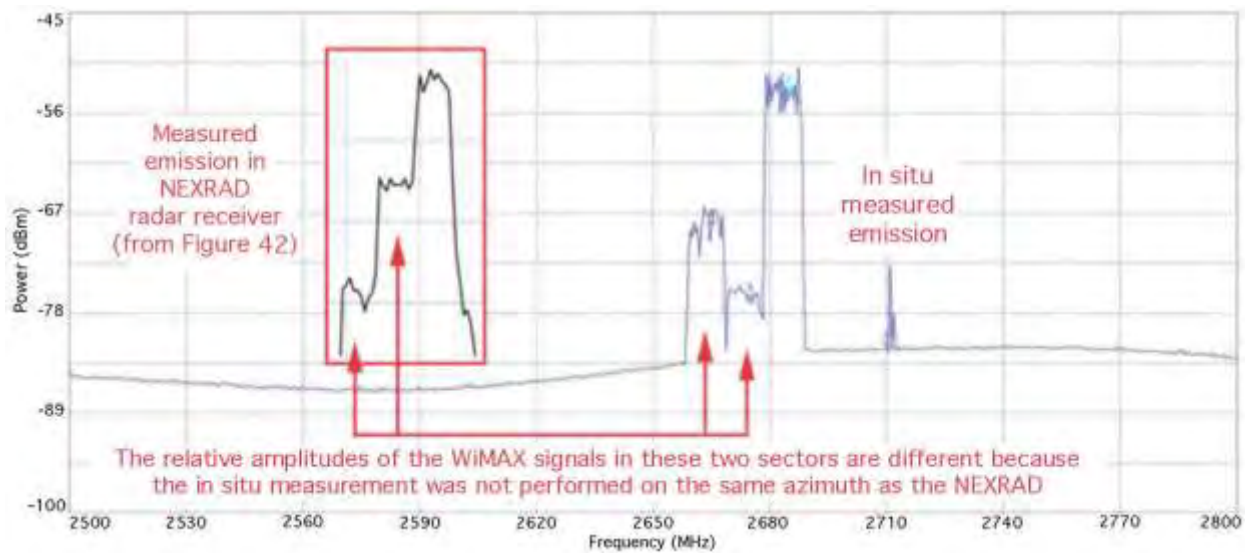


Figure 50. In situ measurement of tower emissions at 294.6°, Calvin Ave SE and Kalamazoo Ave SE, Grand Rapids, Michigan.

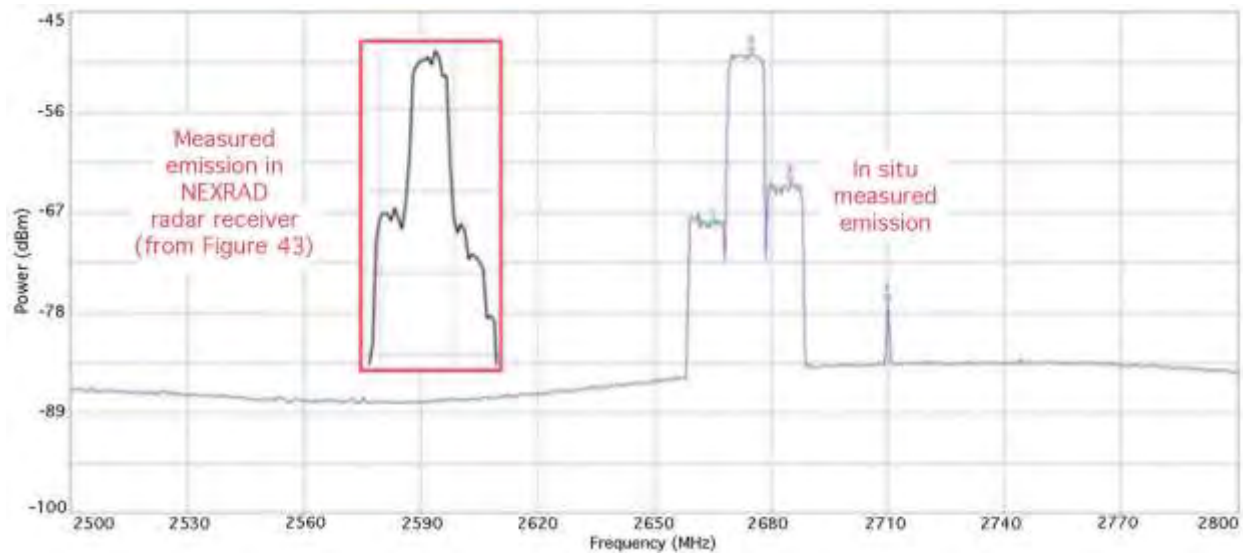


Figure 51. In situ measurement of tower emissions at 296.0°, water tank at Shaffer Ave. SE and 29th St. SE, Grand Rapids, Michigan.

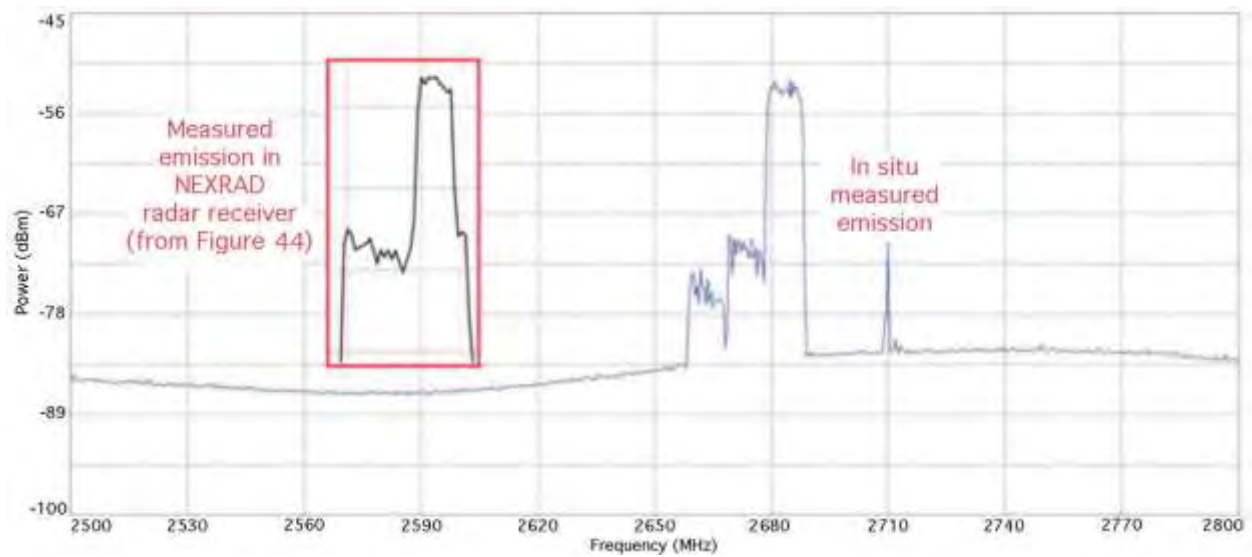


Figure 52. In situ measurement of tower emissions at 304.8°, Boston SE and Plymouth SE, Grand Rapids, Michigan.



Figure 53. Images of four Grand Rapids BRS/EBS towers where the signals shown in Figures 41–44 were transmitted. Azimuths are as measured from the Grand Rapids NEXRAD station location. Photos by author Sanders.

6 DEVELOPMENT OF AN OUTPUT FILTER

6.1 Interference-to-Noise (I/N) Signal Strength on Each Azimuth

A previous multi-agency study [14] has indicated that an I/N ratio of about -10 dB is needed to mitigate interference from relatively high duty cycle interference sources to meteorological radars. While no such study has yet been performed on the specific effects of BRS/EBS interference to any individual radar systems, [13] and [14] indicate that the I/N threshold for interference mitigation in NEXRAD receivers should be about -10 dB; [14] indicates an I/N threshold of about -6 dB for ASR receivers.

The I/N ratios of the interference on each of the measured azimuths are listed in Table 7. These are the peak-power levels of the interference relative to the average noise-floor limit of the radar receiver. For each azimuth, the amount of interference decoupling that would be required to achieve an I/N level of -10 dB is also listed.

Table 7. I/N levels of the Grand Rapids (GR) and Jacksonville (JAX) NEXRAD interference on each azimuth.

Interference Azimuth	I/N Level of the Interference	Figure Showing Measured I/N Data	Decoupling required to achieve $I/N = -10$ dB
289.4° (GR)	42 dB	Figure 35	-52 dB
294.6° (GR)	35 dB	Figure 36	-45 dB
296.0° (GR)	35 dB	Figure 37	-45 dB
304.8° (GR)	32 dB	Figure 38	-42 dB
75.5° (JAX)	21 dB	Appendix B Fig. B-1	-31 dB
84.5° (JAX)	20 dB	Appendix B Fig. B-2	-30 dB
101.0° (JAX)	13 dB	Appendix B Fig. B-3	-23 dB
116.0° (JAX)	23 dB	Appendix B Fig. B-4	-43 dB
135.5° (JAX)	20 dB	Appendix B Fig. B-5	-30 dB
143.5° (JAX)	13 dB	Appendix B Fig. B-6	-23 dB
148.5° (JAX)	11 dB	Appendix B Fig. B-7	-21 dB
151.0° (JAX)	7 dB	Appendix B Fig. B-8	-17 dB
157.0° (JAX)	16 dB	Appendix B Fig. B-9	-26 dB
160.7° (JAX)	12 dB	Appendix B Fig. B-10	-22 dB
192.0° (JAX)	24 dB	Appendix B Fig. B-11	-34 dB
200.3° (JAX)	25 dB	Appendix B Fig. B-12	-35 dB

6.2 Approach for Developing EMC Curves

Since OOB energy from BRS/EBS base stations occurs on the frequencies of NEXRAD receivers, there is no way to resolve the problem by installing filtering on NEXRAD receivers. There are several technical methods for decoupling interference from NEXRADs. These include

careful local frequency planning to maximize frequency differences between BRS/EBS base stations and radars, control of the down-tilt angles of base station antennas, and filtering of BRS/EBS WiMAX base station emissions. All of these approaches are described in more detail below.

6.2.1 Development of a Filtering Option for BRS/EBS WiMAX Base Station Transmitters

If adequate filtering can be installed on transmitters that are operating within some defined frequency range and physical radius from radar receivers, then all presently available spectrum may be used in both the BRS/EBS band and the radar band even if other mitigation options should prove to be infeasible at particular locations. Such filtering could be either lowpass (near 2690 MHz) or bandpass (approximately 2496–2690 MHz). (Notch filtering could work, but notches would have the disadvantage of needing to be custom-tuned for every individual radar station frequency. With lowpass or bandpass filters, a uniform filter design could be installed at any WiMAX station.) Bandpass filters can have faster roll-off on their upper-frequency edges than lowpass filters and are therefore preferred in this application.

Referring to the WiMAX emission spectrum of Figure 44 (tuned to the highest available frequency in the BRS/EBS band at a distance of 5 km from a NEXRAD operating at 2710 MHz), the amount of decoupling (-52 dB) needed to obtain an *I/N* level of -10 dB in the NEXRAD receiver would be achieved by the theoretical filter rejection curve shown in Figure 54. Figure 55 shows a theoretical filter rejection curve that would be adequate at a distance of 5 km from a NEXRAD tuned to 2705 MHz, the lowest frequency used nationally in the radar band.¹⁸ Figure 56 shows a measured response curve for a bandpass filter that has been produced to meet these rejection requirements.

¹⁸ There are over a dozen radars listed in the Government Master File (GMF) that are tuned to 2705 MHz, mostly NEXRADs but also some ASRs and GPNs.

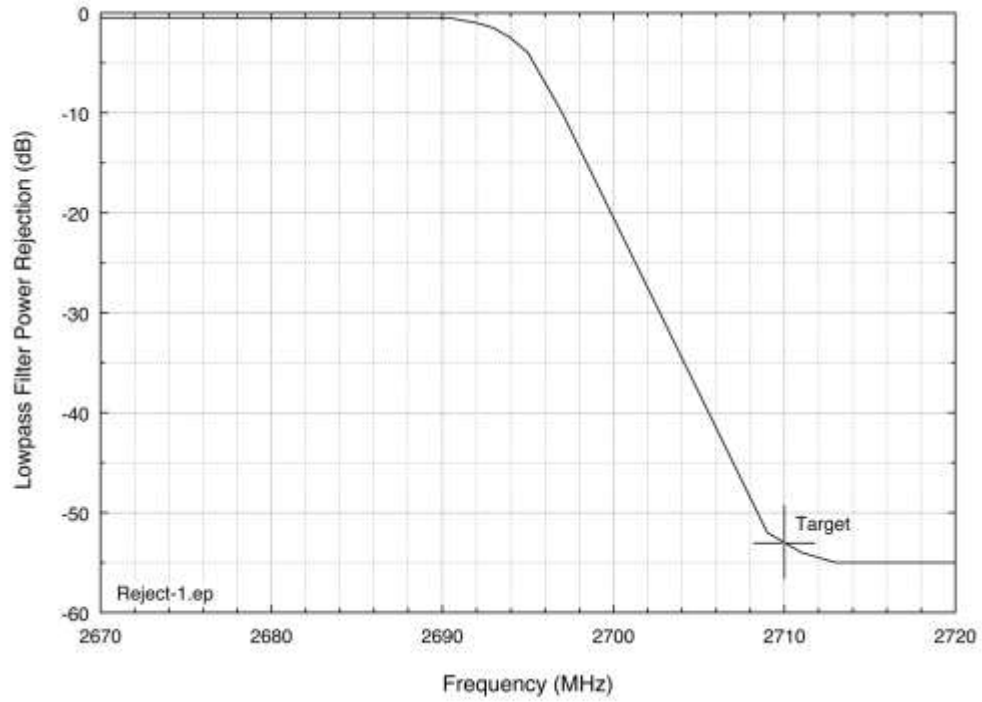


Figure 54. Filter response that would provide compatibility between a WiMAX signal tuned to 2685 MHz (Figure 44) and a NEXRAD receiver 5 km away tuned to 2710 MHz.

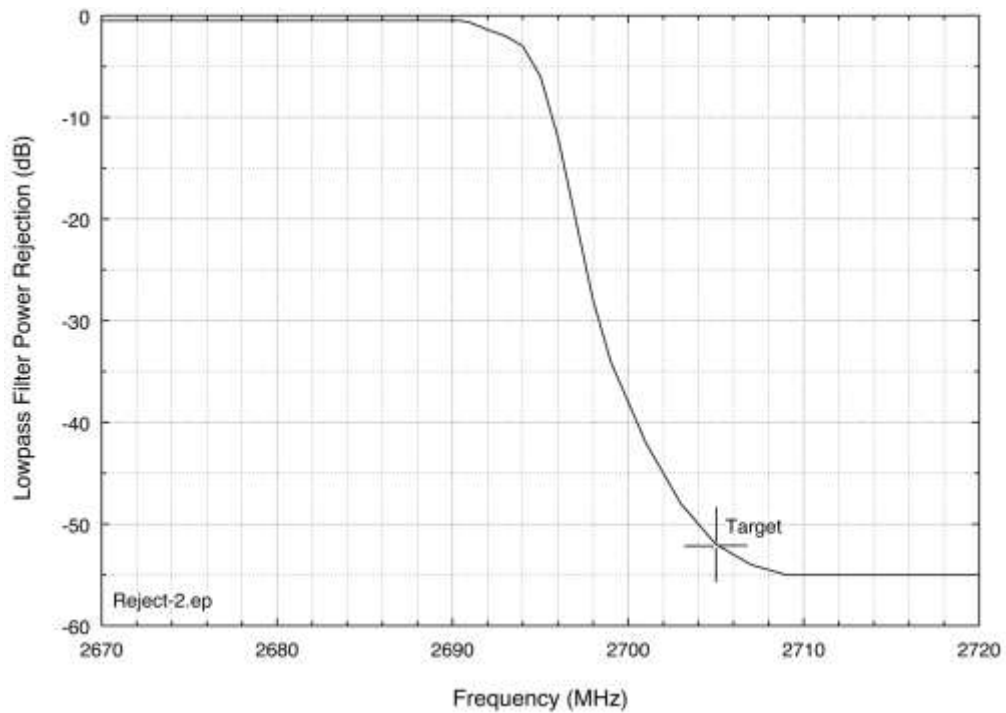


Figure 55. Filter response that would provide compatibility between a WiMAX signal tuned to 2685 MHz and a NEXRAD receiver 5 km away tuned to 2705 MHz.

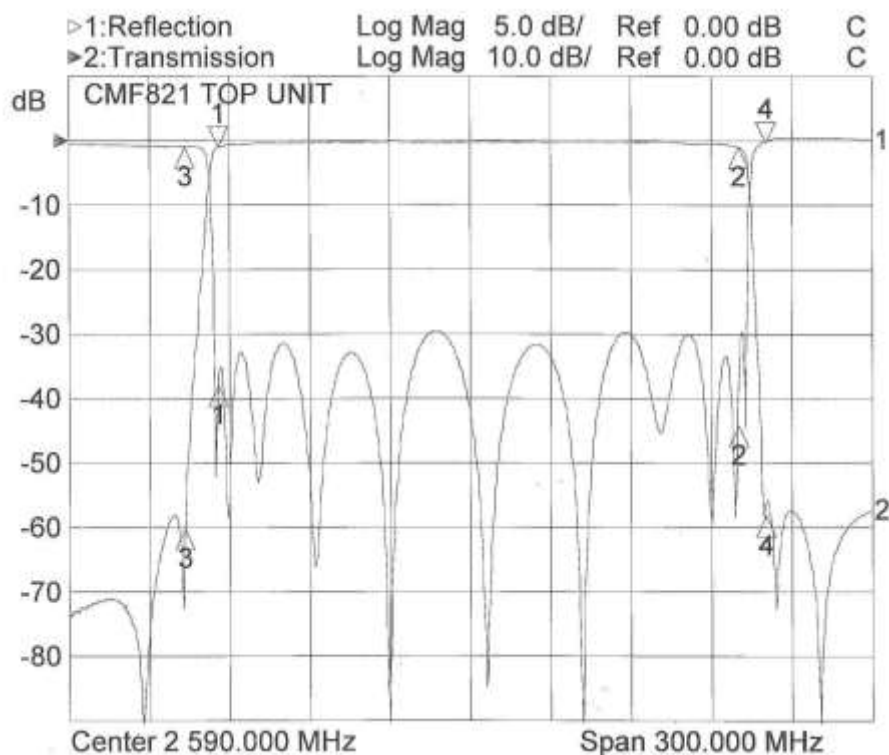


Figure 56. WiMAX output bandpass filter response as measured by the manufacturer, Commercial Microwave Technology (CMT), Inc.

Frequency-distance separation curves may be developed to show the interference-free limits of spatial and frequency separation between radars and WiMAX base stations. These curves may be developed to show minimum separations for WiMAX stations that are not output-filtered versus filtered. To develop these curves, it is necessary to know the emission spectra of WiMAX base stations. With such spectra, the additional factors of antenna coupling, spatial distance, and I/N thresholds for radar receivers may all be systematically incorporated into a model that will give the conditions under which compatibility issues and solutions (filtering, frequency plans, antenna down-tilt angles) need to be assessed. Without such spectrum data, a methodical approach to the problem is not possible.

Based on the maximum measured I/N ratios of the interference that was recorded in the NEXRAD receivers in Michigan and Florida, the service provider procured a bandpass filter (Figure 56) that reduced the out-of-band WiMAX emissions to a level that was calculated to protect the radar receivers (Figures 54–55).

The emission spectra of WiMAX Radios 1, 2, and 3 were measured with the bandpass filter installed at their outputs (see the bandpass filter path shown in Figure 26). The resulting emission spectra are shown in Figures 57–60. These figures are normalized to the center frequencies of the WiMAX transmitters.

Figure 57 shows that the bandpass filter meets its design goal of 52 dB of rejection at 2705 MHz, as determined to be needed at Grand Rapids. The power level of the unfiltered emissions

is -60 dBm. The measurements of the filtered emissions are below the noise floor of the measurement system; however, the line of the filtered emissions can be extended to see where it intersects at 2705 MHz. Figure 57 shows that this occurs at about -112 dBm, which is the predicted value given the filter response.

Figure 58 shows the spectrum measurement results for the WiMAX Radio 2 base station. The figure shows that the bandpass filter meets its design goal of 52 dB of rejection at 2705 MHz. The power level of the unfiltered emissions is -55 dBm. The measurements of the filtered emissions are below the noise floor of the measurement system; however, the line of the filtered emissions can be extended to see where it intersects at 2705 MHz. The figure shows that this occurs at -107 dBm, which is the predicted value for the filter response.

Figure 59 shows measured spectra for the WiMAX Radio 3 base station. This figure shows that the bandpass filter meets its design goal of 52 dB of rejection at 2705 MHz. The power level of the unfiltered emissions is -46 dBm. The measurements of the filtered emissions are below the noise floor of the measurement system; however, the line of the filtered emissions can be extended to see where it intersects at 2705 MHz. Figure 59 shows that this occurs at about -98 dBm, which is the predicted value given the filter response. Figure 60 shows all six emission spectra (Radios 1–3, both filtered and unfiltered) on a single plot.

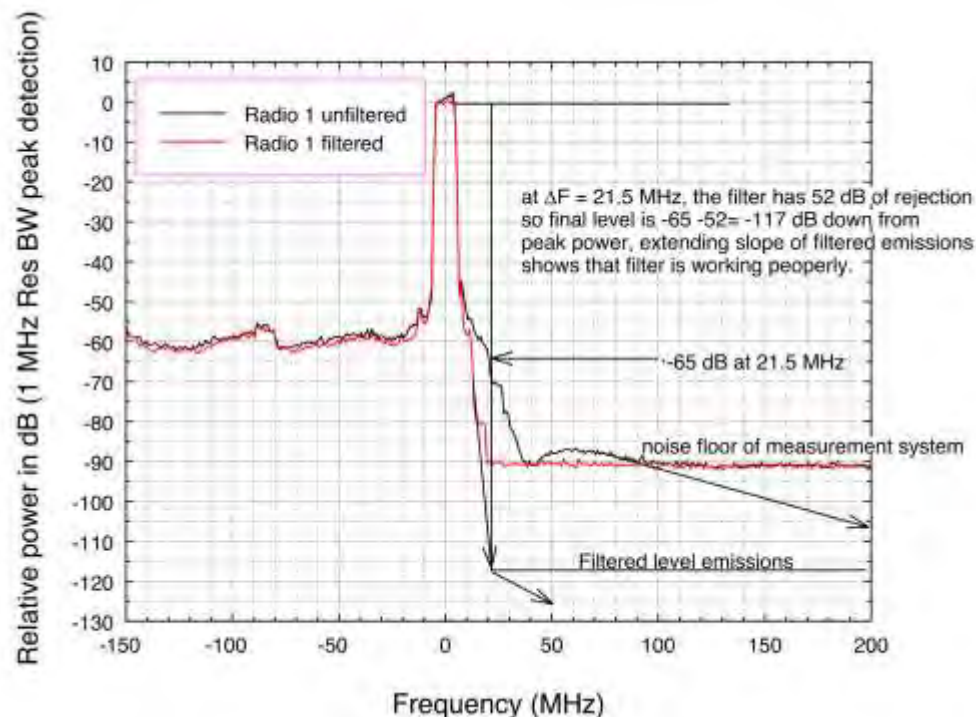


Figure 57. WiMAX Radio 1 base station emission spectra with and without supplemental output filtering.

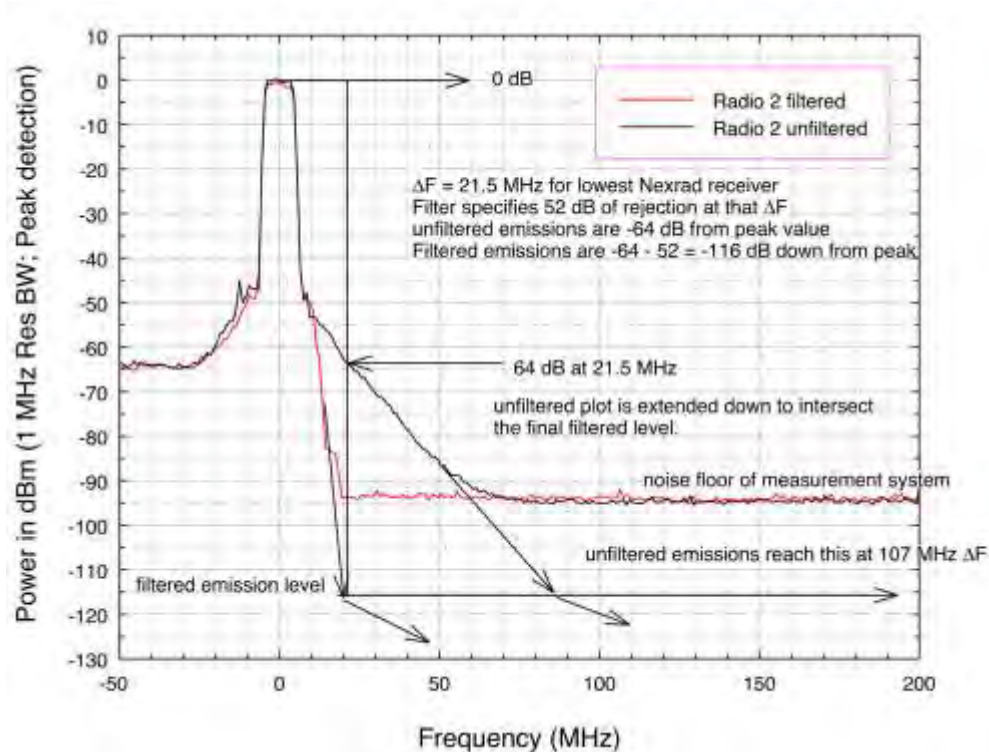


Figure 58. WiMAX Radio 2 emission spectra with and without output filtering.

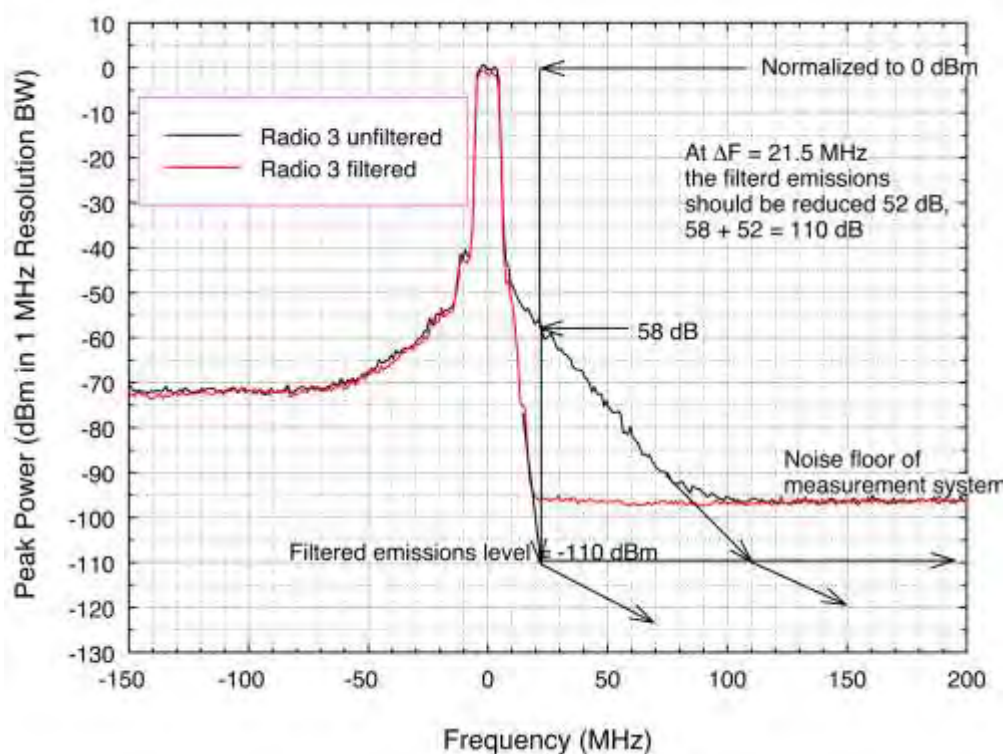


Figure 59. WiMAX Radio 3 emission spectra with and without output filtering.

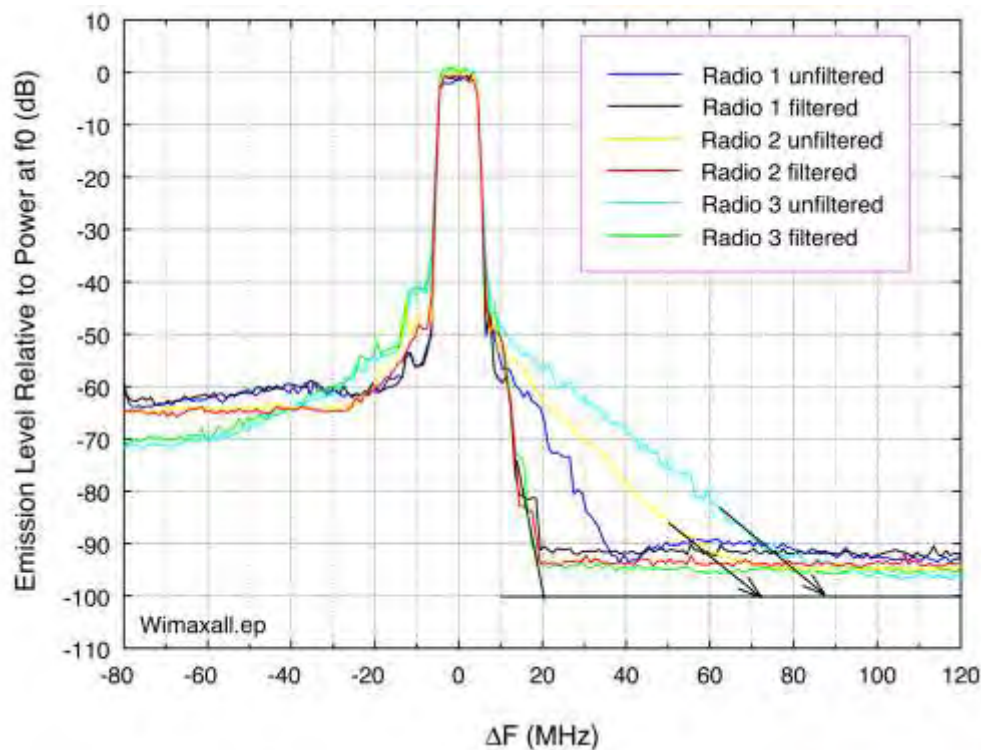


Figure 60. All emission spectra for WiMAX Radios 1-3, filtered and unfiltered, center frequency normalized to zero.

6.3 Testing of WiMAX Output Filtering at Two NEXRAD Field Locations

The WiMAX output filter with the response curve shown in Figure 56 and which was used in the emission measurements shown in Figures 57–60 has been tested on WiMAX transmitters near NEXRADs at Grand Rapids, Michigan, and Norman, Oklahoma, where interference strobes were occurring. Prior to and after the filter installations, staff of the Grand Rapids Weather Forecasting Office (WFO) and Norman ROC gathered raw NEXRAD I and Q data that had not yet been processed by the radar receiver. After analyzing these data, the ROC Engineering Group found no artifacts from WiMAX interference after the filters were installed. Based on this work, NWS concluded that such filters should eliminate interference at other NEXRAD sites.

6.4 Calculation of Minimum Separation Distances With and Without Filters

Appendix D provides detailed calculations of frequency-dependent rejection (FDR) curves developed by OSM for specified amounts of spatial and frequency separation between WiMAX stations and 2700–3000 MHz radar receivers. The results for filtered versus unfiltered WiMAX transmitters are summarized in Table 8. (Results for ASRs were computed from data presented in Appendix C.)

Table 8. Summary of calculated separation distances (km) for $\Delta F = 22$ MHz.

WiMAX Transmitter	NEXRAD		ASR-8		ASR-9		ASR-11	
	No down-tilt	5 Deg. down-tilt	No down-tilt	5 Deg. down-tilt	No down-tilt	5 Deg. down-tilt	No down-tilt	5 Deg. down-tilt
Filtered, for all WiMAX radios	3.7	1.9	14	8.8	0.8	0.3	0.8	0.3
Radio 1 (unfiltered)	25.9	20.1	16.1	10.5	10.1	5.9	10.1	5.9
Radio 2 (unfiltered)	30.5	24.4	16.1	10.5	13.2	8.2	13.2	8.2
Radio 3 (unfiltered)	35.1	28.7	17.4	11.5	16.6	10.9	16.6	10.9

6.5 Summary of WiMAX Filter Development and Effectiveness

Radar receiver performance data presented in this report have been used by a WiMAX service provider to build a bandpass filter that mitigates interference to radar receivers when other methods fail. The filter was designed to meet the decoupling factors specified in Figures 54 and 55, themselves based on measurements of worst-case interference at radar field sites.

The filter's performance has been verified by NTIA measurements of WiMAX emission spectra with the filter installed on three different WiMAX transmitters. Its effectiveness has been verified by NWS through operational testing at two NEXRAD sites.

7 INTERFERENCE MITIGATION OPTIONS

Based on all of the technical work performed in this study, interference into NEXRADs (and ASRs, if it were to occur) from WiMAX (and possibly eventually other types of transmitters) can be mitigated using the following methods, or combinations of them. Both existing and planned base stations should be considered when determining the most appropriate course of action. In situations where minimal amounts of interference are occurring, the simpler and less costly methods may be attempted first to mitigate the interference. Mitigation options are listed here in the order of increasing levels of estimated cost, difficulty, and effort. Pros and cons are discussed for each option.

7.1 Down-Tilting of WiMAX Base Station Transmitter Antennas

As shown in Figure 61, some down-tilting of WiMAX base station antennas will produce additional decoupling of interference energy from radar receivers.

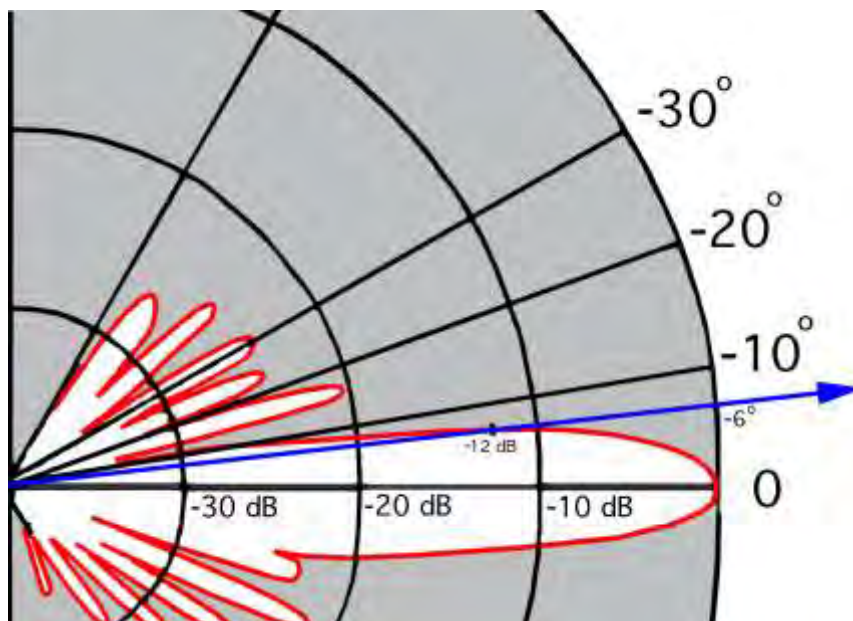


Figure 61. Detail of Figure 17, showing amount of down-tilt needed to achieve 12 dB of decoupling in the antenna pattern.

Pro: Down-tilting the vertical beams of WiMAX base stations can produce some decoupling between WiMAX transmitters and radar receivers. The vertical pattern of commonly used WiMAX base station antennas is very narrow (Figures 17 and 61), so a few degrees of down-tilt can reduce interference coupling by 10 dB or more. The effectiveness of such down-tilting in reducing interference power levels in radar receivers was demonstrated during a test at Grand Rapids, Michigan, in mid-2011, where the *I/N* level was reduced by 12 dB by down-tilting a WiMAX antenna by a few degrees. The down-tilt of some antennas in that provider's network can be remotely controlled, while others need to be adjusted manually on-site.

Con: Down-tilt angles affect WiMAX service coverage. Modification of down-tilts could reduce service to some customers.

7.2 Off-tuning BRS/EBS Base Station Transmitters from Upper BRS/EBS Band Edge

Pro: Experience with local re-arrangement of the BRS/EBS channel-use plan at Grand Rapids has shown that increased frequency off-tuning of unfiltered WiMAX emissions below the upper band edge of 2690 MHz does at some point achieve the same level of interference mitigation as can be achieved by installing bandpass filtering. BRS/EBS networks are typically centrally managed and the base stations can be re-tuned with relative ease. Usually all of the radios in a single market are procured from a single vendor, so network frequency plans are internally consistent and optimal across each market. This makes it easier to concentrate use of channels near the bottom of the BRS/EBS band in market areas near NEXRAD stations.

Con: Changing the channel of even a single BRS/EBS base station has a ripple effect across the entire network in each market area, so thorough and careful planning is required before channel assignments are modified. Centralized frequency management causes single changes to cascade through the entire market, making retuning logistically challenging. Revised frequency plans are not trivial to develop and new ones can require a day or two to be established and verified on each network. This process may adversely affect the service to some customers during that time period, and thus may temporarily adversely affect operations and revenues. (Note: Not all BRS spectrum is readily available in all markets for such reassignment.)

7.3 Installation of Filters on BRS/EBS Base Station Transmitters

Pro: Installing bandpass filters on BRS/EBS WiMAX transmitters will permit them to operate on their highest allocated frequency (2683.5 MHz) without causing interference at a separation distance of 5 km at an antenna height that is approximately the same as the height of NEXRAD receiver antennas. Filter installation is the most completely effective option among all possible approaches. The filters are relatively inexpensive to include during the installation of new BRS/EBS WiMAX base stations, at a cost of about five hundred dollars per filter. However, current transmitters require four filters per station. At some locations, more than one station is operated per sector. There are also ancillary costs (one per filter at a cost of about \$100/each), and a cost to weatherproof the new connections.

Con: Retrofitting bandpass filters at *existing* BRS/EBS WiMAX base stations can cost five thousand dollars or more per installation, roughly ten times the cost of installing them at new base stations. The main retrofit cost is for labor to access the stations, install the filters, and ensure that all connections are weatherproofed. Access to some locations, such as water towers, requires costly labor expenditures. (BRS/EBS WiMAX service providers commonly contract this work on a market-by-market basis.) Given that other mitigation options are available which can be effective and less costly, blanket installation of bandpass filters at all base station sites would be unnecessary and needlessly costly. It may be best to resort to filter installation only at base stations where the need for interference mitigation has been established and where other, less costly mitigation approaches have been attempted but have been found to be ineffective.

7.4 Establishing Larger Physical Separation Distances Between WiMAX Transmitters and Radar Receivers When Frequency Separations are Small

Pro: If the frequencies of a WiMAX and a NEXRAD station are so close as to potentially cause interference to the NEXRAD, then the interference can be mitigated by maintaining a sufficiently large physical separation distance between them. This distance would be at or beyond the radio LOS between their respective antennas. Establishment of separation distances beyond radio LOS between WiMAX transmitters and radar receivers requires minimal additional intervention within each of the systems.

Con: Many NEXRAD radars are located near population centers to provide effective alerts for severe weather and other phenomena. WiMAX networks routinely need to serve those same population centers. So it will generally not be practical (cost and time to relocate being substantial) to use geographical separation alone to mitigate existing interference between stations. However, careful pre-planning for the frequencies of new WiMAX stations can provide for larger separation distances from local NEXRADs when frequency separations need to be small.

7.5 Reduction in the Heights of WiMAX Base Station Transmitter Antennas

Pro: NEXRADs utilize antenna gains of +45 dBi. While the WiMAX base station antenna gains are not so large, the antennas of these two systems are typically located at comparable heights of 24–30 m (80–100 ft) AGL and both systems direct their antenna beams at vertical angles that are close to the horizon. NEXRAD antennas are located on 24 m (80 ft) towers to provide relatively clutter-free coverage toward and above the horizon, while WiMAX antennas are placed high to achieve maximal coverage for their base stations toward and below the horizon. So mainbeam coupling will sometimes occur, maximizing interference. Reducing the heights of some WiMAX base station antennas could reduce the maximum system-to-system coupling levels.

Con: WiMAX antenna heights and beam angles have been established to provide optimal network coverage versus base station costs. Reducing the heights of some WiMAX base station antennas would affect network coverage and could reduce service to some customers. High labor costs might also be incurred on a station-by-station basis and some new, costly gap-filling base stations might need to be established if WiMAX antenna heights were reduced.

7.6 Retuning NEXRAD Frequencies Enough to Mitigate Interference

Taking factors of gain and loss for base station transmitters and NEXRAD receivers into account, for a separation distance of 1.6 kilometers (one mile) or more, NEXRAD stations operating at a frequency of 2723.5 MHz or higher should not experience impacts from BRS/EBS base stations. This is supported by empirical observations; NEXRAD stations reporting strobes have all been tuned below 2720 MHz.

Pro: Retuning the radar can reduce OOB emissions from transmitters in the BRS band enough to mitigate interference by positioning the radar frequency at a more aggressive point in the filter roll-off of the WiMAX station. Stated another way, if a NEXRAD is experiencing WiMAX

interference, retuning it to a sufficiently higher frequency can decouple its receiver enough from WiMAX OOB energy as to eliminate the interference.

Cons: NEXRADs use custom-built RF front-end bandpass filters that would have to be replaced in the event of retuning. Other NEXRAD components (the RF diplexer, circulator, and transmitter klystron) would also need to be adjusted or replaced to accommodate that change; these modifications would be expensive and time-consuming. Some new parts may not be readily available since NEXRADs are now out of production. Retuned NEXRADs would need to be recertified. In addition, changing the frequency of a single NEXRAD can have a ripple effect on the frequency assignments of other NEXRAD, ASR, and GPN radars in a geographic area. This could cause multiple radars in an area to need to be retuned (with front-end filters needing to be replaced in ASR-9s and equivalent GPNs) and operationally recertified if a single NEXRAD is retuned.

8 SUMMARY AND CONCLUSIONS

8.1 Summary

Although a particular interference source has been identified (BRS/EBS base stations utilizing WiMAX technology), the interference is not a direct result of any unique aspect of WiMAX waveforms or emissions. In this study, interference from BRS/EBS base stations operating below 2700 MHz to nearby radar receivers operating above 2700 MHz in Grand Rapids and Jacksonville has been examined. The problem has only been documented as occurring in NEXRAD radar receivers.¹⁹ The problem occurs at NEXRAD stations when they are relatively close to BRS/EBS base stations in both frequency and spatial separation. The possibility of interference to FAA ASRs has been analyzed but due to the lower antenna gains and heights of those radars, the potential for interference from BRS/EBS stations to ASRs is relatively low. The specific conclusions that have been developed in this study are provided below.

This report documents an approach for analyzing an EMC problem and determining solutions to that problem. This study provides readers with a single case-study road-map of procedures (initial analysis, measurement of receiver characteristics, measurement of transmitter spectra, determination of interference coupling mechanism, and determination of a range of mitigation options) that can be more generally applied in a wide range of EMC studies. The methodology (identification of interference sources and engineering analysis of transmitter and receiver characteristics to determine interference mechanism) and range of solutions described in this study may be applicable to other interference scenarios.

8.2 Conclusions

1. Measurement data show that NEXRAD receivers that are tuned close to 2700 MHz are experiencing interference from BRS/EBS base stations at Grand Rapids and Jacksonville. Although these are individual instances of a potentially more widespread problem, additional situations and circumstances may need to be evaluated on case-by-case basis across the country using the same analytical approach.
2. Interference to ASRs from BRS/EBS base stations has not been documented. The lower antenna gains and heights of ASRs make these radar receivers less likely to experience interference effects from BRS/EBS base stations.
3. Measurement data indicate that OOB emissions from BRS/EBS base stations appear to be the cause of interference to NEXRADs; front-end receiver amplifier overload seems to have been ruled out by the same data.
4. The measured characteristics of NEXRAD (Section 2) and ASR-9 receivers (Appendix C) show that front-end overload should not occur in these receivers; OOB emissions from

¹⁹ Appendix E presents procedures for assessing interference sources at ASR stations if the need should arise in the future.

BRS/EBS base stations should be the only interference mechanism of concern for these systems.

5. The measured characteristics of ASR-8 and ASR-11 receivers (Appendix C) indicate that these could be vulnerable to both OOB and front-end overload interference from WiMAX base stations. However, the measured overload thresholds of these receivers' front-end LNAs are not likely to ordinarily be exceeded by WiMAX base station emissions.
6. Using measurement data and known characteristics of WiMAX base stations, frequency-separation distance separation curves have been developed for WiMAX base stations located in the vicinity of 2700–3000 MHz radars.
7. A set of mitigation options that will resolve all known or likely incidences of interference from WiMAX base stations to 2700–3000 MHz radar receivers has been developed and is presented in Section 7 of this report.
8. Most mitigation options can be implemented with relative ease and at relatively low cost. All mitigation options require some level of coordination between WiMAX service providers and Federal agencies that operate radars in other bands.
9. Output RF filtering of WiMAX base station emissions can provide an effective solution to interference problems without the need to sacrifice any use of spectrum. This option is less costly to install on new base stations than on existing base stations. Most WiMAX base stations should not need such filtering. But in cases in which interference to radars in other bands occurs and no other mitigation options are effective or feasible, this option ultimately provides an assured method of mitigation.

9 ACKNOWLEDGEMENTS

The authors thank George Engelbrecht of the ITS Telecommunications Engineering, Analysis and Modeling Division for his technical assistance and support during the Grand Rapids radar interference measurements. The staff of the Grand Rapids Weather Forecasting Office and the Jacksonville Weather Office are also recognized and thanked for their assistance with the measurements presented in this report; without this assistance, the work in this study could not have been accomplished. Particular thanks are extended to Don Howell and Ivan Gonzales, the NEXRAD technicians who operated the NEXRAD receivers during the tests and measurements at Grand Rapids and Jacksonville, respectively, and provided technical access within these radars from their antennas to their IF outputs.

The assistance and cooperation of the fourth generation wireless communications industry was a critical component of all of the interference mitigation analysis and implementation that is described in this report. NTIA thanks the industry participant for this assistance and cooperation.

The authors thank the staff of the Jacksonville ASR-9 for their support of this work, and also the staff of the Jacksonville Naval Air Station for providing access to that radar.

Finally, but not least, the FCC field office in Tampa, Florida, especially Don Roberson, is thanked for assistance with the work in Jacksonville and Grand Rapids, including the coordination of turn-off testing with the BRS licensee in Jacksonville.

10 REFERENCES

- [1] Wang, Z., M. Ganley, Bal Randhawa and I. Parker, “Interference from radars into adjacent band UMTS and WiMAX systems,” ERA Report (Cobham Technical Services, CTS) report for Ofcom, ERA report number 2007-0554, Sep. 2007.
<http://stakeholders.ofcom.org.uk/binaries/research/technology-research/2007-0554.pdf>.
- [2] Ganley, M. and S. Munday, “Assessment of the potential for interference into an ‘S-band’ air traffic control radar from 2500 to 2690 MHz systems,” ERA Technology (Cobham Technical Services) report for Ofcom, ERA report number 2008-0456, Issue 4, Oct. 2008.
http://stakeholders.ofcom.org.uk/binaries/spectrum/spectrum-awards/awards-in-preparation/757738/588_Assessment_of_the_Poten1.pdf.
- [3] Ganley, M. and Z. Wang, “Potential impact of out-of-band emissions from the 2.6 GHz auction on S-band maritime radar,” ERA Technology (Cobham Technical Services) report for the UK Maritime and Coast Guard Agency (MCA), report number 2009-0258, Jun. 2009. http://www.dft.gov.uk/mca/2009-0258_final_-_mca-2.pdf.
- [4] C. Blackler, “Watchman radar: Receiver selectivity improvements in the 2700-3100 MHz band,” SELEX Systems Integration, report number SSI-PS0305-ENG-405, 1 Dec. 2009.
http://stakeholders.ofcom.org.uk/binaries/spectrum/spectrum-awards/awards-in-preparation/757738/592_Watchman_Radar_Receiver1.pdf.
- [5] Helios Company report, “Review of radar receiver adjacent channel thresholds of UK S-band ATC radars: final report,” summarizing work performed by Cobham Technical Services (CTS) and SELEX for Ofcom, 10 Dec. 2009.
http://stakeholders.ofcom.org.uk/binaries/spectrum/spectrum-awards/awards-in-preparation/757738/594_Review_of_Radar_Receive1.pdf.
- [6] L. Ashton, “Phase 2 of 2.6 GHz trials at RAF Honington Aug 2009,” ERA Technology for Ofcom and UK Ministry of Defense (MoD), Issue 2, 4 Nov. 2009.
http://stakeholders.ofcom.org.uk/binaries/spectrum/spectrum-awards/awards-in-preparation/757738/590_Mepward_Report_Phase_1.pdf.
- [7] L. Ashton, “Phase 2 of 2.6 GHz trials at Portland Aug 2009,” ERA Technology for Ofcom and UK MoD, Issue 2, 4 Nov. 2009.
http://stakeholders.ofcom.org.uk/binaries/spectrum/spectrum-awards/awards-in-preparation/757738/591_Mepward_Report_Phase_1.pdf.
- [8] Ofcom report, “Coexistence of S band radar systems and adjacent future systems,” 11 Dec. 2009. <http://stakeholders.ofcom.org.uk/binaries/spectrum/spectrum-awards/awards-in-preparation/infoupdate.pdf>.
- [9] Louth, G. “Consultation on assessment of future mobile competition and proposals for combined award of 800 MHz and 2.6 GHz spectrum,” Ofcom Briefing for Stakeholders, 22 Mar. 2011. <http://stakeholders.ofcom.org.uk/binaries/consultations/combined-award/annexes/briefing.pdf>.

- [10] Real Wireless Ltd., “Airport deployment study: final report,” Real Wireless for Ofcom, 19 Jul. 2011. http://www.ofcom.org.uk/static/spectrum/Airport_Deployment_Study.pdf.
- [11] Ofcom report, “Communications signals in the 2.6 GHz band and maritime radar - technical assessment of interference,” 2 Aug. 2011. http://stakeholders.ofcom.org.uk/binaries/spectrum/spectrum-awards/awards-in-preparation/2011/Maritime_technical_report.pdf.
- [12] Electronic Communications Committee (ECC) of the European Conference of Postal and Telecommunications Administrations (CEPT), “Compatibility between the mobile service in the band 2500–2690 MHz and the radiodetermination service in the band 2700–2900 MHz,” ECC Report 174, Mar. 2012. <http://www.erodocdb.dk/docs/doc98/official/pdf/ECCRep174.pdf>.
- [13] International Telecommunications Union, Radiocommunication Sector (ITU-R), “Technical and operational aspects of ground-based meteorological radars,” ITU-R Recommendation M.1849, Jun. 2009. http://www.itu.int/dms_pubrec/itu-r/rec/m/R-REC-M.1849-0-200906-I!!PDF-E.pdf.
- [14] Sanders, F. H., R. Sole, B. Bedford, D. Franc and T. Pawlowitz, “Effects of RF interference on radar receivers,” NTIA Technical Report TR-06-444, U.S. Dept. of Commerce, Sep. 2006. <http://www.its.bldrdoc.gov/publications/2481.aspx>.
- [15] U.S. Department of Commerce, Office of Spectrum Management, “Manual of Regulations and Procedures for Federal Radio Frequency Management,” Chapter 5, Jan. 2008 Edition, May 2011 Revisions. http://www.ntia.doc.gov/files/ntia/publications/manual_5_11.pdf.
- [16] Sanders, F. H., R. L. Hinkle, and B. J. Ramsey, “Measurement procedures for the Radar spectrum engineering criteria (RSEC),” NTIA Technical Report TR-05-420, U.S. Dept. of Commerce, Mar. 2005. <http://www.its.bldrdoc.gov/publications/2450.aspx>.
- [17] Sanders, F. H., “The rabbit ears pulse-envelope phenomenon in off-fundamental detection of pulsed signals,” NTIA Technical Memorandum TM-12-487, Jul. 2012, <http://www.its.bldrdoc.gov/publications/2678.aspx>.
- [18] Sanders, F. H., R. L. Hinkle and B. J. Ramsey, “Analysis of electromagnetic compatibility between radar stations and 4 GHz fixed-satellite earth stations,” NTIA Technical Report TR-94-313, U.S. Dept. of Commerce, Jul. 1994. <http://www.its.bldrdoc.gov/publications/2340.aspx>.

APPENDIX A: PROCEDURES FOR MEASURING INTERFERENCE AT NEXRAD STATIONS

A.1 Introduction

A problem that has been posed is to observe time-domain and frequency-domain characteristics of interference inside NEXRAD receivers for the purpose of identifying the likely source(s) of interference. This Appendix provides detailed procedures for such observations. NEXRADs need to be taken out of operation while these procedures are being performed.

Interference in NEXRAD receivers is not always manifested as visible strobes on the radar data display; strobes only occur when interference is present at relatively high interference-to-noise (I/N) levels. These procedures are designed to identify interference sources even if their power levels in NEXRAD receivers are below the strobe-generation threshold.

A.2 Recommended Measurement Hardware

It is assumed that the hardware complement for these measurements will need to be portable. The only required equipment is a portable spectrum analyzer with capabilities for both peak detection and RMS average detection, with miscellaneous RF cables and connectors. The inclusion in the spectrum analyzer of a built-in low-noise amplifier (preamplifier) that operates at frequencies up to 3 GHz and can be manually turned on or off is desirable.

A.3 Procedures for Observing Interference Energy in the NEXRAD IF Stage

Part I: Build a Catalog of NEXRAD Interference Source Azimuths.

1. Put the NEXRAD into receive-only mode, with the transmitter klystron either turned off or running into a dummy load.
2. Adjust the NEXRAD antenna elevation angle to either 0° or 0.5° . (The lowest angle will usually provide maximal coupling into interference sources but 0.5° will more accurately reproduce the minimum scan elevation angle of the radar when it is performing volume scans.)
3. Adjust the NEXRAD antenna azimuth to true north (0°).
4. Turn on the spectrum analyzer and connect it to J3 in the NEXRAD receiver cabinet.
5. Tune the spectrum analyzer center frequency to 57.56 MHz, the center frequency of the NEXRAD IF output.
6. Set the spectrum analyzer to zero-hertz span. It will now show the time domain, not the frequency domain.

7. Set the spectrum analyzer input attenuation level to 0 dB.
8. Set the spectrum analyzer resolution (IF) bandwidth to 1 MHz.
9. Set the spectrum analyzer video bandwidth to be equal to or greater than 1 MHz.
10. Set the detection mode to RMS average. If the analyzer does not have an average detection mode, then set the detection mode to “sample” and adjust the video bandwidth to 10 kHz, leaving the resolution bandwidth at 1 MHz.
11. Set the spectrum analyzer trace mode to clear-write.
12. Verify that the noise level displayed on the spectrum analyzer is actually the noise level of the NEXRAD receiver. Do this by momentarily disconnecting the spectrum analyzer signal input while observing the noise. If the displayed noise level drops when the analyzer input is disconnected, then the displayed noise level is confirmed as being that of the radar receiver; skip to Step (14).
13. If the displayed level does not drop when the analyzer is disconnected, then turn on the spectrum analyzer’s internal low noise amplifier (preamplifier) and perform Step (12) again. If the radar receiver noise is still not visible when the preamplifier is on, verify that the receiver circuitry is operative and that the analyzer is connected to the receiver at J3, and try again.
14. Put the spectrum analyzer into “single sweep” mode, in which a single sweep can be manually triggered at the front panel of the analyzer.
15. With one person operating the radar antenna and another person operating the sweep trigger on the analyzer, agree to a reasonable time interval within which the radar antenna can be scanned through 0 to 360 degrees. This might be, for example, three minutes (2 degrees/second antenna scan rate). The radar antenna operator will know a good scan rate to use. Set the spectrum analyzer sweep time to be equal to the anticipated antenna scan interval and prepare to start a manually triggered sweep on the analyzer.
16. Coordinating verbally with the radar antenna operator, perhaps with a short verbal countdown, begin the NEXRAD antenna rotation at the same moment as the manually triggered sweep on the spectrum analyzer. (This process will probably involve a few false starts before it works successfully.)
17. As the NEXRAD antenna rotates, the analyzer sweep progresses. Interference sources will become visible as bumps above the radar noise floor.
18. When the sweep is completed, stop the NEXRAD antenna rotation and view and record the analyzer sweep.
19. For each bump on the analyzer display, correlate the time during the sweep to the corresponding azimuth angle of the NEXRAD antenna. For example, if a bump occurs at the 60 second point in a 180 second sweep, then the corresponding azimuth is $(60/180) \times 360^\circ =$

120°. In actual practice these azimuths will only be accurate to about 2–3 angular degrees, but they are close enough for the next steps.

20. Make a list of each azimuth where interference energy has been noted.

The first part of the interference-analysis process is now complete, with a catalog of interference azimuths having been compiled. Some of these will correspond to visible strobe azimuths, but others will probably have been found for which no strobes are visible. RMS average detection is used to compile this catalog because too many impulsive ticks tend to appear in the 360° scan when peak detection is used. At this point, however, the analyzer detection mode will be switched to positive peak so as to show the full I/N ratio of each individual interference source.

Part II: Determine Exact Interference Azimuths.

1. Keep the NEXRAD in receive-only mode, with the transmitter klystron either turned off or running into a dummy load.
2. Switch the spectrum analyzer detector mode to positive peak. (This is *not* maximum-hold trace mode; keep the analyzer in its clear-write trace mode.)
3. Using the catalog of interference azimuths compiled in Part I, identify the first azimuth that will be examined.
4. Subtract 5 degrees from that azimuth. Ask the NEXRAD antenna operator to move the NEXRAD antenna to this position.
5. With the antenna operator, prepare to move the NEXRAD antenna through 10 degrees of azimuth at a slow rate, perhaps 0.5° per second. This will therefore require 20 seconds to move through 10 degrees of arc.
6. Set the spectrum analyzer sweep time to this interval and prepare to take a single sweep when the start-sweep button is pushed.
7. Repeating the earlier-established coordination process for synchronizing a single spectrum analyzer sweep with the NEXRAD antenna rotation, take an analyzer sweep while the NEXRAD antenna moves.
8. When the interference power maximizes on the spectrum analyzer screen, the analyzer operator should call out “mark” to the antenna operator, who should note the antenna azimuth at that moment. If the action seems too fast, slow down the antenna scan rate and lengthen the corresponding analyzer sweep time, and repeat this process at a slower rate.
9. In the azimuths-of-interference catalog, note this more-exact interference azimuth.
10. Repeat steps 3–8 for each azimuth in the original catalog.

Note: If several interference azimuths are close to each other, they do not necessarily need to be individually assessed. Instead, swing the NEXRAD antenna through several of the azimuths as a

group. But be sure to start at an azimuth that is at least 5 degrees lower than the first azimuth in the group and end the sector scan at an azimuth that is at least 5 degrees greater than the last azimuth in the group. Call out “mark” for each azimuth in the group as the antenna swings through the peak level on each one, with the NEXRAD antenna operator noting the exact antenna azimuth each time a mark is called out.

The end result of Part II is an improved catalog of exact azimuths (each accurate to about 1 angular degree) for each interference bump that is observed in the NEXRAD IF stage.

Part III: Observe and Record Interference Power Level and Time-Domain Characteristics on Each Azimuth.

1. Keep the NEXRAD in receive-only mode, with the transmitter klystron either turned off or running into a dummy load.
2. Using the catalog of exact interference azimuths compiled in Part II, identify the first azimuth that will be examined in the time domain.
3. Move the NEXRAD antenna to that azimuth while examining the interference level on the spectrum analyzer. Fine-tune the azimuth, if necessary, to maximize the interference power level. Confirm the NEXRAD antenna azimuth.
4. Holding the NEXRAD antenna azimuth fixed on this azimuth, set the analyzer sweep time to 50 msec.
5. The analyzer display should now show the interference characteristics in the time domain. If more or less resolution is needed for this observation, adjust the analyzer’s sweep time appropriately.
6. Perform a recording or screen capture of this interference. *Be sure to correlate the recording with the NEXRAD antenna azimuth.* This recording documents both the peak power of the interference and its time-domain behavior.
7. Move the NEXRAD antenna to the next interference azimuth and repeat steps (3) through (6) until all azimuths have been examined.

When this process has been completed, the interference level, I , and the time domain characteristics of the interference on each azimuth will have been documented. The work is now ready to proceed to examination of the RF spectrum via observations that will be performed at the NEXRAD antenna feed, inside the bubble at the top of the antenna tower.

A.4 Procedures for Observing Interference Energy in the NEXRAD RF Stage

Proceed with the spectrum analyzer to the top of the NEXRAD tower.

1. Disconnect the NEXRAD antenna output *ahead* of the RF bandpass filter.

2. Adjust the NEXRAD antenna elevation angle to the same elevation angle (0° or 0.5°) as was used for the IF measurements.
3. Turn on the spectrum analyzer and connect it to the NEXRAD antenna output inside the pedestal, confirming that the bandpass filter is *not* in the path.
4. Tune the spectrum analyzer to sweep from 2600 MHz to a frequency slightly higher than that of the NEXRAD.
5. Set the spectrum analyzer input attenuation level to 0 dB.
6. Turn on the spectrum analyzer internal preamplifier.
7. Set the spectrum analyzer resolution (IF) bandwidth to 1 MHz.
8. Set the spectrum analyzer video bandwidth to be equal to or greater than 1 MHz.
9. Set the detection mode to positive peak.
10. Set the spectrum analyzer trace mode to clear-write.
11. Call to the NEXRAD antenna operator and request that the antenna azimuth be rotated to the first interference azimuth in the catalog.
12. Set the spectrum analyzer trace mode to maximum-hold.
13. Allow the spectrum envelopes of various emitters to fill in, and then record (i.e., screen capture or equivalent) the spectrum analyzer display. *Be sure to correlate each spectrum scan with the NEXRAD antenna azimuth.*
14. Repeat steps 10–13 until all the interference spectra on all azimuths have been examined and recorded.

**APPENDIX B: INTERFERENCE TIME WAVEFORMS ON TWELVE AZIMUTHS OF
THE JACKSONVILLE NEXRAD RECEIVER**

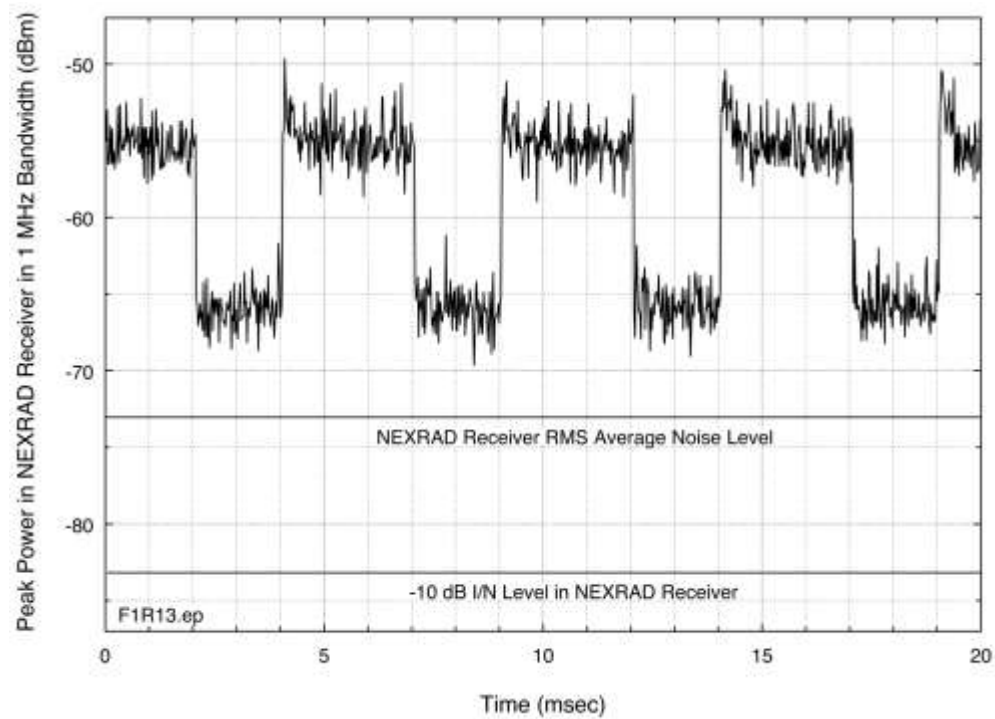


Figure B-1. WiMAX interference, Jacksonville NEXRAD, 75.5° azimuth.

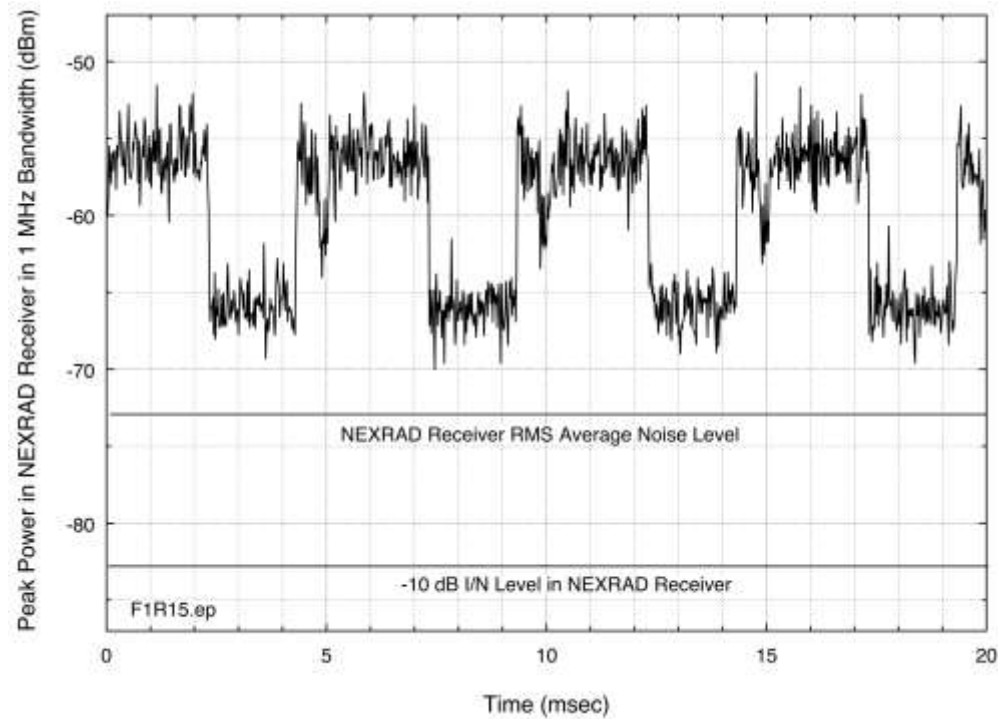


Figure B-2. WiMAX interference, Jacksonville NEXRAD, 84.5° azimuth.

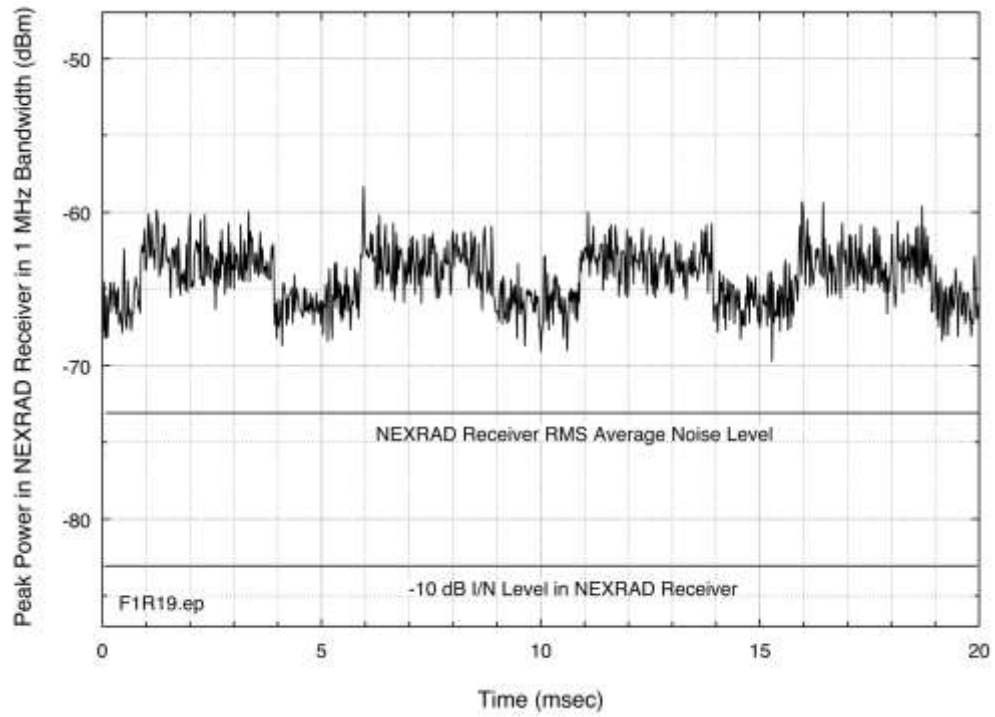


Figure B-3. WiMAX interference, Jacksonville NEXRAD, 101.0° azimuth.

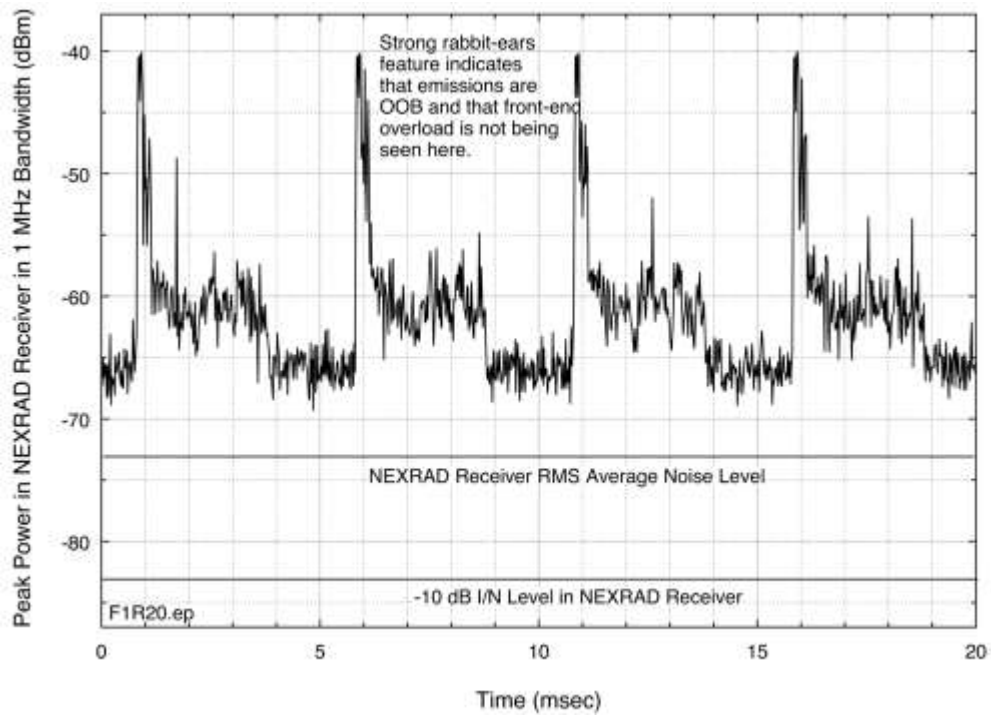


Figure B-4. WiMAX interference, Jacksonville NEXRAD, 116.0° azimuth.

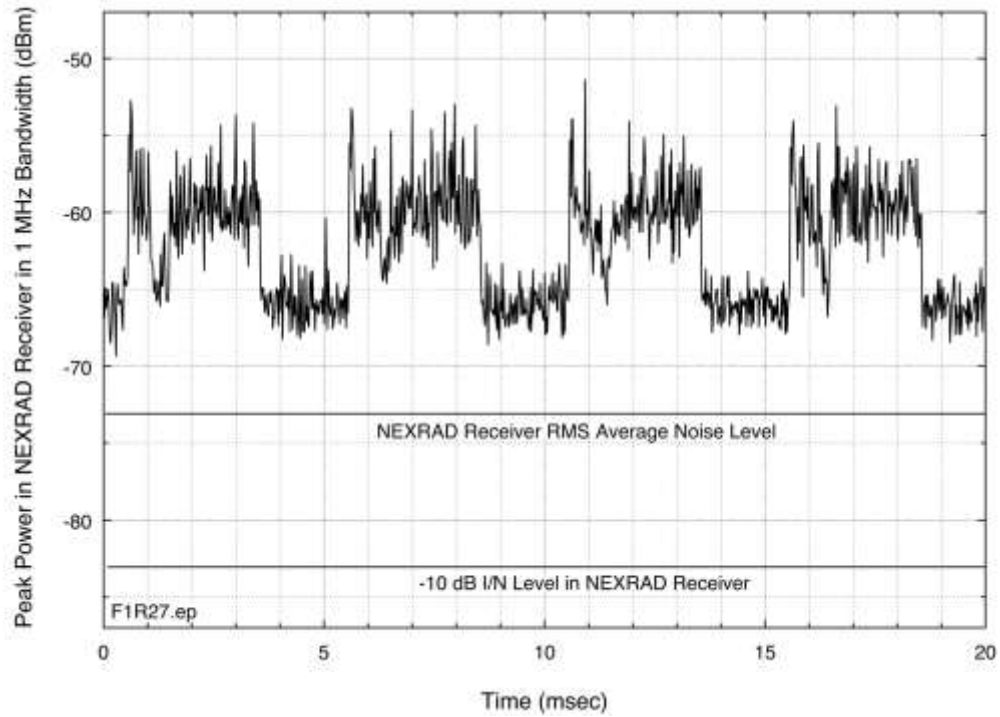


Figure B-5. WiMAX interference, Jacksonville NEXRAD, 135.5° azimuth.

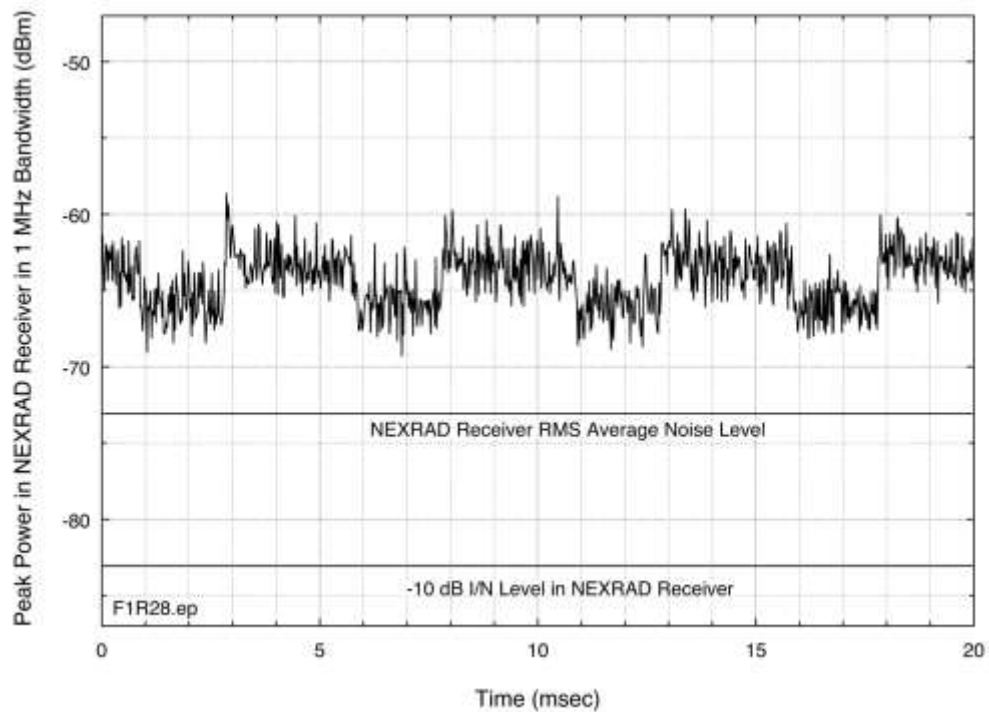


Figure B-6. WiMAX interference, Jacksonville NEXRAD, 143.5° azimuth.

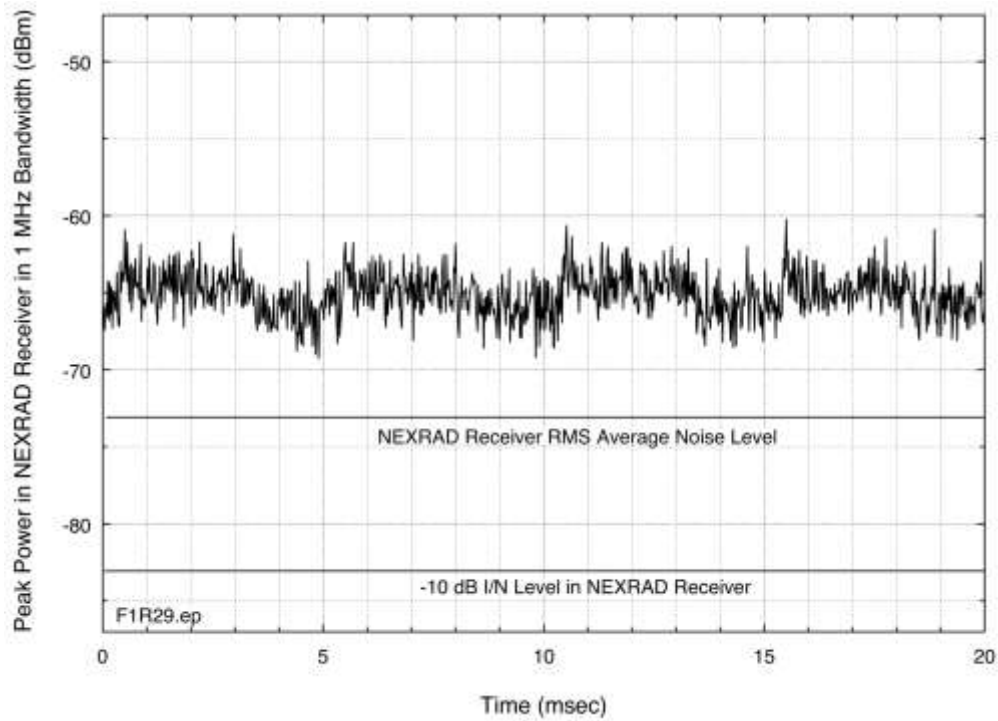


Figure B-7. WiMAX interference, Jacksonville NEXRAD, 148.5° azimuth.

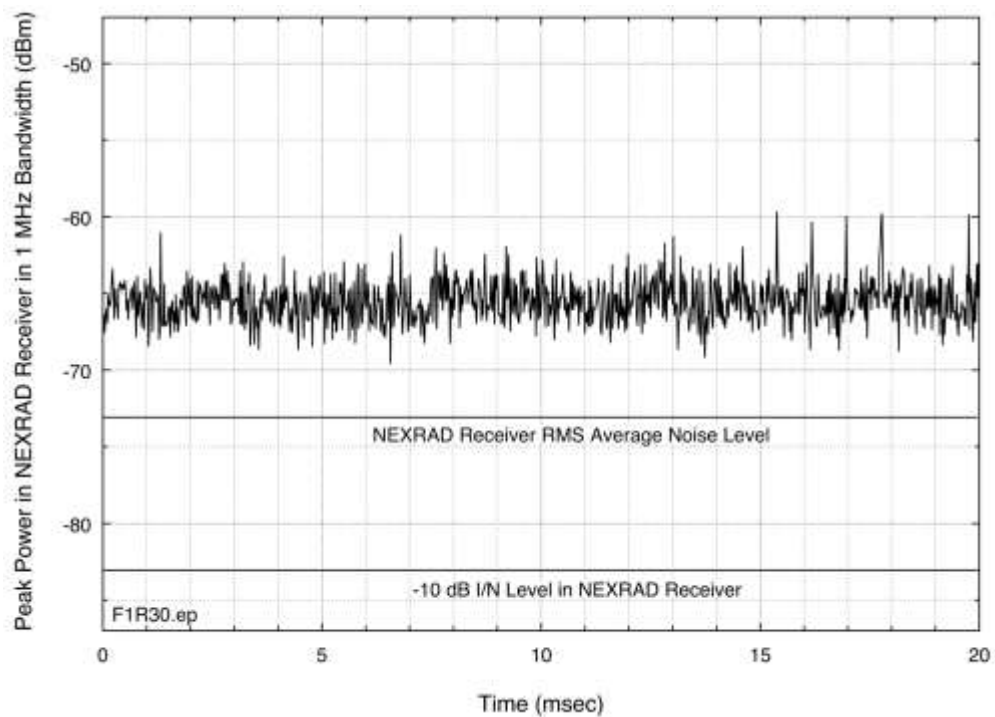


Figure B-8. WiMAX interference, Jacksonville NEXRAD, 151.0° azimuth.

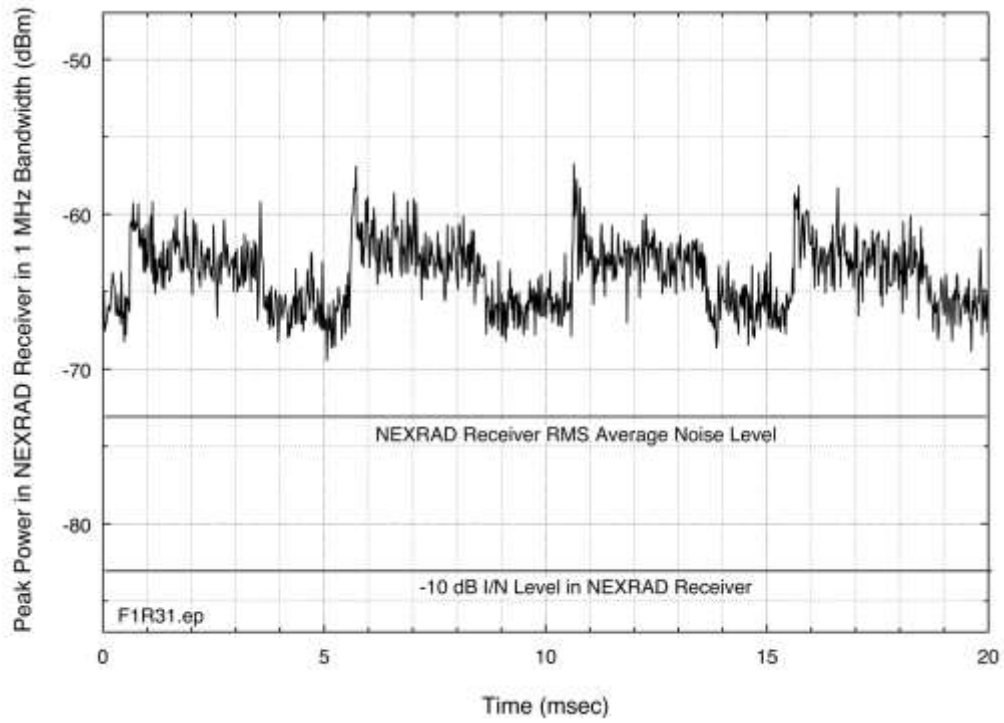


Figure B-9. WiMAX interference, Jacksonville NEXRAD, 157.0° azimuth.

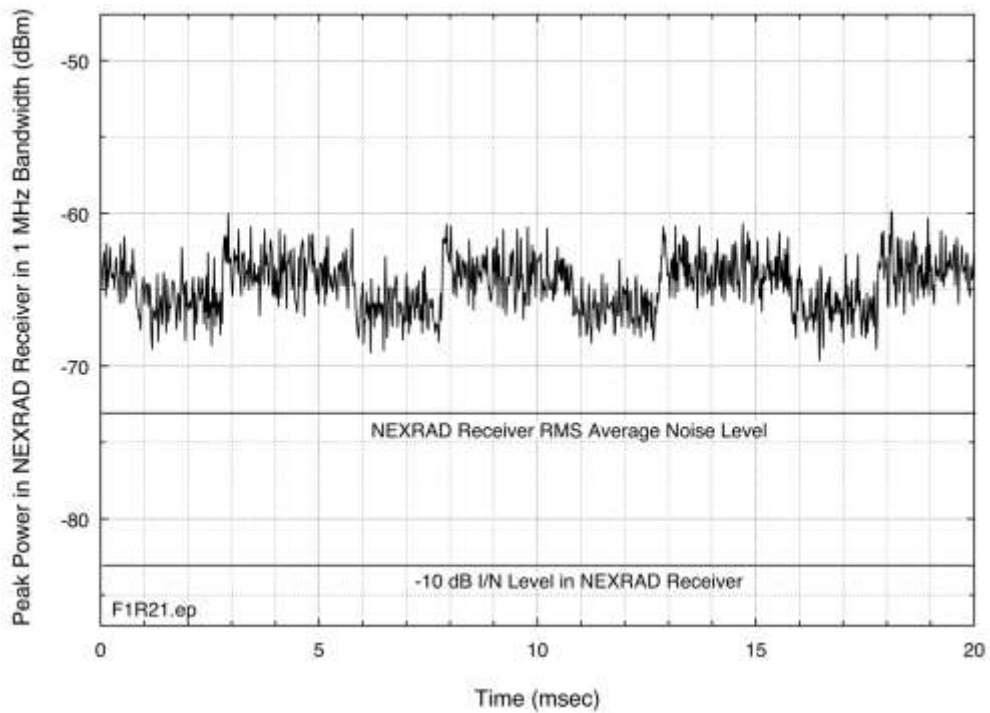


Figure B-10. WiMAX interference, Jacksonville NEXRAD, 160.7° azimuth.

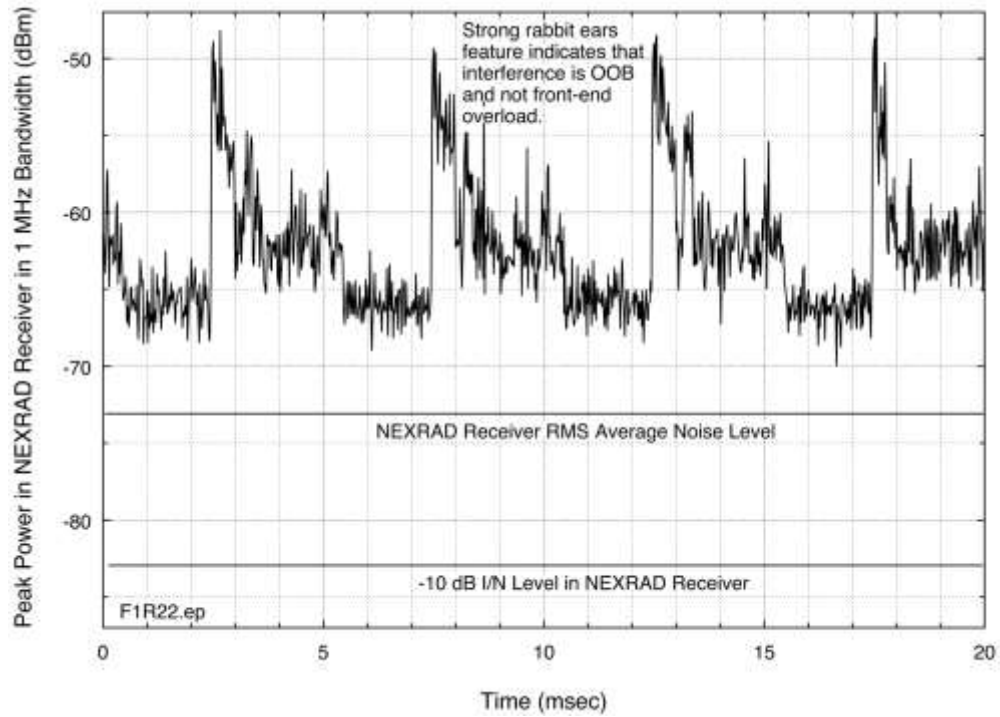


Figure B-11. WiMAX interference, Jacksonville NEXRAD, 192.0° azimuth.

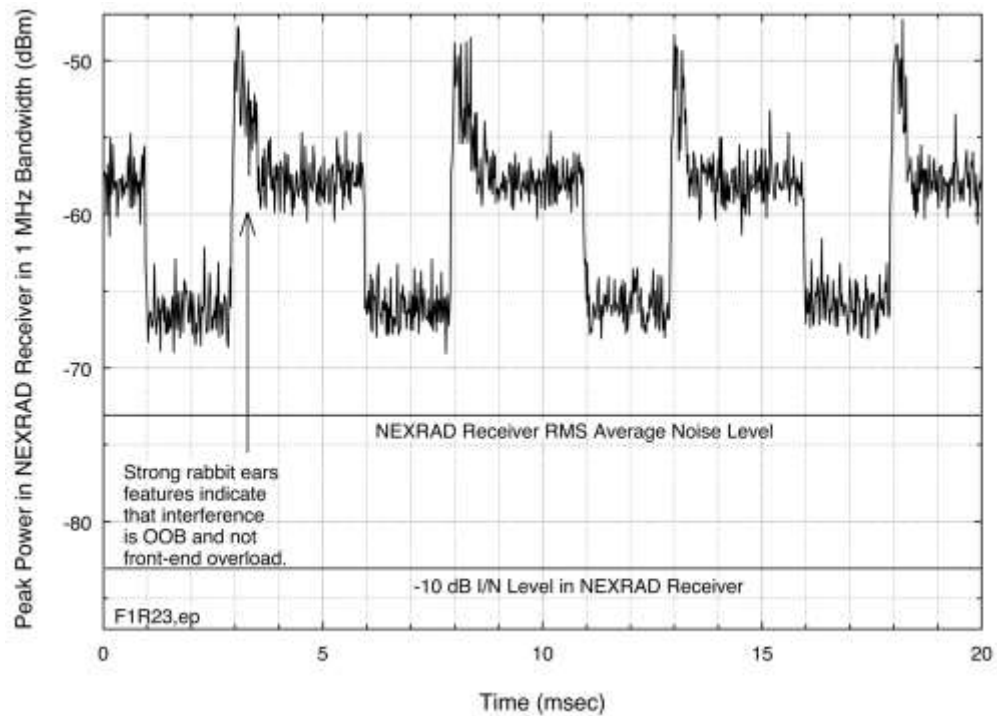


Figure B-12. WiMAX interference, Jacksonville NEXRAD, 200.3° azimuth.

APPENDIX C: ASR TECHNICAL CHARACTERISTICS

C.1 ATC Radars Operating in the Band 2700-2900 MHz

The ASR-8, -9, and -11 are airport-area air traffic control (ATC) radars used in the United States for the safe operation of aircraft in the safety-of-life National Airspace System (NAS).²⁰ The Department of Defense (DoD) operates electronically equivalent ground radar navigation (GPN) radars, models 20, 22, 27, and 30, for non-safety-of-life air surveillance. The ASR-11 is the newest ASR design to have been integrated into the NAS. The ASR-8 and ASR-9 transmitters use high-power klystron tubes. The ASR-11 uses a solid-state transmitter.

ASR-8 and -9 radars transmit unmodulated (called P0N in the Government Master File (GMF)) pulses in staggered sequences. The ASR-11 transmits staggered sequences of pairs of P0N and frequency-modulated (chirped) pulses. The P0N pulses of all three radars are close to 1 μ s long, but the ASR-11 chirped pulse is about one hundred times longer (Table C-1).

The maximum range for ASRs is about 220 km (120 nmi); however, they most effectively operate out to 110 km (60 nmi). The ASR-8 and ASR-9 systems have been in service longer than the ASR-11; their high power klystrons transmit relatively short (approximately 0.8 μ s) pulses. They provide air surveillance coverage with fan-beam, high-gain antennas with a typical height above ground of tens of meters, as shown in Figure C-1, with the lower edges of the antenna patterns angled slightly upwards. Fan-beam coverage provides range and azimuth information for aerial targets, but elevation-angle (height) information is not provided for ASR targets. Table C-1 lists technical characteristics of ASRs.

All ASRs are RSEC Criteria D radars.²¹ RSEC D criteria were originally developed to allow tighter, more efficient spectrum packing of the 2700–2900 MHz band by ASRs. Since the advent of RSEC D, these radars' designs have emphasized efficient RF design for both the transmitters and the receivers. For ASR transmitters this meant abandoning magnetron transmitter tubes in favor of more expensive but higher-performance klystron tubes for the ASR-8 and ASR-9 and solid-state transmitters for the ASR-11.

Historically, ASR receivers were expected to operate in environments where signals in other bands were not expected to provide EMC design challenges. This assumption no longer holds true. In late 2010, NTIA engineers performed detailed receiver-characteristics measurements on ASR receivers at the FAA's Mike Monroney Aeronautical Center in Oklahoma City to determine the extent to which the ASR receivers are compatible with high-power signals in other bands.

²⁰ A few older ASR-7 radars continue to operate in the United States, but most have been replaced with newer ASR models.

²¹ RSEC D requires that the radar receiver bandwidths be commensurate with transmitted pulse widths; these bandwidths are typically about 1 MHz.



Figure C-1. An airport surveillance radar antenna (here an ASR-11) as typically deployed on a tower. The beacon antenna is part of an electronically separate system.

Table C-1. Summary of ASR technical characteristics (as provided by FAA).

Parameter	ASR-8 Value	ASR-9 Value	ASR-11 Value
Peak transmitter power	1 MW	1.32 MW	25 kW
Transmitter type	klystron tube	klystron tube	solid state
Operational frequency range	2700–2900 MHz	2700–2900 MHz	2700–2900 MHz
Antenna type	modified parabolic reflector with stacked feed horns	modified parabolic reflector with stacked feed horns	modified parabolic reflector with stacked feed horns
Antenna gain	34 dBi	34 dBi	34 dBi
Typical antenna height above ground	12 m (40 ft)	12 m (40 ft)	12 m (40 ft)
Antenna beam type	1/(cosecant squared) vertical fan beam	1/(cosecant squared) vertical fan beam	1/(cosecant squared) vertical fan beam
Antenna beam width	2.3° (horizontal) 0.3°–30° (vertical)	2.3° (horizontal) 0.3°–30° (vertical)	2.3° (horizontal) 0.3°–30° (vertical)
Antenna polarization	right & left circular	right & left circular	vertical
Antenna sidelobe levels	At least 25 dB below main-beam gain	At least 25 dB below main-beam gain	At least 25 dB below main-beam gain
Antenna beam-scanning protocol	0°–360° rotational	0°–360° rotational	0°–360° rotational
Antenna beam-scanning rate	12.5 rpm (4.8 sec/scan)	12.5 rpm (4.8 sec/scan)	12.5 rpm (4.8 sec/scan)
Transmitted pulse widths	0.6 μs	1.05 μs	1 μs (CW pulse) 89 μs (linear FM)
Transmitted pulse modulation	P0N (unmodulated CW pulses)	P0N (unmodulated CW pulses)	P0N and Q3N (unmodulated CW pulses paired with linear FM pulses)
Transmitted pulse repetition rates	1014 pulses/sec (average) in a 4-stagger* sequence	1156 pulses/sec (average) in a 4-stagger* sequence	856 pulses/sec (average) in a 4-stagger* sequence
Receiver target-processing bandwidth	1.2 MHz	0.7 MHz	1.1 MHz
Nominal receiver noise figure	2 dB	2 dB	2 dB
Thermal noise level in receiver bandwidth (computed)	-111.2 dBm	-113.2 dBm	-111.6 dBm

*Stagger sequences are groups of pulses with non-integer-divisible time divisions between them. Staggering of pulses eliminates Doppler-processing blind speeds in moving-target-indicator (MTI) air traffic control data processing.

C.2 Objectives

The objectives of the measurements described in this section were to measure and record, for each of the ASR-8, ASR-9 and ASR-11 receivers, the following characteristics:

1. The frequency-domain response of the RF front end filter
2. The frequency-domain response and gain-compression characteristics of the LNA
3. The frequency-domain response of the IF stage
4. The frequency response of the overall receiver, consisting of the filter, the LNA and the IF stage
5. The receiver's overall architecture (i.e., the inventory and ordering of components in the receiver)

C.3 Measurement Procedures

The receiver-characteristics measurements were performed via hardline-coupled carrier-wave signals that were injected into each radar receiver at various points to measure the frequency responses for the RF filters, LNAs, and IF stages. The response data were collected and stored as ASCII data files.

C.4 LNA and Bandpass Filter Frequency-Response Measurements

Each radar receiver's RF front-end filter characteristics were measured as follows. With the radar transmitter taken out of operation, a signal generator was connected to the waveguide ahead of all filter and amplifier stages, using a coupled port if available and a hardline connector if necessary. The signal generator was configured to produce a continuous wave (CW) signal that was pre-programmed to step, in small increments, across the frequency band of interest; the response was measured and recorded using the Agilent E4440 spectrum analyzer, set to the appropriate bandwidth and detector. Figure C-2 shows a general notional diagram of the various measurement configurations for these measurements.

C.5 LNA Gain Compression Measurements

While the measurement system and the radar receiver were configured to measure the LNA frequency response, the spectrum analyzer was also used to measure the power-compression behavior of the LNA. For this measurement, the signal generator was fixed-tuned to the radar's operational frequency. While the LNA output was observed with the spectrum analyzer in a zero-hertz-span mode, the signal generator output power was increased in 10 and 1 dB steps until the response was observed to become non-linear. The response was recorded by the analyzer and later plotted to show LNA output power as a function of input power.

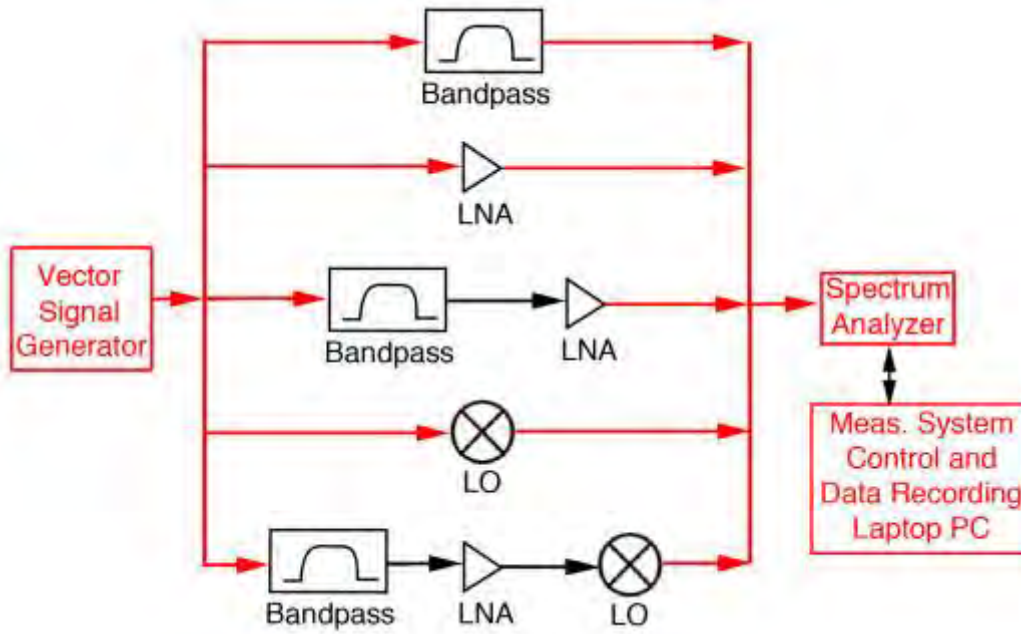


Figure C-2. Schematic measurement block diagram for characterization of the RF and IF stages in ASR receivers. The signal generator was programmed to step in small increments across the frequency bands of interest, and the data were recorded on a computer connected to a spectrum analyzer.

C.6 IF Stage Frequency Response Measurement

When possible, a measurement was performed on the frequency response of the IF alone. This was accomplished by coupling a stepped- frequency CW signal into the LO mixer input while measuring the output of the IF with a spectrum analyzer. Secondly, the IF frequency response was (in effect) measured by using the stepped-frequency CW signal at the input to the first stage of the RF front end while measuring the IF output, as shown in Figure C-2. The RF front-end coupling was the same for the IF response measurements as required for the RF response measurements.

C.7 Measurement Results for ASR Receivers

The results for each of the radars are contained in the following sections.

C.7.1 ASR-8 Receiver Measurement Results

C.7.1.1 ASR-8 Receiver System Architecture

A simplified block diagram of the ASR-8 receiver is shown in Figure C-3. The ASR-8 channel that was examined in these measurements was tuned to 2710 MHz.

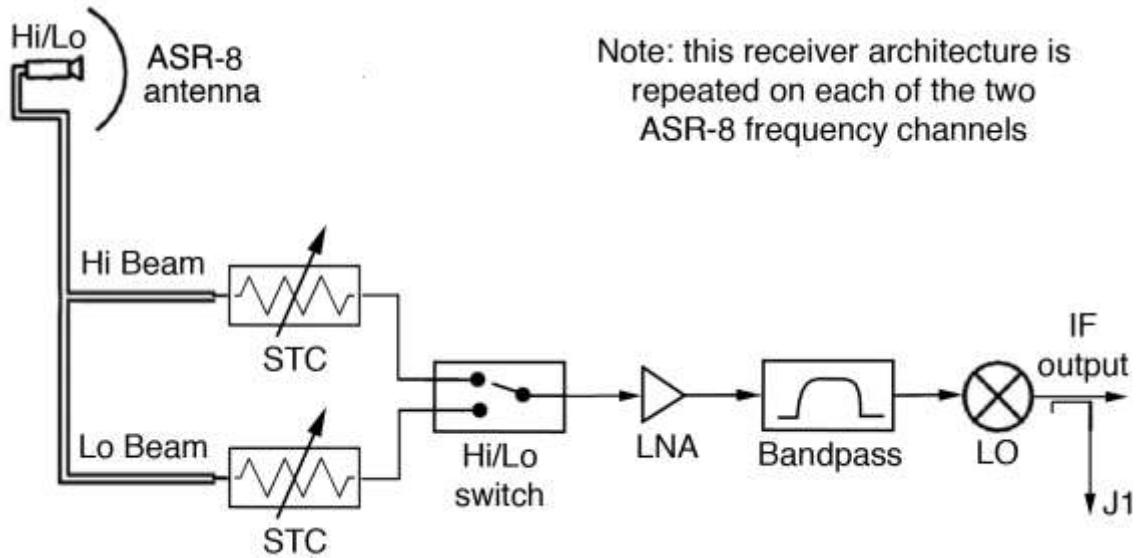


Figure C-3. Simplified block diagram of the ASR-8 receiver.

As shown in Figure C-3, the received RF signal first passes through a step attenuator called sensitivity time control (STC).²² Passing through an antenna switch that selects between high and low antenna beams, it is fed into an LNA. The LNA output then passes through a bandpass (channel) filter and a phase shifter (not shown), and finally a mixer and an IF preamplifier (not shown). The IF signal goes to a video detector which generates pulses that appear as “blips” on the radar’s plan position indicator (PPI) display.

The ASR-8 was designed in the mid-1970s. The spectrum allocations of that era differed substantially from their current designations; the ATC radar designers of that time were not faced with issues of high power communication systems operating in other bands, nor had the NTIA RSEC Criteria D yet been developed.

C.7.1.2 ASR-8 Receiver LNA Frequency Response and Gain Compression

The measured frequency response of the ASR-8 LNA is shown in Figure C-4, the measurement having been performed with a stepped-frequency CW input as described above.

The LNA response is optimized for the 2700–2900 MHz band in which ASRs operate. Substantial response also occurs for frequencies outside this band, and this out-of-band response may become a technical issue of concern regarding communication systems in, for example, the 2496–2690 MHz band.

²² STC is used to attenuate echo returns from objects close to the radar. Such echoes produce unwanted features on radar displays, and STC is a clutter-reduction feature of most radar designs.

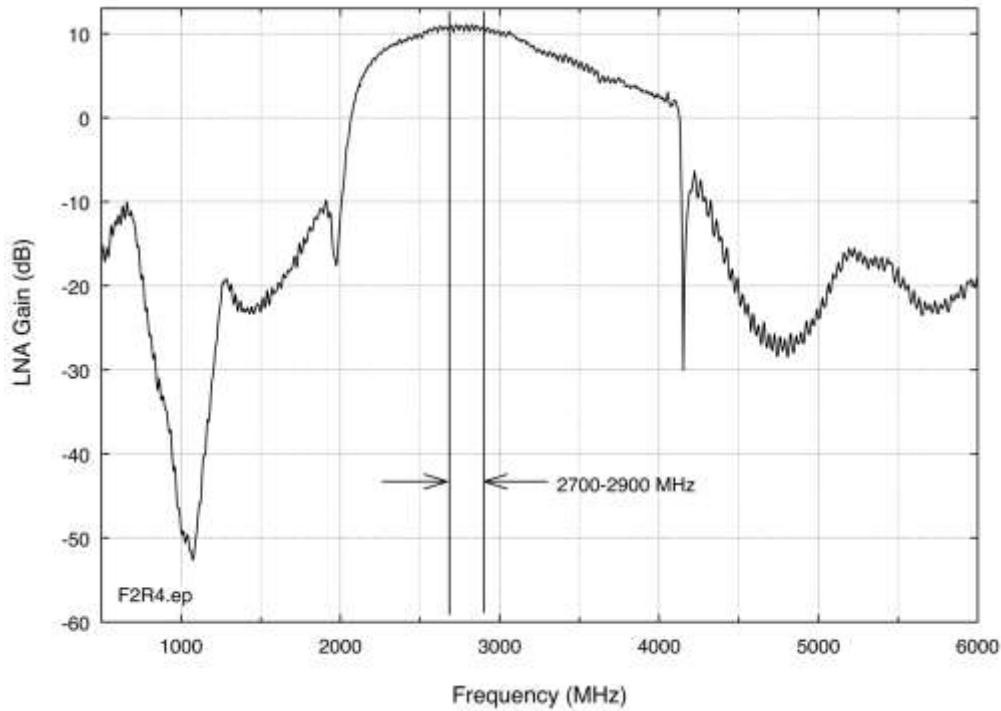


Figure C-4. ASR-8 receiver LNA frequency response.

For receivers such as the ASR-8 that lack filtering in front of the first LNA stage, knowledge of the out-of-band gain response of the LNA is necessary to determine the circumstances under which out-of-band front-end overload of the LNA may occur, with concomitant loss of in-band LNA performance and consequent occurrence of interference effects, as described in [18].

The gain compression characteristic of the LNA was assessed by increasing input power of a carrier wave at 2710 MHz in 1 dB increments from a starting point of -10 dBm while measuring the corresponding increase in output power from the LNA. The measurement continued until the increases in output power were substantially less than 1 dB. The results are shown in Figure C-5.

C.7.1.3 ASR-8 Receiver RF Selectivity

The frequency response of the ASR-8 RF preselector was measured with the stepped-frequency CW signal generator connected to its input and the spectrum analyzer connected to its output, as diagrammed schematically in Figure C-2. Figure C-6 shows the frequency response of the filter. The filter passband is for a single operational radar channel; its design, which is tunable, only passes signals within a portion of the 2700–2900 MHz band.

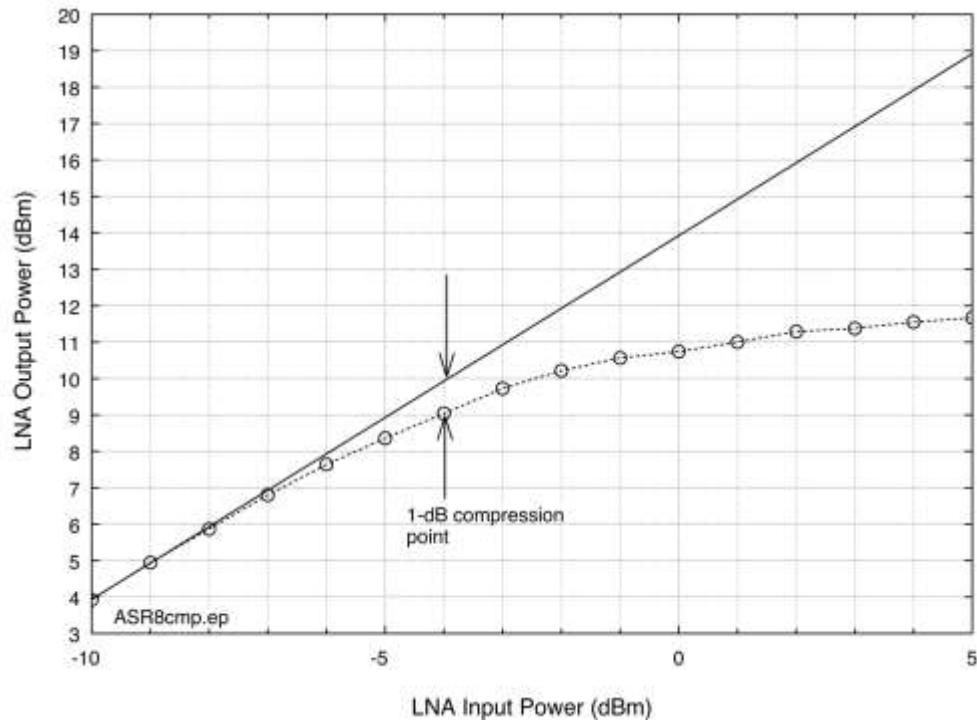


Figure C-5. ASR-8 receiver LNA compression-response curve.

C.7.1.4 ASR-8 Receiver IF Selectivity

The frequency response of the ASR-8 RF filter plus the IF stage was measured. The stepped-frequency CW signal was moved across a frequency range exceeding that of the IF while maintaining a constant input power level. Figure C-7 shows the result.

C.7.1.5 ASR-8 Total Signal Path Selectivity

The total selectivity of the ASR-8 signal path was measured by injecting the signal at the LNA input and measuring the response at the IF output. Figure C-8 shows the result.

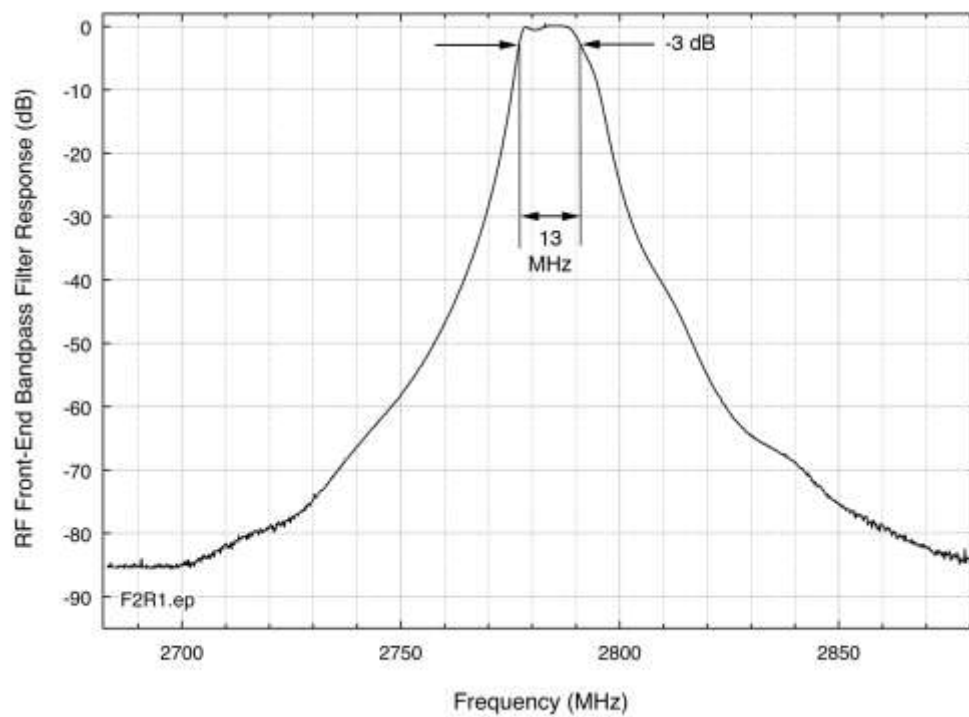


Figure C-6. ASR-8 receiver RF filter response.

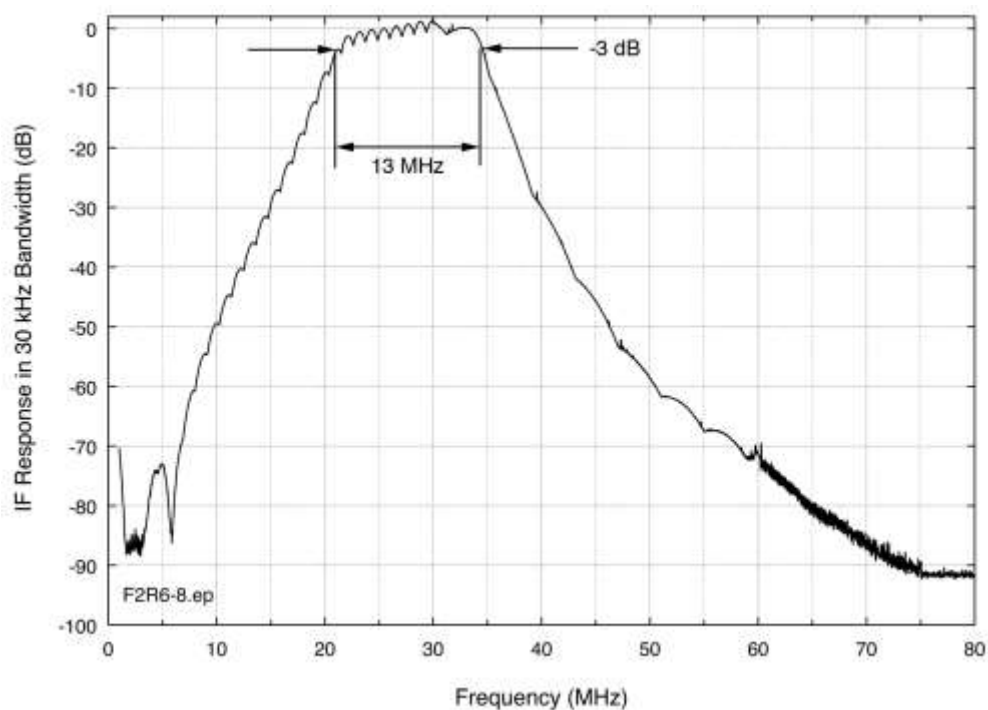


Figure C-7. ASR-8 receiver RF filter plus IF frequency response.

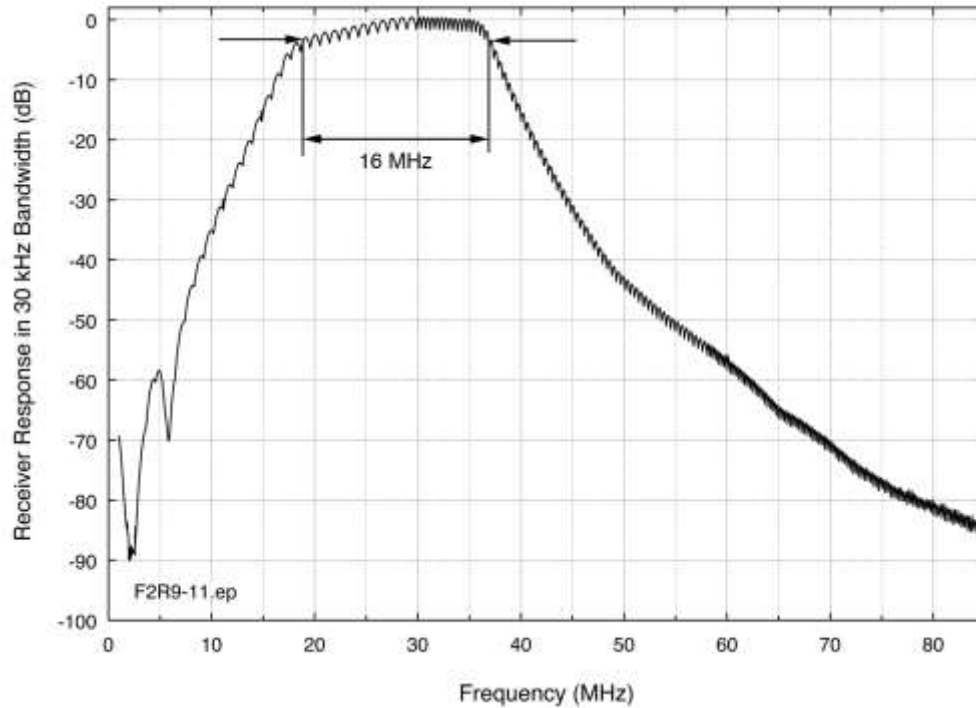


Figure C-8. ASR-8 total receiver selectivity.

C.7.2 ASR-9 Receiver Measurement Results

C.7.2.1 ASR-9 Receiver System Architecture

The ASR-9 was designed in the early 1980s. In contrast to the decision made for the ASR-8 design, the designers of that era placed the preselector RF filter *ahead* of the LNA to provide the receiver with better protection from out-of-band signals and to comply with RSEC Criteria D. Figure C-9 is a block diagram of the receiver architecture for the ASR-9. For these tests, the radar was tuned to 2730 MHz.

C.7.2.2 ASR-9 Receiver LNA Response and Gain Compression

The frequency response of the ASR-9 LNA was measured in isolation from the rest of the receiver. Figure C-10 shows the gain response of the LNA. The gain-compression response of the ASR-9 LNA was measured with the frequency of the signal generator held fixed at 2730 MHz while the input signal power was increased in 1 dB steps starting at -15 dBm. The result is shown in Figure C-11.

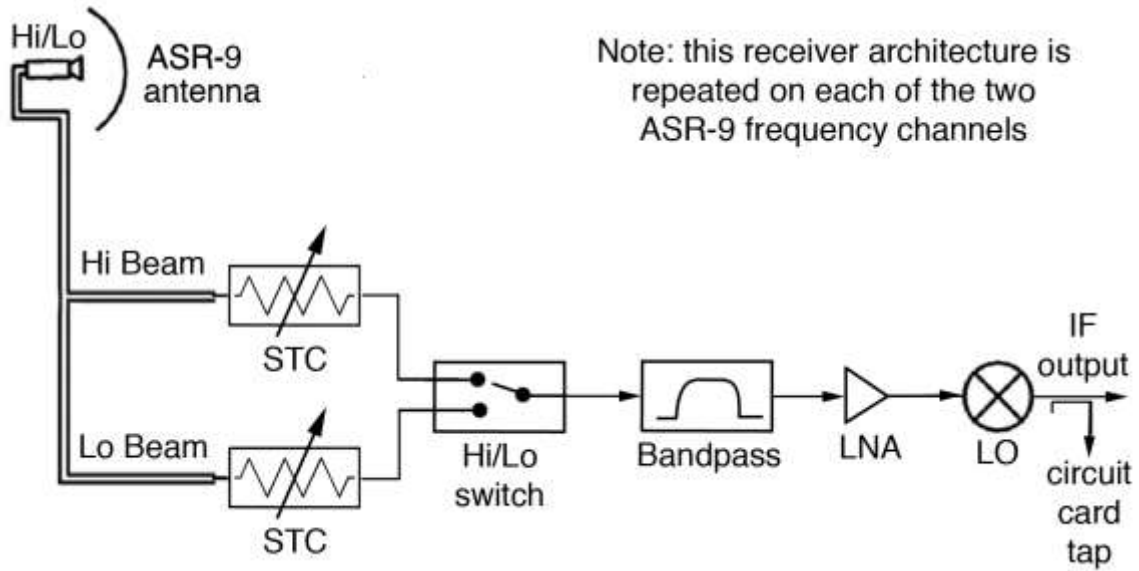


Figure C-9. Simplified block diagram of the ASR-9 receiver.

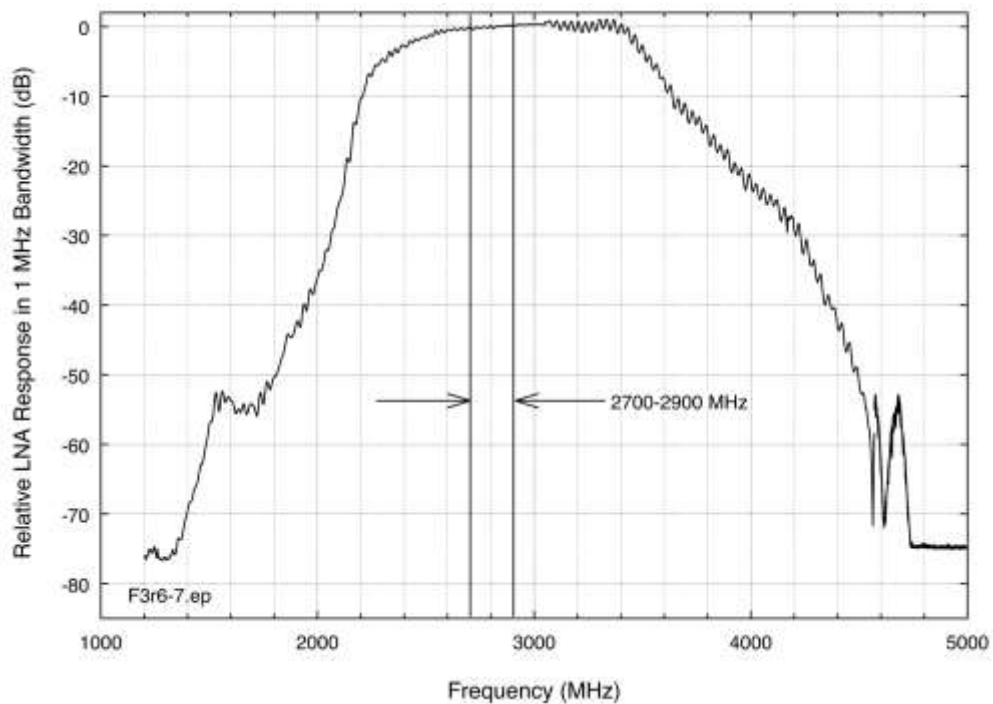


Figure C-10. ASR-9 receiver LNA frequency response.

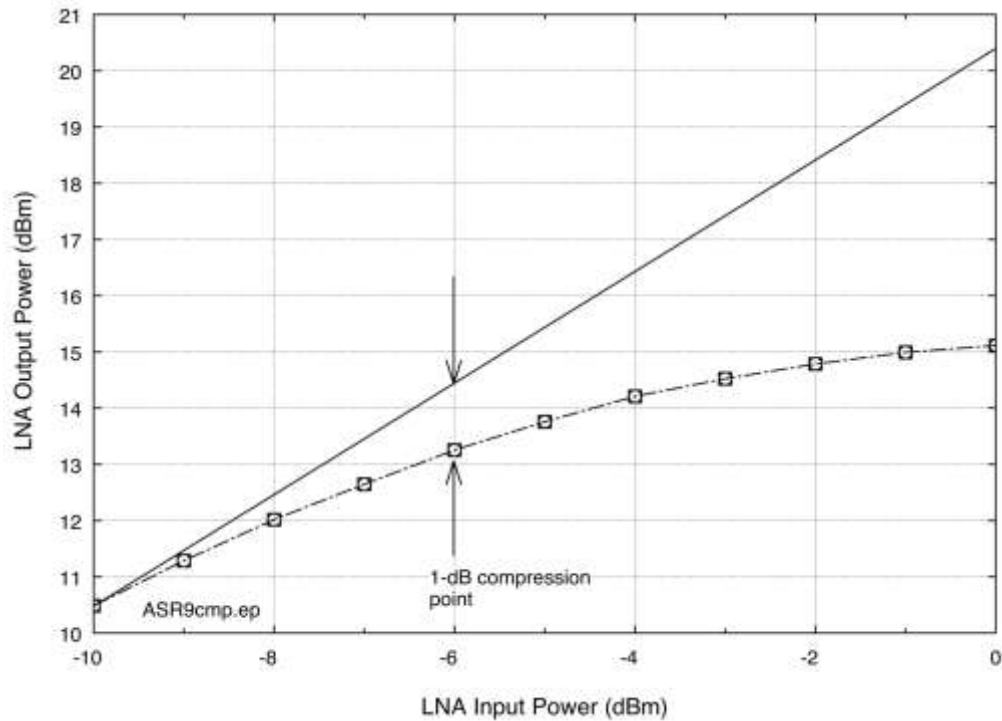


Figure C-11. ASR-9 receiver LNA gain compression response.

C.7.2.3 ASR-9 Receiver RF Selectivity

The frequency response of the ASR-9 RF preselector filter was measured in isolation from the rest of the receiver. Figure C-12 shows the result. This is a tunable channel filter that only passes signals within a portion of the 2700–2900 MHz band. The filter that was used for this measurement was tuned to 2705 MHz; it was not the same filter as the one used in the radar itself, but was the same model. The frequency response of the combination of the RF filter and the LNA is shown in Figure C-13.

C.7.2.4 ASR-9 Receiver IF Selectivity

The frequency response of the combination of the ASR-9 receiver RF filter, LNA, and IF stage was measured; the result is shown in Figure C-14. Effectively, since the IF stage provides the limiting bandwidth in this combination, this is also the IF stage frequency response.

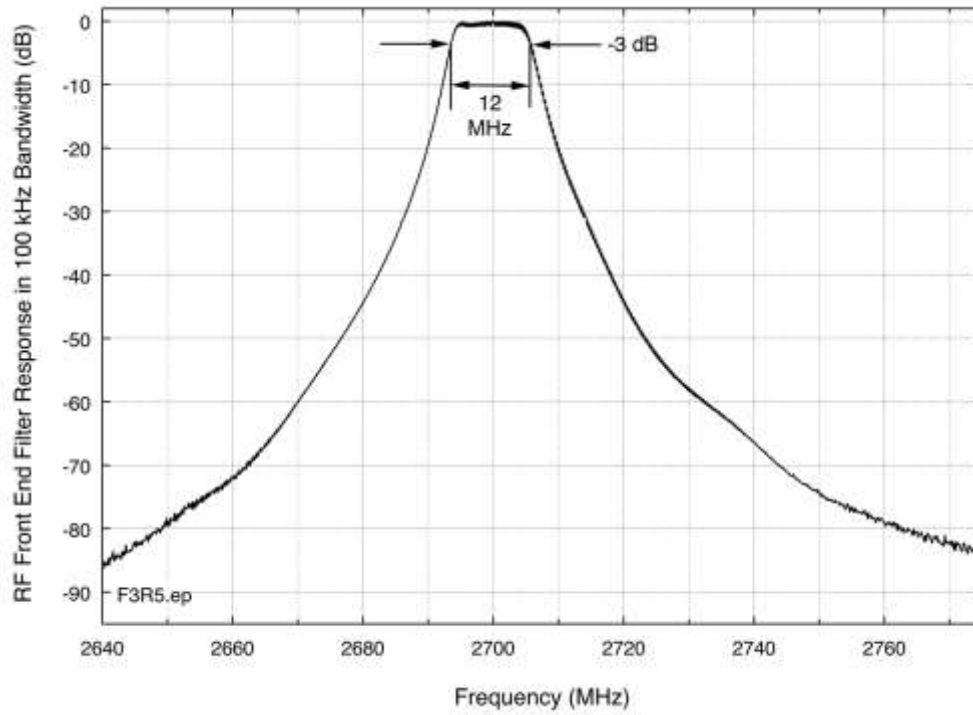


Figure C-12. ASR-9 receiver RF filter response.

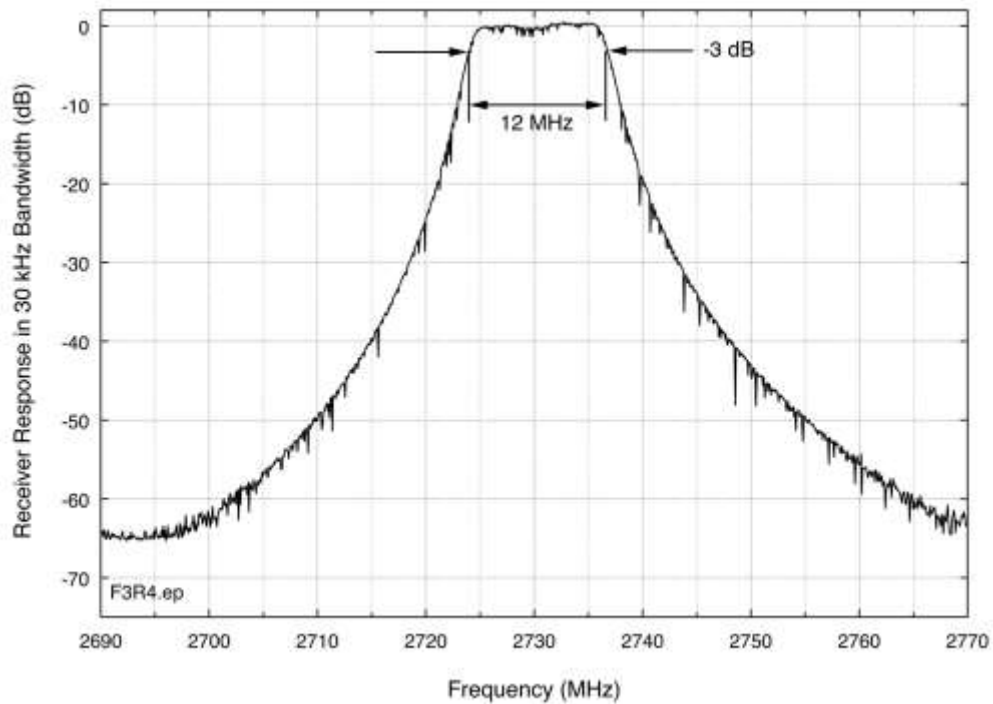


Figure C-13. ASR-9 receiver RF filter plus LNA response.

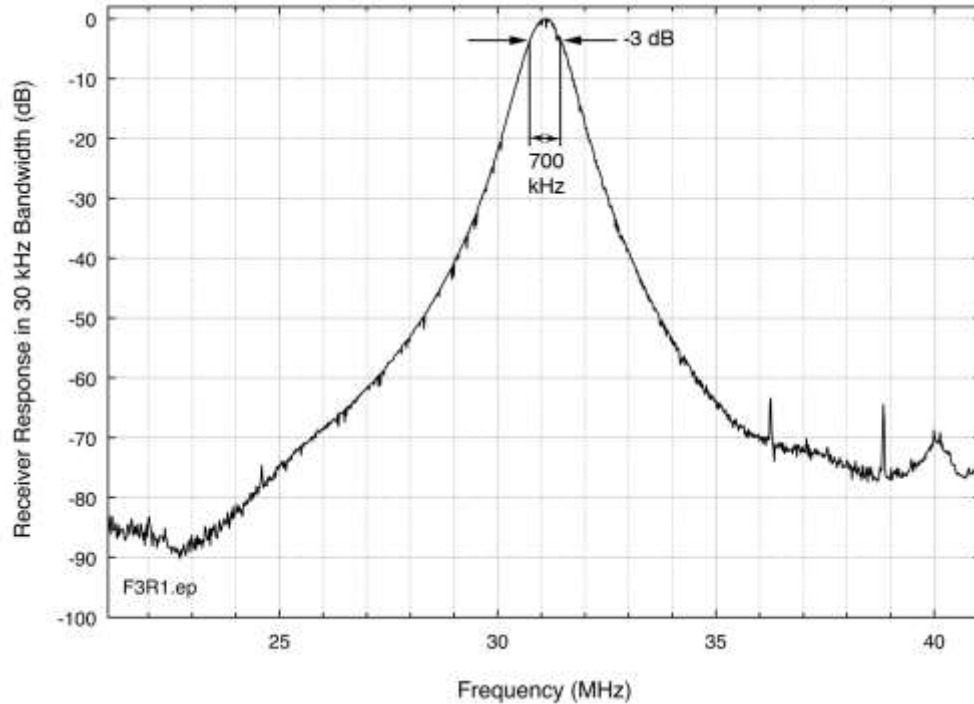


Figure C-14. Overall frequency response of the ASR-9 receiver. This is also the effective frequency response of the ASR-9 IF stage, as that stage provides the limiting bandwidth of the system.

C.7.3 ASR-11 Receiver Measurement Results

C.7.3.1 ASR-11 Receiver System Architecture

The ASR-11 was designed in the mid-1990s. It uses an array of solid-state amplifiers rather than a tube to generate RF pulses and was designed to comply with RSEC Criteria D. The designers placed the preselector RF filter *ahead* of the LNA to provide better receiver protection from out-of-band signals. Figure C-15 is a simplified block diagram of the architecture of the ASR-11 receiver.

C.7.3.2 ASR-11 Receiver LNA Response and Gain Compression

The frequency response of the ASR-11 LNA was measured in isolation from the rest of the receiver by stepping the frequency of a CW signal in small increments across 500–6000 MHz while maintaining a constant input power level. Figure C-16 shows the frequency response of the LNA; Figure C-17 shows its gain-compression response.

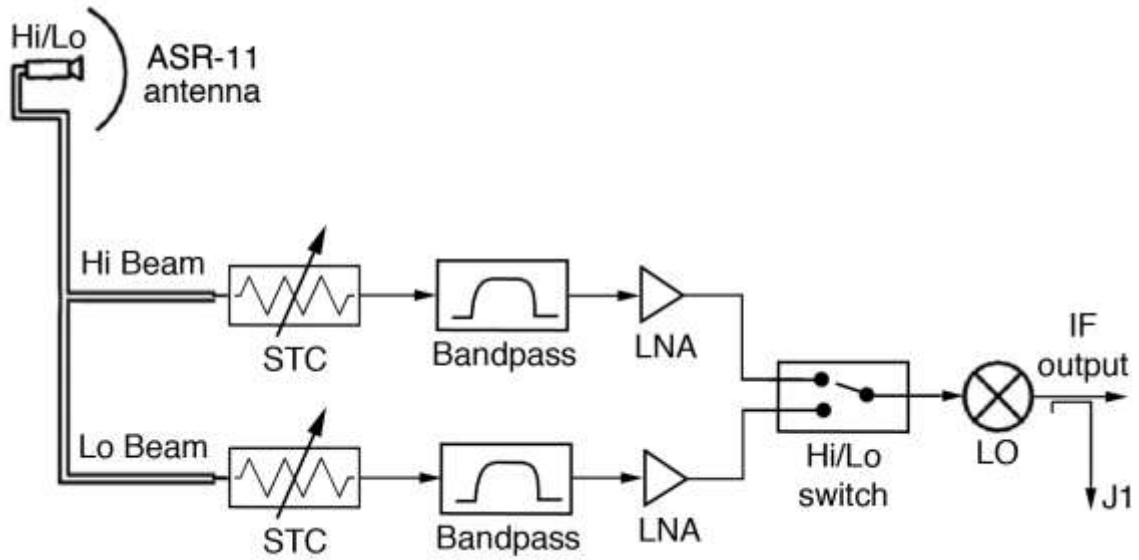


Figure C-15. ASR-11 receiver simplified block diagram.

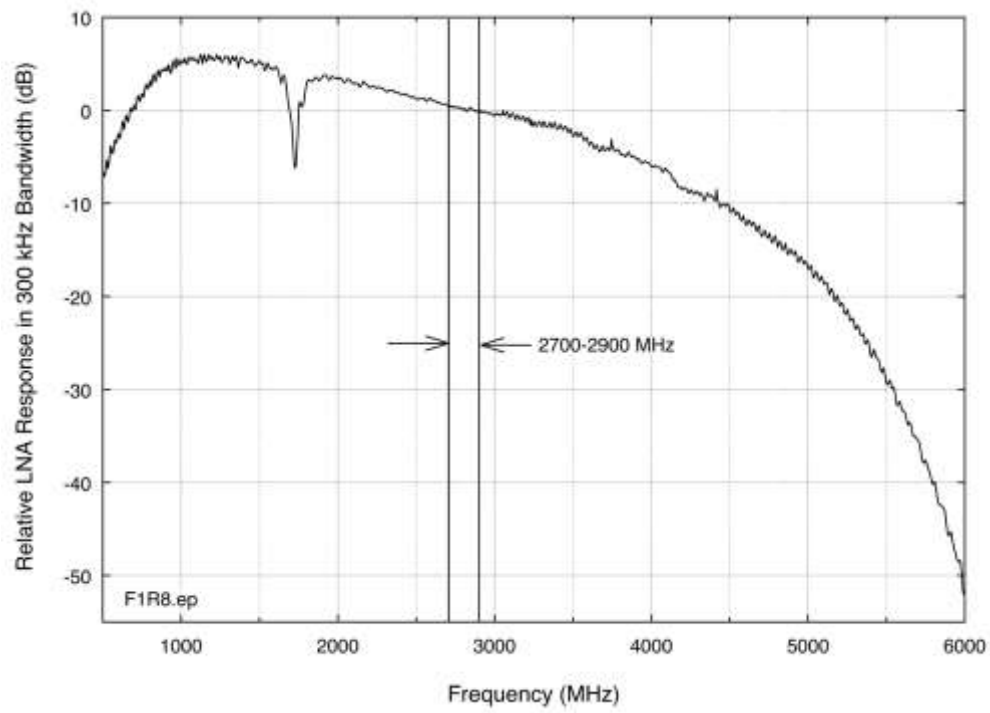


Figure C-16. ASR-11 LNA frequency response.

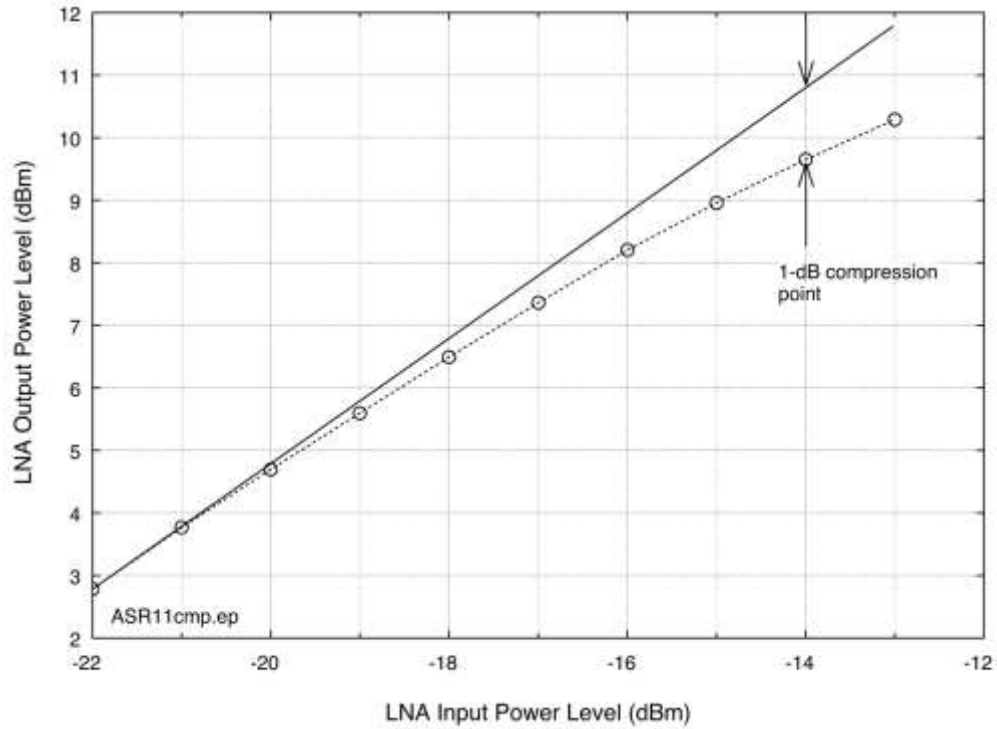


Figure C-17. ASR-11 LNA gain-compression response.

C.7.3.3 ASR-11 Receiver RF Selectivity

The frequency response of the ASR-11 RF preselector filter was measured in isolation from the rest of the receiver; the result is shown in Figure C-18. The filter is a full passband for the spectrum used by ASRs; unlike the preselectors for the ASR-8 and ASR-9 receivers, it is not a narrow-bandwidth channel filter.

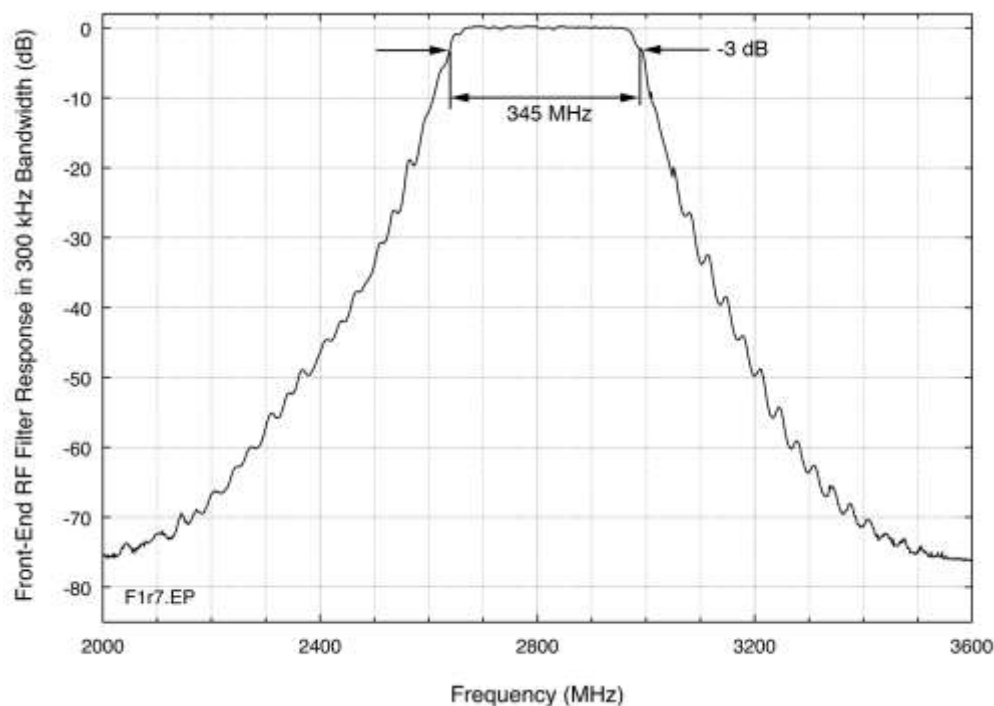


Figure C-18. ASR-11 RF filter frequency response.

C.7.3.4 ASR-11 Receiver IF Selectivity

The frequency response of the ASR-11 IF stage was measured in isolation from the rest of the receiver, between its input and output. The result is shown in Figure C-19.

C.7.3.5 ASR-11 Total Receiver Signal Path Selectivity

The total selectivity of the ASR-11 signal path was measured by injecting the signal at the input of its limiter, ahead of the STC attenuator. The frequency responses of the bandpass filter, LNA, and IF stage were incorporated in this measurement; Figure C-20 shows the frequency response of the entire ASR-11 receiver path.

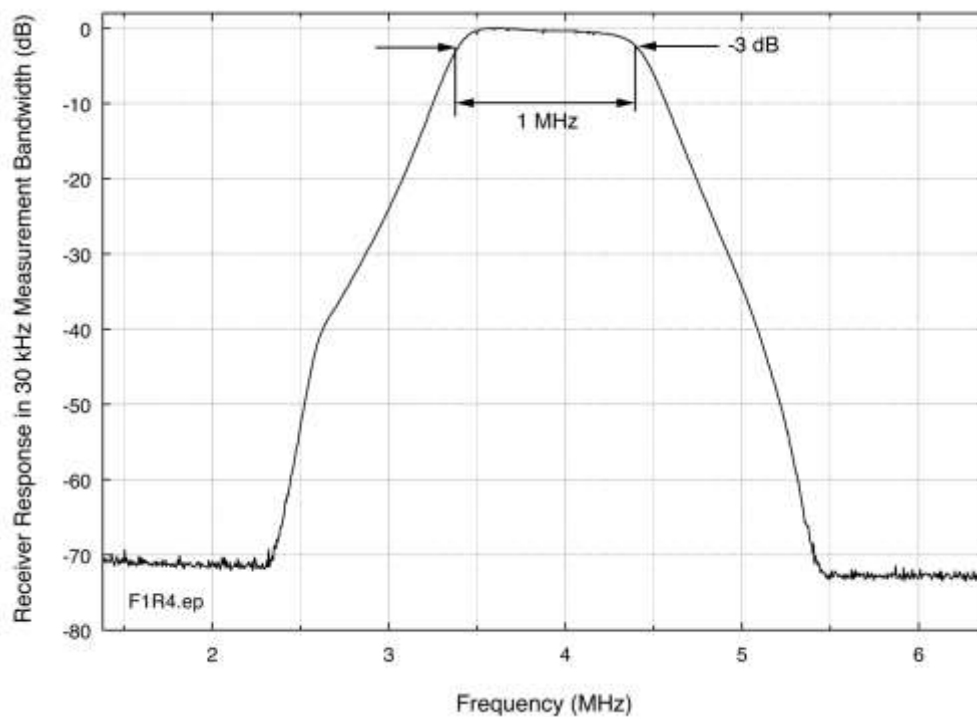


Figure C-19. ASR-11 receiver IF-stage frequency response.

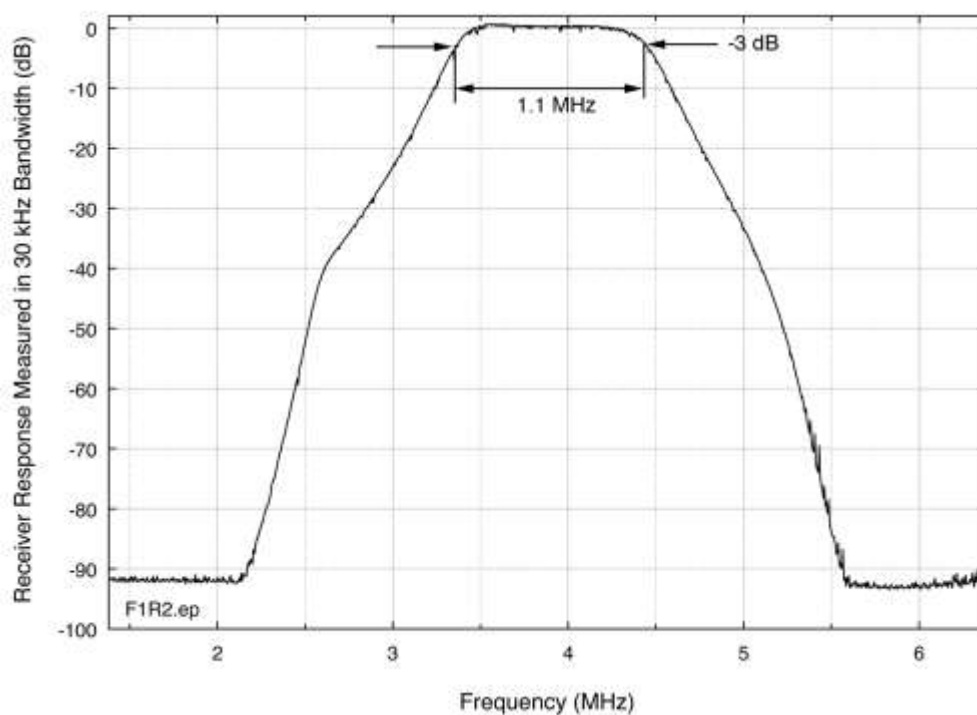


Figure C-20. ASR-11 total receiver frequency response.

C.8 ASR Receiver Characteristics Data Summary

Table C-2 contains the summary of the measured data for ASR receiver characteristics.

Table C-2. Summary data table of measured ASR receiver characteristics.

Radar	RF Filter 3 dB Bandwidth (MHz)	IF 3 dB Bandwidth (MHz)	RF Filter Ahead of LNA	LNA 3 dB Bandwidth	LNA 1 dB Compress. Point (dBm)
ASR-8	13	13*	No	1 GHz (2300-3300 MHz)	-4
ASR-9	12	0.7	Yes	1.1 GHz (2400-3500 MHz)	-6
ASR-11	345	1.1	Yes	1.4 GHz (1800-3200 MHz)	-14

*The final ASR-8 receiver processing bandwidth is assumed to be commensurate with inverse of transmitted pulse width, which would be 1.2 MHz. But at the only accessible linear-IF test point in the receiver the bandwidth was 13 MHz.

C.9 Future Work on ASR Receiver Characteristics and Interference Responses

The data that have been collected on ASR receiver characteristics could be used in future EMC analyses of ASR receiver responses to WiMAX and long-term evolution (LTE) signals. Future work on ASR receivers may include the generation of target probability of detection (P_d) curves as a function of I/N levels for each radar receiver using pre-recorded WiMAX and LTE signals as interference sources. These interference signals will be injected at various power levels and frequency offsets from the tuned frequencies of radar receivers. NTIA may also perform similar measurements on NEXRAD receivers.

APPENDIX D: FDR Curves for WiMAX-to-Radar EMC Analysis

D.1 Objectives of EMC-Curve Development Effort

The objectives of the EMC-curve development were to:

1. Perform a comprehensive set of emission spectrum measurements on three WiMAX base station transmitters in the service-provider's inventory (designated Radio 1, Radio 2, and Radio 3), with and without supplemental output RF filters installed. The measurements were performed via hardline coupling in an underground RF-shielded room at the service provider's facility near Washington, DC, to ensure that extraneous signals did not corrupt the emission spectra. The stations were fixed-tuned to a center frequency of 2683.5 MHz, which is the highest available WiMAX channel center frequency in the band.
2. Measure the frequency response of a WiMAX base station transmitter antenna at the NTIA/ITS laboratory in Boulder.
3. Calculate and plot the frequency dependent rejection (FDR) of the NEXRAD and ASR-8, -9, and -11 receivers versus the filtered and unfiltered emissions for all three WiMAX transmitters.

Calculate the distances required to protect the radar receivers from interference using the appropriate protection criteria and radar system characteristics for all three WiMAX transmitters.

D.2 Calculation of Frequency Dependent Rejection (FDR)

Frequency dependent rejection (FDR) is a key element in EMC link budget calculations. NTIA OSM calculated each receiver's FDR response for each transmitter with and without the filter using the FDR program that is included in NTIA Microcomputer Spectrum Analysis Models (MSAM) software. The minimum frequency separation between the radars and the WiMAX transmitters is 21.5 MHz, with the WiMAX operating below the radar.

The emission spectrum data for the WiMAX transmitters was normalized in power and frequency for the FDR program. The radars' IF selectivity were also normalized in power and frequency for the FDR program. For the filtered case, the roll-off on the transmitter emission spectra was 10 dB per decade once it reached the level where it intercepted the predicted level. For the unfiltered case, the roll-off was 10 dB per decade once it intercepted the level where the emissions met the predicted filtered level. The implementation of this method is indicated graphically in Figures 57–59 (see Section 6.2.1, above). The unfiltered emissions of WiMAX Radio 1 intercepted the filtered emissions well above the band edge.

D.3 FDR for NEXRAD Radar

NTIA had previously measured the IF response of the NEXRAD receiver at the Severe Storm Warning Center at Norman, Oklahoma, and those data were used for these calculations. The IF

response was measured to a level of -60 dB, and for these calculations the curve was extended to the -100 dB point and given a roll-off of 20 dB per decade (Figure D-1).

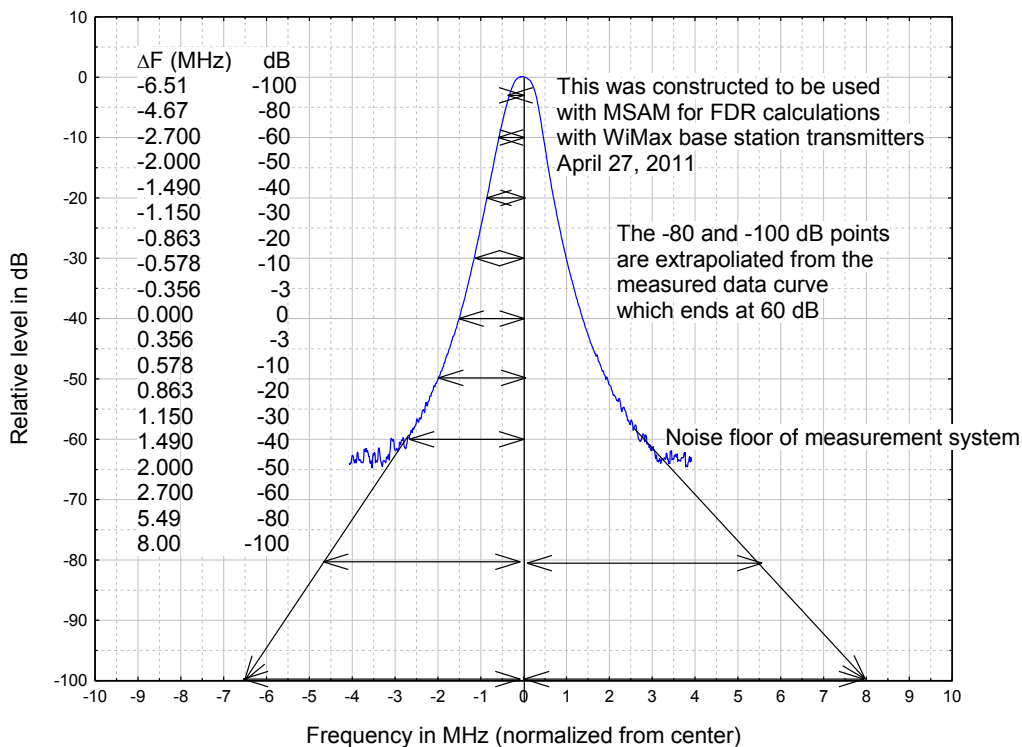


Figure D-1. Measured NEXRAD IF frequency-response curve.

The FDR that were calculated for the NEXRAD receiver versus the filtered and unfiltered emissions for the WiMAX transmitters are shown in Figure D-2. This figure shows that at 21.5 MHz of frequency separation the filtered FDR was 110 dB. At that delta frequency the unfiltered WiMAX Radio 1 FDR was 80 dB, the Radio 2 FDR was 76 dB, and the Radio 3 FDR was 72 dB. Clearly the filter did, at a minimum, increase the FDR by 30 dB. Figure D-2 also shows that the filtered FDR continued to increase as the frequency separation became larger, since both the transmitter and the receiver were rolling off.

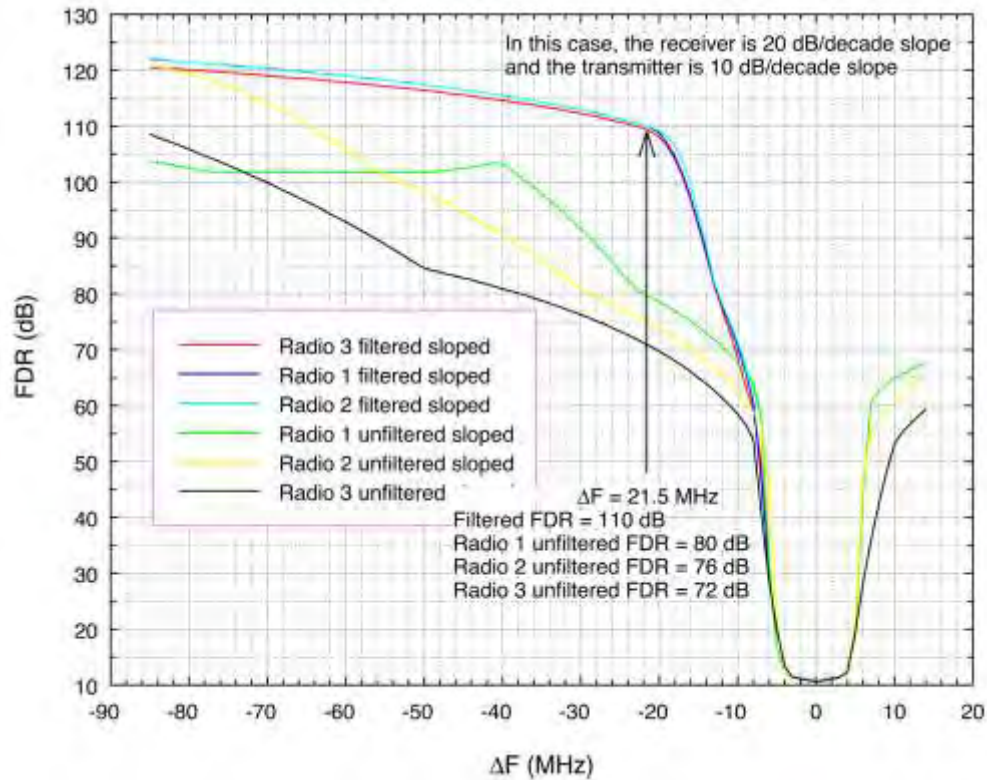


Figure D-2. FDR plot for NEXRAD receiver versus WiMAX transmitters.

D.4 FDR for ASR-8 Radar

NTIA had previously measured the IF response of the ASR-8 at the FAA Mike Monroney Aeronautical Center in Oklahoma City, Oklahoma, and that data was used for these calculations (Figure D-3). The roll-off of the data was 20 dB per decade after the last measured data point. Note that the IF of this radar is relatively wide at 13 MHz and the dynamic range of the measurement was 90 dB.

The FDRs that were calculated for the ASR-8 receiver versus the filtered and unfiltered emissions for the WiMAX transmitters are shown in Figure D-4. This figure shows that at 21.5 MHz of frequency separation the filtered FDR was 57 dB. At that delta frequency the unfiltered Radio 1 FDR was 57 dB, the Radio 2 FDR was 57 dB, and the Radio 3 FDR was 54 dB.

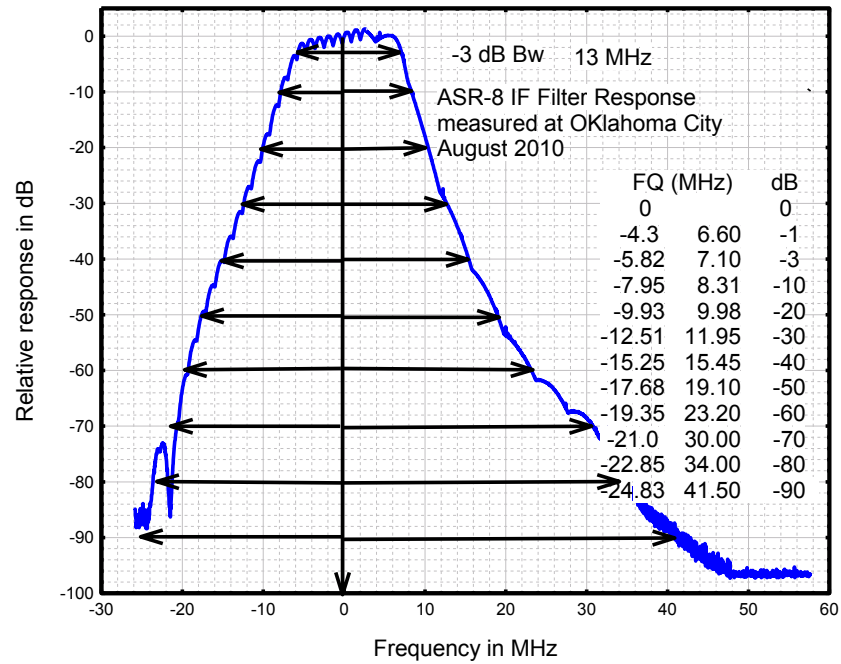


Figure D-3. ASR-8 IF plot.

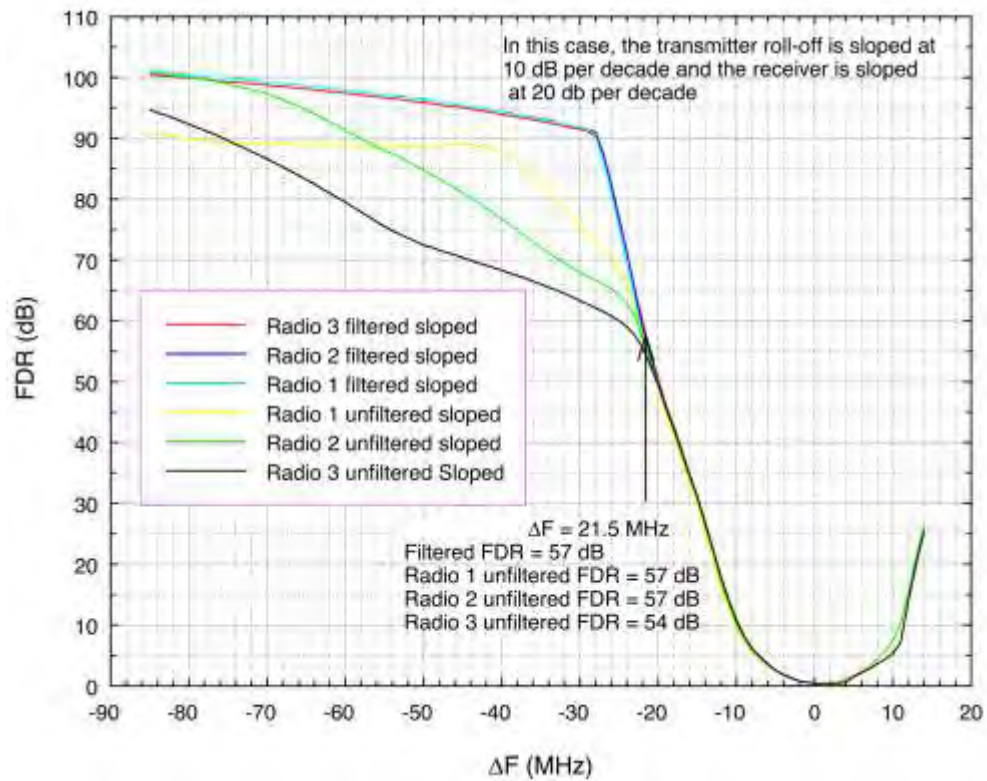


Figure D-4. FDR plot for ASR-8 receiver versus WiMAX transmitters.

D.5 FDR for ASR-9 Radar

NTIA had previously measured the IF response of the ASR-9 at the FAA Mike Monroney Aeronautical Center in Oklahoma City, Oklahoma, and those data were used for these calculations (Figure D-5). For these calculations the slope was extended to the -100 dB point, after that the roll-off was 20 dB per decade. The measured IF response was 90 dB. The FDR that were calculated for the ASR-9 receiver versus the filtered and unfiltered emissions for the WiMAX transmitters are shown in Figure D-6.

Figure D-6 shows that at 21.5 MHz of frequency separation the filtered FDR was 106 dB. At that delta frequency the unfiltered, the WiMAX Radio 1 FDR was 79 dB, the Radio 2 FDR was 75 dB, and the Radio 3 FDR was 71 dB. Clearly the filter did, at a minimum, increase the FDR by 27 dB. Figure D-6 also shows that the filtered FDR continued to increase as the frequency separation became larger, since both the transmitter and the receiver were rolling off.

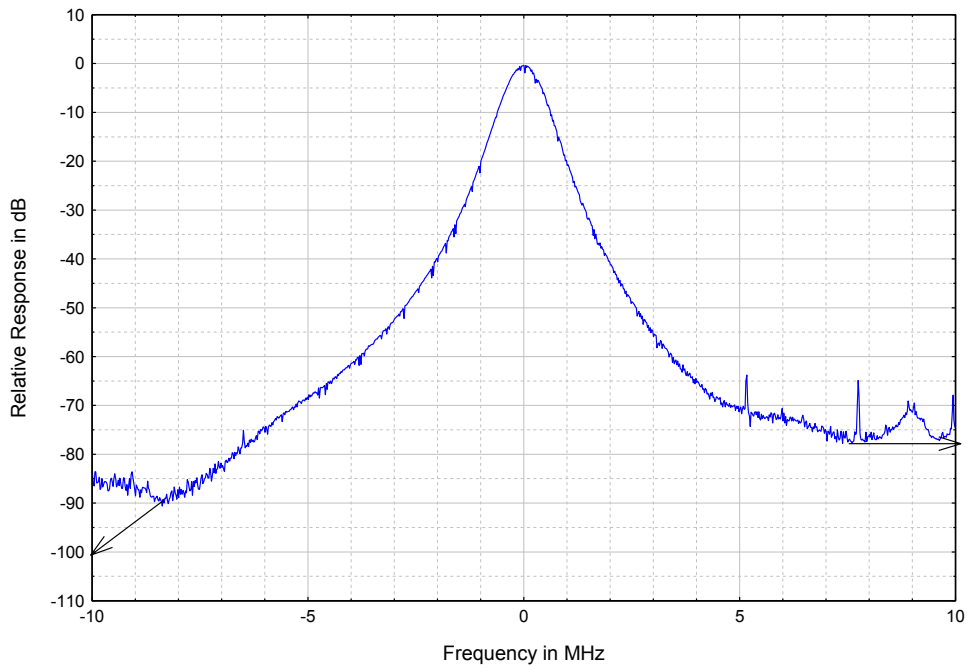


Figure D-5. ASR-9 IF response plot.

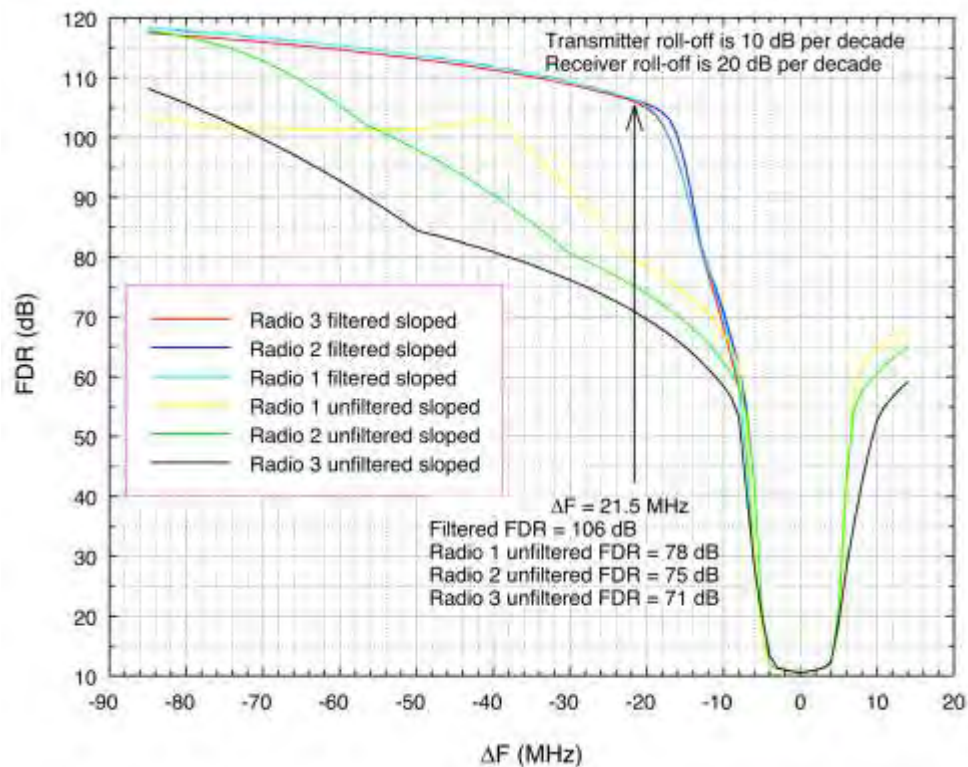


Figure D-6. FDR plot for ASR-9 receiver versus WiMAX transmitters.

D.6 FDR for ASR-11 Radar

NTIA had previously measured the IF response of the ASR-11 at the FAA Mike Monroney Aeronautical Center in Oklahoma City, Oklahoma, and those data were used for these calculations (Figure D-7). For this calculation the slope was extended to the -100 dB point; after that the roll-off was set at 20 dB per decade. The FDR that were calculated for the ASR-11 receiver versus the filtered and unfiltered emissions for the WiMAX transmitters are shown in Figure D-8.

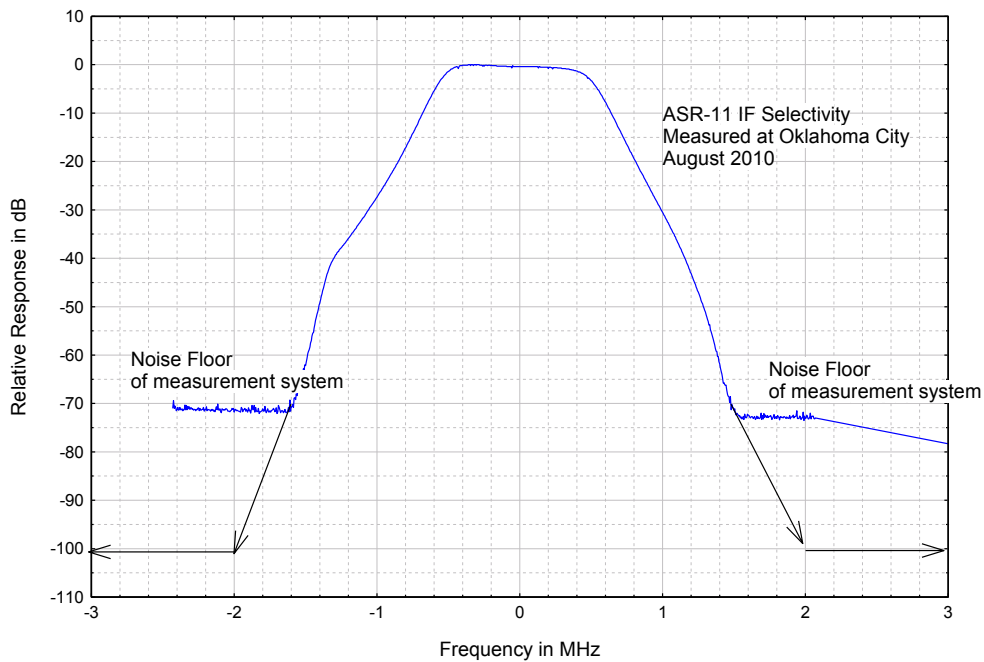


Figure D-7. ASR-11 IF plot.

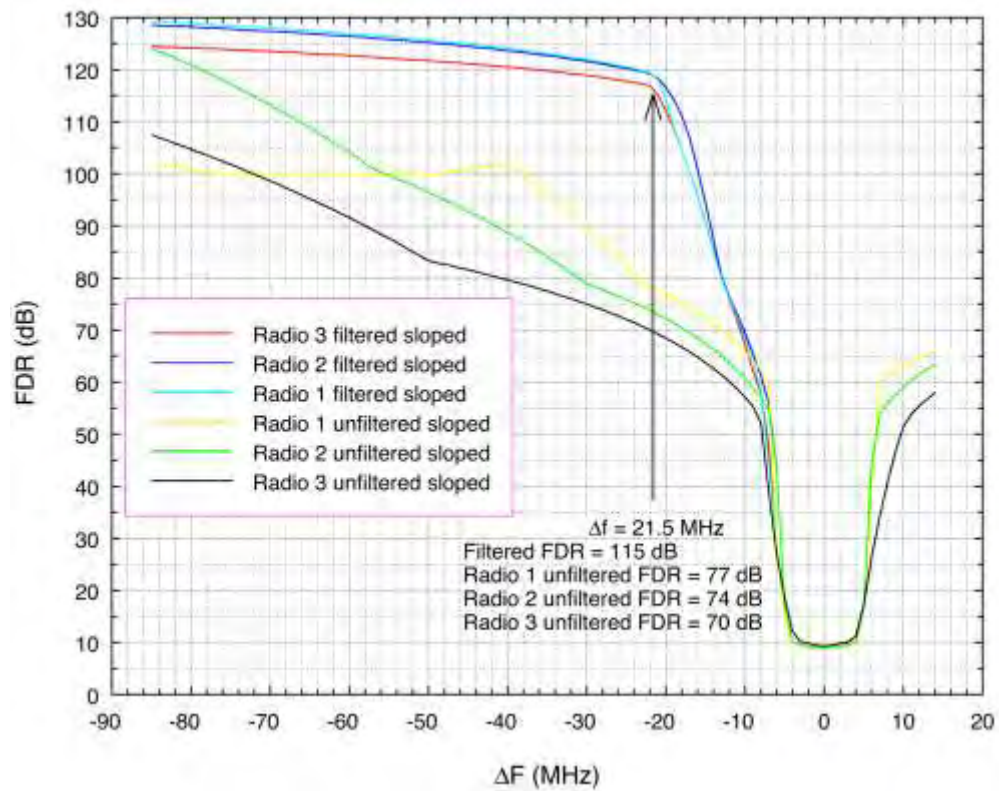


Figure D-8. FDR plot for ASR-11 receiver versus WiMAX transmitters.

Figure D-8 shows that at 21.5 MHz of frequency separation the filtered FDR was 115 dB. At that delta frequency the unfiltered, the Radio 1 FDR was 77 dB, the Radio 2 FDR was 74 dB, and the FDR was 70 dB. Clearly the filter did, at a minimum, increase the FDR by 38 dB. The figure also shows that the filtered FDR continued to increase as the frequency separation became larger, since both the transmitter and the receiver were rolling off.

D.7 Calculation of Protection Distances

The minimum required separation distance to protect each radar receiver from a BRS/EBS base station transmitter is calculated using the Irregular Terrain Model (ITM) propagation model, after link budget analyses have determined the maximum interference power and corresponding path loss. The separation distances are calculated for the filtered and unfiltered emissions for each WiMAX transmitter, under the condition that the WiMAX antenna down-tilt angle is either 0 degrees or 5 degrees below the local horizon. The results are shown in Figures D-9 through D-16. The following link-budget equation is used:

$$I_{Max} = P_T + G_T - L_P - FDR + G_R - L_S$$

where:

I_{Max} = Maximum interference level (dBm);
 P_T = Transmitted Power (dBm);
 G_T = Transmitter antenna gain (dBi);
 L_P = Atmospheric path loss (dB);
 FDR = frequency-dependent rejection (dB);
 G_R = Antenna gain of the receiver (dBi)
 L_S = Insertion loss within the receiver front-end (dB).

Re-arranging terms:

$$L_P = P_T + G_T - I_{Max} - FDR + G_R - L_S.$$

The ITM propagation model is run in reverse mode, to calculate the distance at which the path loss meets the required values. The ITM model settings are shown in Table D-1 and the radar EMC characteristics are shown in Table D-2.

Table D-1. ITM model settings for WiMAX-to-radar EMC analysis.

ITM Parameter	ITM Parameter Value
Mode of Variability	Broadcast
Delta H	90
WiMAX Transmitter Height (m)	33
Receiver Height (m)	NEXRAD = 33; ASR = 23
Transmitter Site Criteria	Very Careful
Receiver Site Criteria	Random
Dielectric	15

ITM Parameter	ITM Parameter Value
Conductivity	0.005
Surface Refractivity	301
Radio Climate	Continental Temperate
Percent Time	50
Percent Location	50
Percent Confidence	50
Polarity	Horizontal

Table D-2. Radar parameters for EMC analysis.

Parameter	NEXRAD	ASR-8	ASR-9	ASR-11
3 dB IF BW (MHz)	0.712	13	0.564	1
Noise Figure (dB)	2.5	4	3	3
Protection Criteria (I/N , in dB)	-10	-6	-6	-6
Receiver Noise Power (dBm/MHz)	-113	-98	-113	-111
Maximum Interference Level (dBm/MHz)	-123	-105	-120	-117
Antenna Gain (dBi)	45	32	32	32
System Loss (dB)	2	2	2	2
Antenna Height (m)	33	23	23	23

WiMAX transmit power, P_T , is set to 42 dBm, and WiMAX antenna gain, G_T , is set to 14 dBi. For the ASRs the Microsoft Excel© models were run for mainbeam coupling for worst case scenario.

In Figures D-9 to D-12 the results are shown for WiMAX antenna down-tilt angles of 0 degrees. In Figures D-13 to D-16 the results are shown for WiMAX antenna down-tilt angles of 5 degrees below the horizon. The down-tilt results were based on the antenna pattern of Figure 61 with corresponding decoupling values as a function of down-tilt angle as shown in Table D-3.

D.7.1 Calculated Separation Distances for 0 Degrees of WiMAX Antenna Down-Tilt

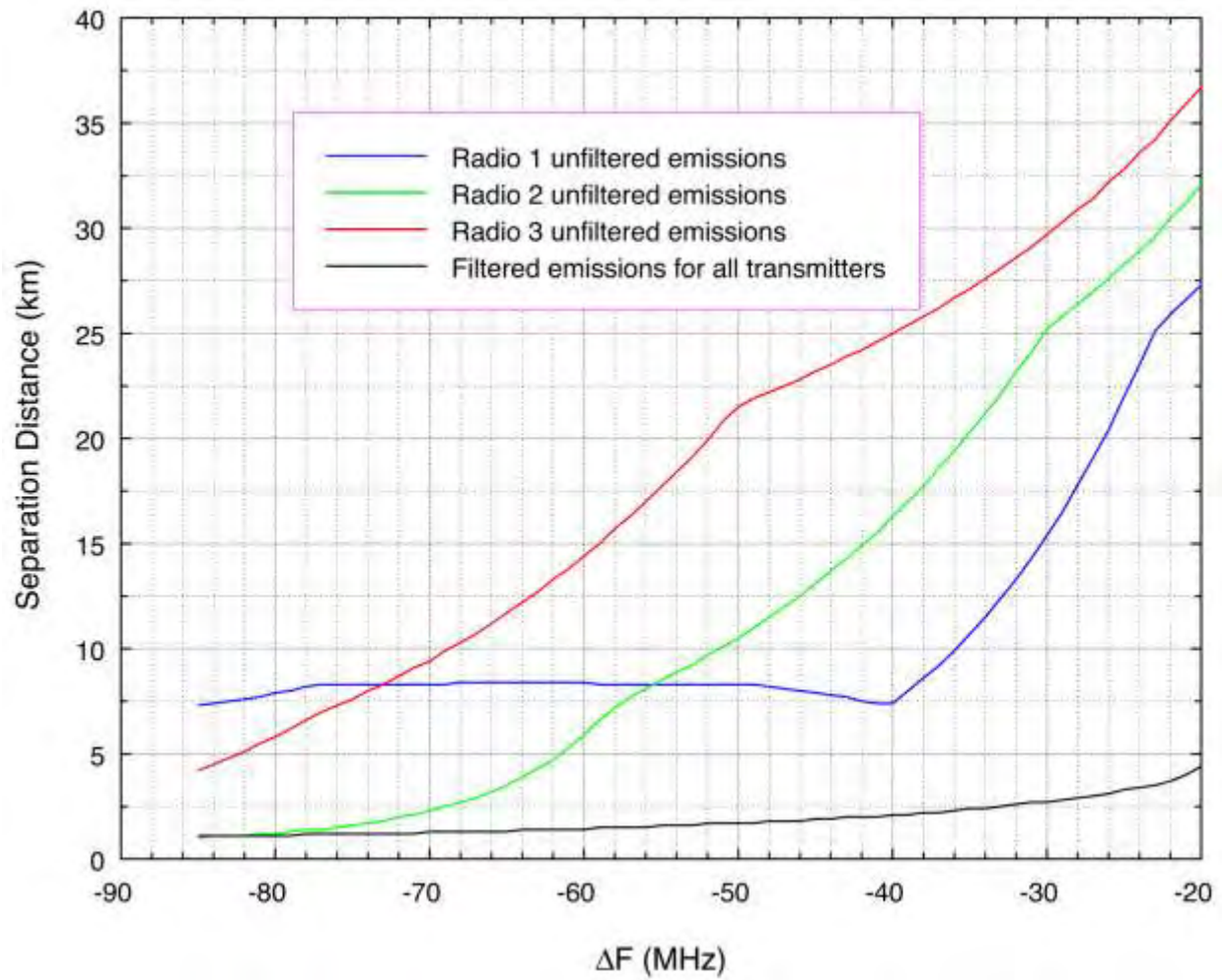


Figure D-9. Distance-frequency separation distance curves for NEXRAD and WiMAX, with WiMAX down-tilt angle = 0 degrees.

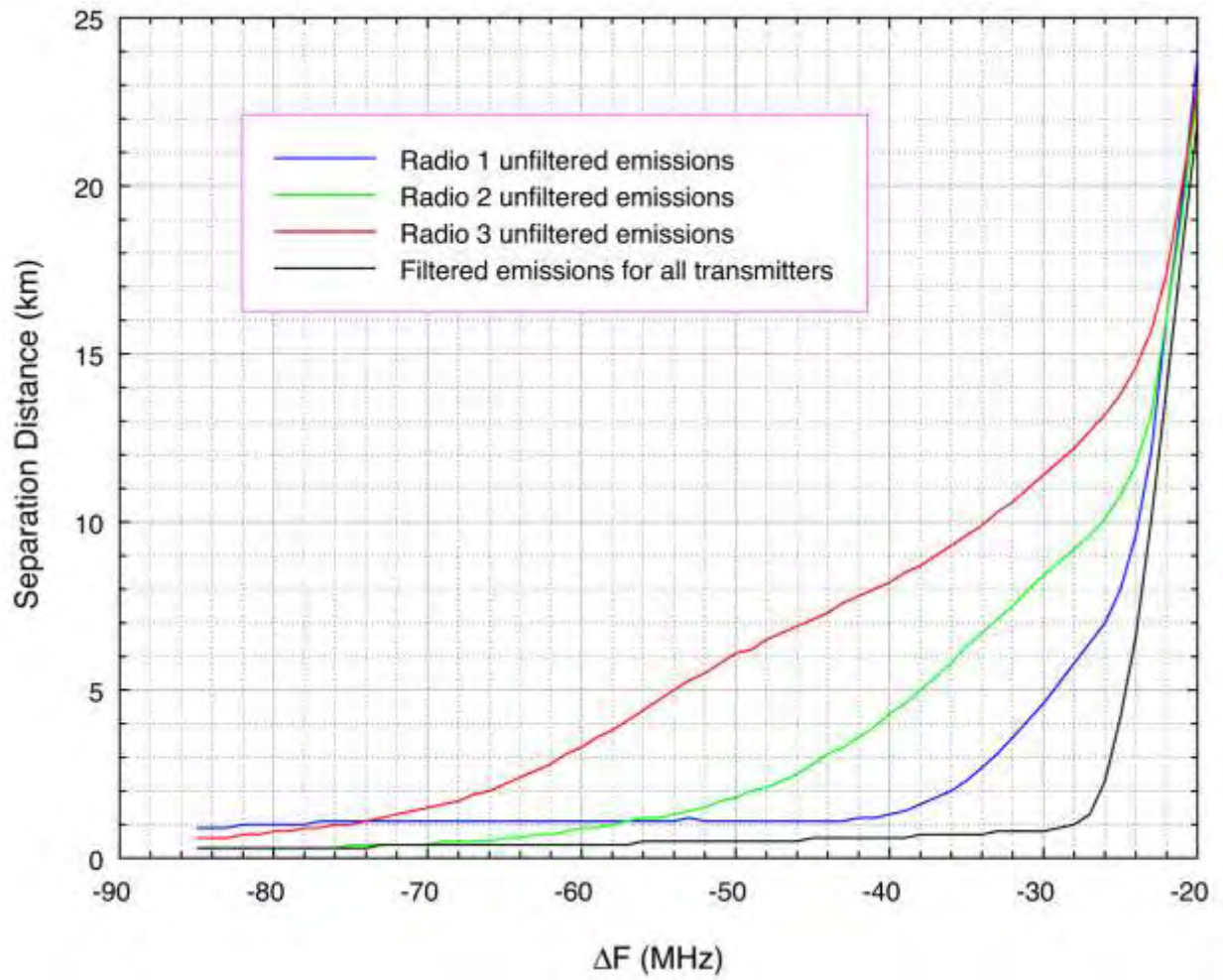


Figure D-10. Distance-frequency separation curves for ASR-8 and WiMAX, with WiMAX down-tilt angle = 0 degrees.

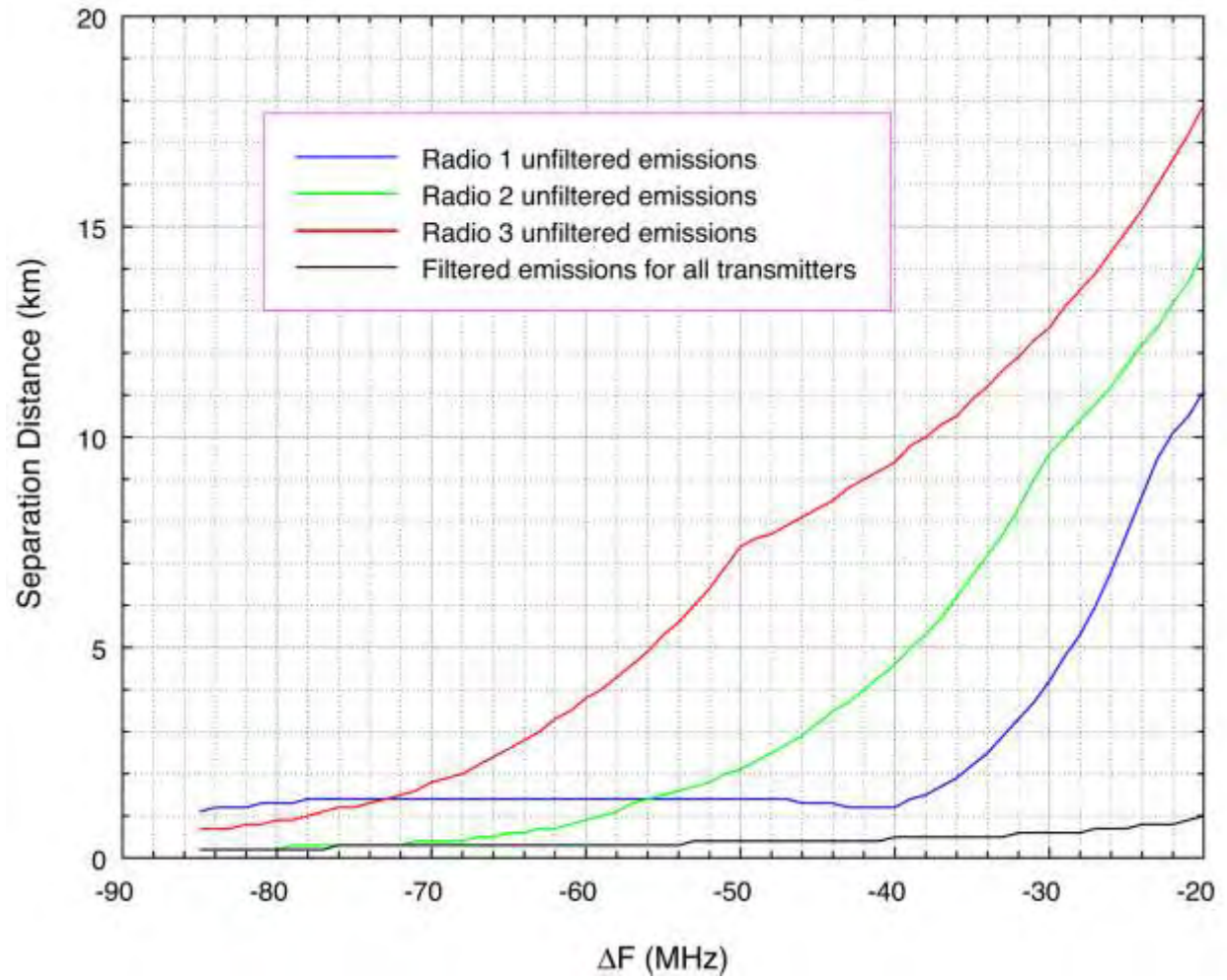


Figure D-11. Frequency-separation distance curves ASR-9 and WiMAX, with WiMAX down-tilt angle = 0 degrees.

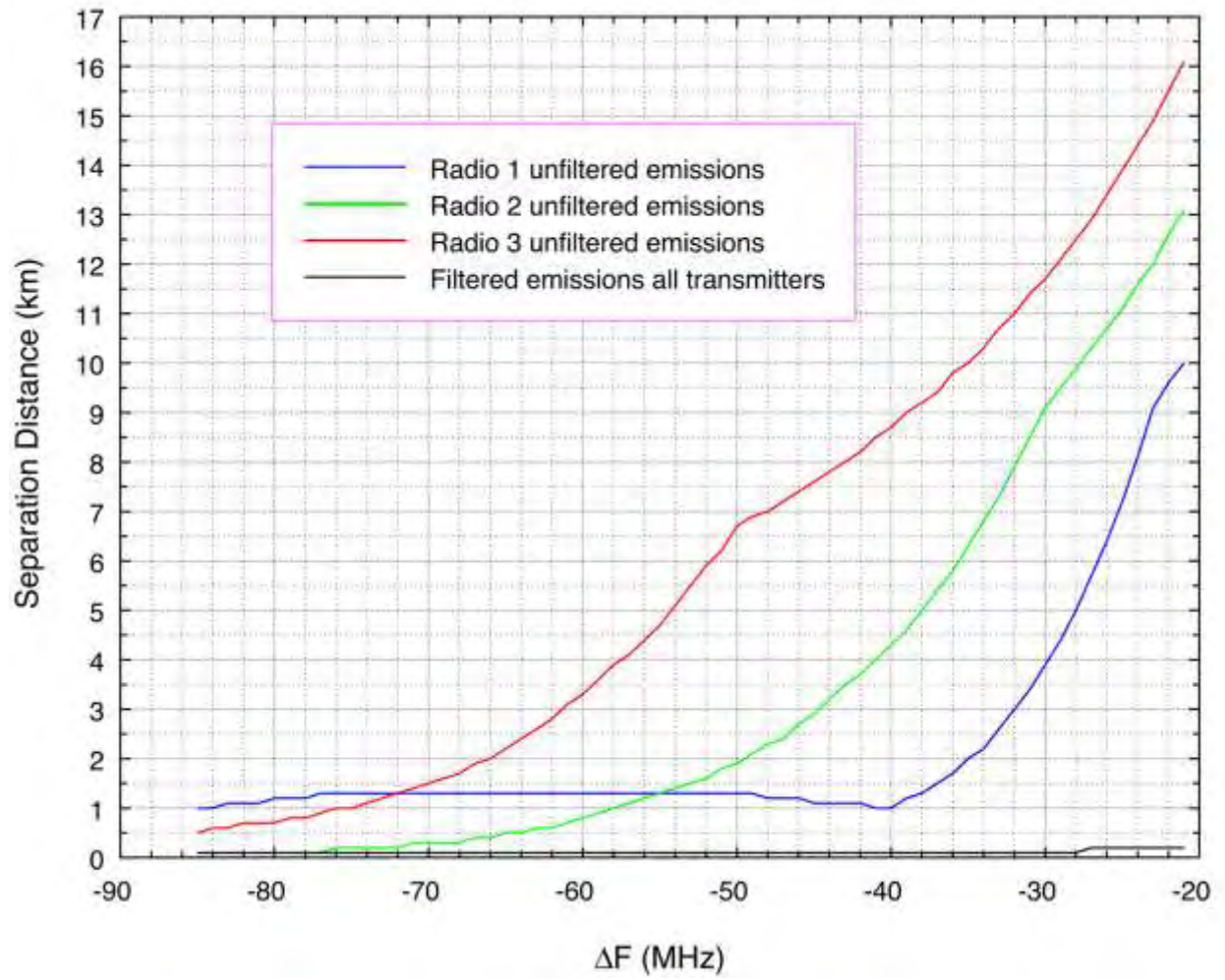


Figure D-12. Frequency-distance separation curves for ASR-11 and WiMAX, with WiMAX down-tilt angle = 0 degrees.

D.7.2 Calculated Separation Distances for 5 Degrees of WiMAX Antenna Down-Tilt

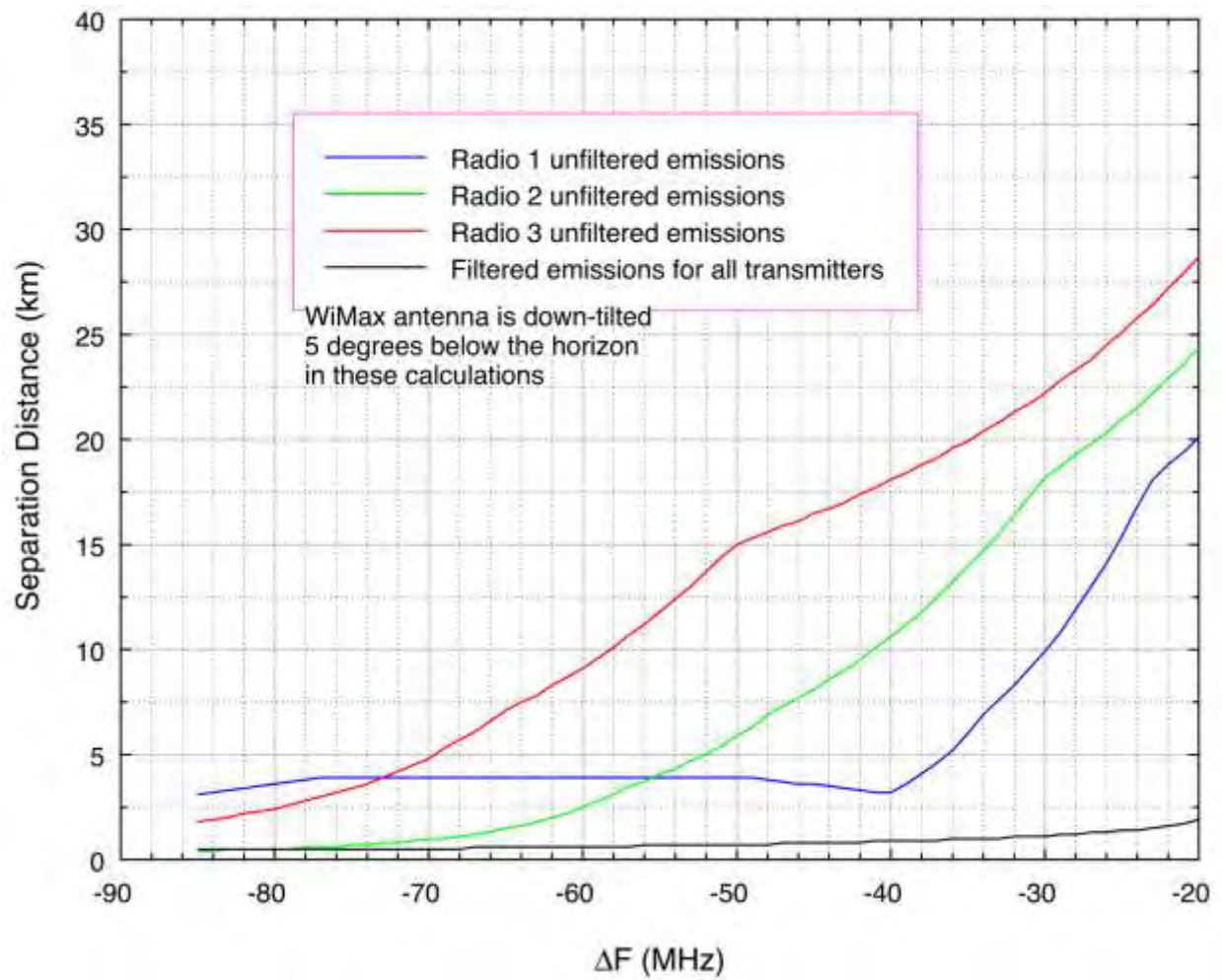


Figure D-13. Frequency-distance separation curves for NEXRAD and WiMAX, with WiMAX down-tilt angle = 5 degrees.

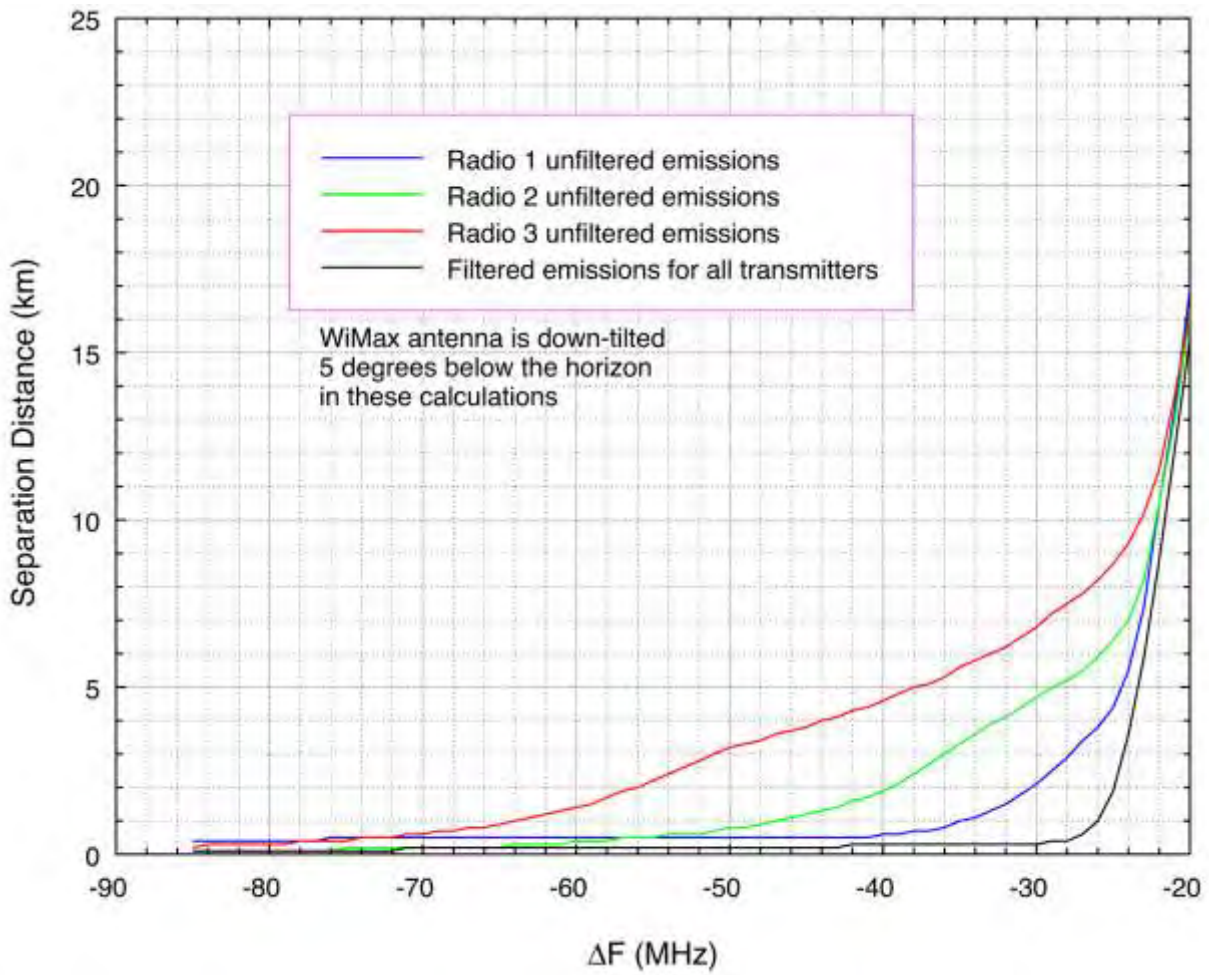


Figure D-14. Frequency-distance separation curves for ASR-8 and WiMAX, with WiMAX down-tilt angle = 5 degrees.

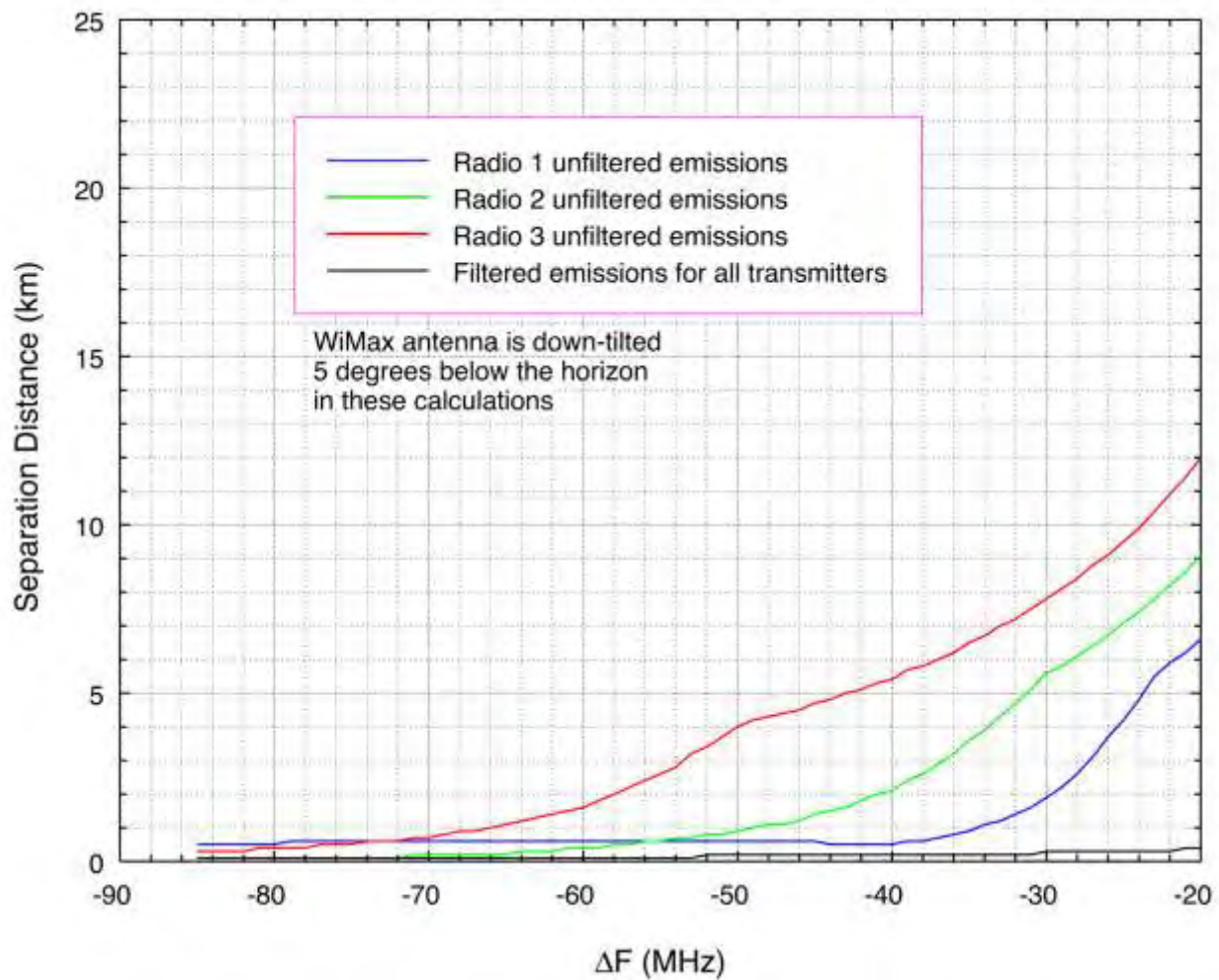


Figure D-15. Frequency-distance separation curves for ASR-9 and WiMAX, with WiMAX down-tilt angle = 5 degrees.

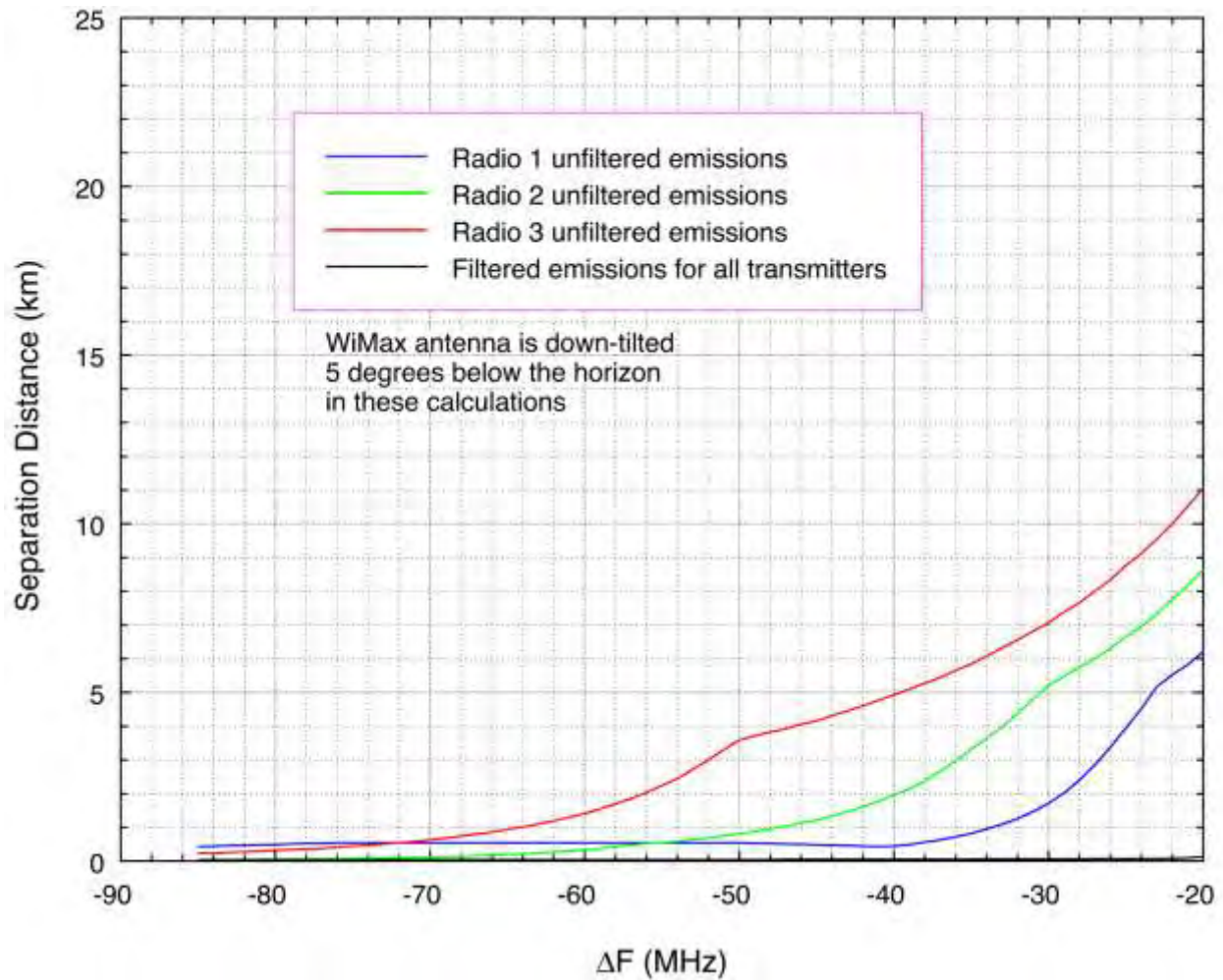


Figure D-16. Frequency-distance separation curves for ASR-11 and WiMAX, with WiMAX down-tilt angle = -5 degrees.

Table D-3. WiMAX antenna gain reduction as a function of down-tilt angle.

Angle (degrees)	Gain reduction (dB)
0	0
1.5	1.5
2.5	2.5
5.0	7.5
7.5	15
>10	20

D.8 Summary of EMC Frequency-Separation Distance Curves

A methodical approach to the problem of measuring interference levels in situ, determining the interference mechanism (co-channel energy on the victim receivers' frequencies in this case),

establishing the IF-response characteristics of the subject receivers, and measuring the emission spectra of the interfering transmitters with and without supplemental output RF filtering results in the frequency-distance separation curves shown in Figures D-9 through D-16. These curves may be used to establish compatible operations between WiMAX transmitters and radar stations if none of the other possible mitigation approaches (as described below) prove to be effective.

Table D-4 summarizes the results of the various scenarios and compares the separation distances for filtered and unfiltered WiMAX emission, along with WiMAX antenna down-tilting. The required separation distances collected in Table 12 are for the case of the ΔF between the WiMAX transmitter and the radar receivers being 22 MHz. The actual closest ΔF is 21.5 MHz, but the models were run with 1 MHz increments starting at $\Delta F = 20$ MHz.

Table D-4. Summary separation distances (km) for $\Delta F = 22$ MHz.

WiMAX Transmitter	NEXRAD		ASR-8		ASR-9		ASR-11	
	No down-tilt	5 Deg. down-tilt	No down-tilt	5 Deg. down-tilt	No down-tilt	5 Deg. down-tilt	No down-tilt	5 Deg. down-tilt
Filtered	3.7	1.9	14	8.8	0.8	0.3	0.8	0.3
Radio 1 (unfiltered)	25.9	20.1	16.1	10.5	10.1	5.9	10.1	5.9
Radio 2 (unfiltered)	30.5	24.4	16.1	10.5	13.2	8.2	13.2	8.2
Radio 3 (unfiltered)	35.1	28.7	17.4	11.5	16.6	10.9	16.6	10.9

The results in Table D-4 show that the filter significantly reduces the separation distances that are required between the WiMAX transmitters and the radar receivers. The worst case is the Radio 3 transmitter with the NEXRAD receiver, requiring 35.1 km of separation distance when it is unfiltered and uses a 0 degree vertical tilt angle. When its emissions are filtered, the required separation distance for the Radio 3 transmitter and the NEXRAD and *all other* WiMAX transmitters is 3.7 km. When the WiMAX antenna is down-tilted to -5 degrees *with* the emissions being filtered, the distance reduces to 1.9 km. It is anticipated that these relatively small separation distances should be able to be coordinated between the NWS and communication service providers.

If the Radio 1 emissions are not filtered and the Radio 3 antenna is down-tilted by 5 degrees, the required separation distance is 20.1 km. For the unfiltered Radio 2 transmitter this down-tilt only distance is 24.4 km and for the unfiltered Radio 3 transmitter the down-tilt only distance is 28.7 km. The data for the ASRs in Table D-4 can be interpreted using the same methodology as for the NEXRAD.

APPENDIX E: PROCEDURES FOR MEASURING INTERFERENCE AT ASR STATIONS

E.1 Introduction

A problem that has been posed is to observe characteristics of interference at airport surveillance radar (ASR) receivers without interrupting radar operations. While this is difficult, and while it would be ideal to be able to observe such interference with the ASR transmitter turned off, it is possible to perform some effective assessment measurements while these radars are operating normally. This Appendix provides procedures for such observations.

E.2 Recommended Measurement Hardware

It is assumed that the hardware complement for these measurements will need to be portable, so that it can be shipped to a site in about two shipping boxes. The required inventory is:

1. A portable spectrum analyzer with capabilities for both peak detection and RMS average detection.
2. A ½ meter diameter parabolic antenna with a feed that works at least across the 2–4 GHz frequency range. A parabolic antenna will *minimize* energy coupled from the ASR, while *maximizing* the energy coupled from local interference sources. The feed may be either circularly or linearly polarized.
3. *Optional:* A manually tunable RF notch filter with a tuning range of at least 2700–2900 MHz.
4. *Optional:* A low-noise amplifier (LNA) with at least a 2–4 GHz frequency response. See Section E.4 below for information on how to select an LNA with optimal characteristics for this type of work.
5. *Optional:* A battery or small power supply to power the LNA.
6. *Optional:* A 2700 MHz lowpass filter.
7. A tripod on which the antenna can be mounted and rotated manually. The rotating tripod head should be marked in 5 degree or smaller azimuth increments.
8. Miscellaneous RF cables and connectors.

E.3 Procedures for Observing Interference Energy

Note: If it is ever possible to observe the interference without having the radar's transmitter turned on, the procedures as described below can still be implemented, and should be easier to perform and more effective; the radar antenna itself can be used manually as an excellent

direction finder. But the procedures are presented here with the assumption that the radar's transmitter is *on* and the radar is operating normally.

Part I (Optional): Be Prepared to Synchronize the Spectrum Analyzer Sweeps with the ASR Rotation

Establish, in advance of visiting the radar station, the voltage of the synch pulse that is produced at the beginning of each ASR PPI scope rotation, at the scope's north mark. Compare this to the maximum allowed voltage for the single-sweep trigger mode for the spectrum analyzer, and build a voltage converter to get the radar synch-pulse voltage into the proper range for the analyzer's triggered-sweep input. (A potentiometer with a manually controlled knob is a useful feature on this voltage converter.)

Part II: (Optional): Try to Observe the Interference in the ASR's IF Stage

1. Turn on the spectrum analyzer and connect it to the IF output of the ASR.
2. Tune the spectrum analyzer center frequency to the center frequency of the ASR IF output. (This is 30 MHz for the ASR-8, 31 MHz for the ASR9-9, and 3.88 MHz for the ASR-11.) *It is crucial that the ASR's linear IF output, which feeds to the radar detection stage, be connected; the output of the ASR receiver's log video stage will not work for this purpose.*
3. Set the spectrum analyzer to zero-hertz span. It will now show the time domain, not the frequency domain.
4. Set the spectrum analyzer input attenuation level to 0 dB.
5. Set the spectrum analyzer resolution (IF) bandwidth to 1 MHz or wider.
6. Set the spectrum analyzer video bandwidth to be equal to or greater than the IF bandwidth.
7. Set the detection to positive-peak. (This is *not* the same as maximum-hold trace mode!)
8. Set the spectrum analyzer trace mode to clear-write.
9. *Optional synchronization of the analyzer's sweeps with the ASR antenna rotation:* If the voltage from the PPI scope output is to be used to synchronize the spectrum analyzer's sweeps with the radar's antenna rotation, then set up the voltage converter between the PPI scope output (J6 on the ASR-9, for example) and the analyzer's sweep-trigger input. Set the analyzer's sweep mode to "continuous" and its trigger mode to "external trigger source." Adjust the trigger threshold level and the input voltage level until they are working together to trigger an analyzer sweep every 4.7 seconds as the ASR antenna swings through north.)

The interference signal might now be seen in the time domain every 4.75 seconds when the ASR antenna rotates past the source azimuth. However, with the ASR transmitter running, only the ASR's own pulses will likely be seen. In order to reduce these pulses' prominence on the display and have a chance of seeing the interference, the operator will now take advantage of the fact that the ASR pulses are relatively low in duty cycle (especially for the ASR-8 and ASR-9) and

that the interference duty cycle is probably relatively high, likely somewhere near 100 percent. This is done by switching the analyzer's detection mode from "peak" to "RMS average" (or, for older analyzers, a facsimile of RMS average as described below). Average detection will give a good response to high duty cycle energy (typically interference) but a reduced response to low duty cycle energy, such as the ASR's own pulses. Proceed as follows:

1. Switch the analyzer's detection mode from "peak" to "RMS average." If the analyzer is an older model that does not have an RMS average mode, then adjust its video bandwidth to 10 kHz and set the detection mode to "sample."
2. The analyzer's display of the ASR's own pulses should drop considerably, but the visibility of interference on any azimuths should be relatively enhanced, appearing as one or more bumps that are visible out of the remaining (residual) internal-pulse energy.
3. Note the azimuth(s) of the interference by correlating the time on the display to the time out of the antenna's 4.7 second rotation period, and multiplying by 360.
4. Record this information (e.g., do a screen capture), if possible.

Part III: Observe the Interference at RF Frequencies Outside the ASR Station

This procedure can be applied if either (a) PPI strobes or target drop-outs have been identified at particular azimuths on the ASR's PPI scope display or (b) interference azimuths have been identified via observations of the ASR IF stage output, as described in the optional Part II, above. In this procedure, the challenge is to observe the interference energy through the high energy level that the ASR transmitter is producing at locations near the station.

1. Take advantage of the fact that the ASR's transmitted field strength is minimal at locations below the ASR antenna, anywhere near the base of the antenna tower platform. Set up the tripod near the base of the tower with a clear view of the sector(s) where interference is believed to be originating, and mount the measurement antenna on the tripod.
2. Orient the antenna feed. If the feed is linear, try to orient it at an intermediate slant between vertical and horizontal, so as to couple any linear interference polarization reasonably well. (Circularly oriented interference will couple equally well on any linear feed orientation.) If the feed must be either horizontal or vertical, then vertical is probably the best-guess choice for terrestrial interference sources.
3. Connect the antenna output to the analyzer input. Do not use an internal or external LNA yet.
4. Set up the spectrum analyzer to sweep across 2700–2900 MHz.
5. Set the spectrum analyzer input attenuation level to 0 dB.
6. Set the spectrum analyzer resolution (IF) bandwidth to 1 MHz.
7. Set the spectrum analyzer video bandwidth to be 3 MHz.

8. Set the detection to RMS average. (If this option is not available, then set the detection mode to “sample” and adjust the video bandwidth to 10 kHz.)
9. Set the spectrum analyzer trace mode to clear-write.
10. Set the sweep time to “auto.”

Note: By setting up the measurement system at the base of the ASR antenna-platform tower, using a dish antenna for the measurement system, and using averaging detection, the measurement system is discriminating as much as possible *against* the ASR’s transmitted energy, and should be coupling as well as possible into interfering signals that are within the beam of the measurement antenna. The 1 MHz bandwidth of the measurement system is replicating fairly closely the effective bandwidth of the ASR receiver that is experiencing interference.

11. Slowly move the measurement antenna around either the entire horizon, or else through the sector(s) where interference is occurring. Watch the analyzer display for any signals, especially near the ASR frequency, that are *not* coming from the ASR.

Note: Using maximum-hold trace mode (*not* peak-detection mode), with the analyzer running in its average-detection mode, may help to bring out the interference signal.

12. *Optional:* Restrict the frequency range of the sweeping to within plus/minus 10 or 20 MHz or so of the ASR frequency and try this procedure again.
13. If interference signal(s) are observed, peak up the dish azimuth on it/them. Tune the analyzer’s center frequency to the frequency of each signal in question. Record screen captures showing the spectrum of the signal(s).

Note: If the signal is out-of-band energy from a transmitter below 2700 MHz, its spectrum may appear to be noise-like, but it may have structure in the time domain.

14. At each signal frequency, set the analyzer frequency span to zero hertz (so that the analyzer is running in the time domain on that frequency), set the sweep mode to “single sweep” and then record 20 ms, 50 ms and 100 ms of the interference signal’s time-domain behavior. Record these time-domain pictures as screen captures.
15. *Optional:* If the interference is *not* centered on the ASR frequency, try inserting the notch filter, turn the analyzer’s internal preamp on (if the analyzer has one), and optionally insert the supplemental external LNA between the measurement antenna and the analyzer input. Then repeat steps 11–14.
16. *Optional:* Use a 2700 MHz lowpass filter in front of the LNA to observe the local signal environment below 2700 MHz.

E.4 Selecting an Optimal LNA for EMC/EMI Measurements

The purpose of an LNA, or preamplifier, is not really to provide gain; rather, an LNA is needed to provide a low noise figure (lower than the spectrum analyzer noise figure) for improved measurement sensitivity, with just enough added gain to cause the LNA's internal noise generation to be easily visible above the noise floor of the spectrum analyzer when the amplifier is connected to the analyzer. The lower the LNA noise figure, the more sensitive the overall measurement system will be. Any LNA gain that goes above and beyond the minimum that is necessary to overdrive the spectrum analyzer noise will not improve this noise figure, but will have the undesired effect of reducing the overall available dynamic range of the measurement system.

E.4.1 Procedure for Determining the Best Combination of Gain and Noise Figure for a Supplemental LNA.

1. Turn on the spectrum analyzer that will be used for the measurements.
2. Terminate the analyzer's input with an external 50 dB load or a 10 or 20 dB attenuator.
3. Tune the analyzer to a frequency within the range where measurements will be performed. (For ASR-band measurements, tune the analyzer to 2800 MHz.)
4. Set the frequency span of the analyzer to zero hertz, so that the analyzer is working in the time domain.
5. Set the analyzer's sweep time to 1 second.
6. Set the analyzer's vertical graticule to 10 dB per division.
7. Set the analyzer's internal attenuation level to 0 dB. *This step is crucial.*
8. *If the analyzer has an option for an internal low-noise amplifier (preamplifier), turn it on.*
9. Set the analyzer's IF (or resolution) bandwidth to 1 MHz.
10. Set the analyzer's video bandwidth to any value larger than 1 MHz.
11. Set the analyzer's detection mode to RMS average. If the analyzer does not have an option for RMS average, then set its detection mode to "sample" and reduce the video bandwidth to 10 kHz.
12. If the displayed noise level is within 10 dB of the bottom of the display, adjust the reference level to get the displayed noise floor to more than 20 dB above the bottom of the display, if possible.
13. Note the displayed noise level on the analyzer screen.

14. Subtract -114 dBm from the value of the measured noise on the analyzer's screen. *The difference between -114 dBm and the displayed noise level is the spectrum analyzer's noise figure.* It is not unusual to obtain a value of 20-30 dB for a spectrum analyzer noise figure. If the analyzer's optional internal preamp is turned on, this noise figure will probably still be 10 dB or more.
15. Call the noise figure NF . The decibel sum of the gain and noise figure of the supplemental LNA should be equal to, or slighter greater than, NF ; the noise figure of the supplemental LNA itself should be relatively low and the gain should be commensurately larger to make up the difference.

E.4.2 Example

With the analyzer set up as described above, suppose that the noise floor is measured at -90 dBm. Then the analyzer's noise figure is $(-90 \text{ dBm} - (-114 \text{ dBm})) = 21 \text{ dB}$.

The decibel sum of the gain and noise figure of the supplemental LNA should therefore be 21–25 dB, if possible. In any event, the sum of the LNA's gain and noise figure should not exceed 30 dB in this case, because as the LNA's gain goes higher, the dynamic range of the measurement system will go lower and the sensitivity of the system (its capability to detect weak signals) won't be improved.

Continuing this example, within the value of 21–25 dB for the sum of ((LNA gain) + (LNA noise figure)), if the lowest available LNA noise figure (as read from a vendor's catalog) is 3 dB, then the corresponding optimal gain value should be between 18 and 22 dB.

Suppose that the vendor's catalog has an LNA with 3 dB noise figure, but the lowest available gain is higher than needed, say 30 dB. In that case, the LNA with 3 dB noise figure and 30 dB of gain can be procured, but when it is used a 10 dB attenuator should be inserted between the LNA output and the spectrum analyzer input; that 10 dB of attenuation will effectively reduce the LNA gain to 20 dB, exactly where it ought to be.

E.4.3 Testing/Verifying the LNA Performance with the Spectrum Analyzer

To verify that the LNA is performing properly (and optimally) with the spectrum analyzer, first set up the spectrum analyzer as described in Steps 1–13 above. Then:

1. Attach the LNA (along with a supplemental attenuator, if previously indicated as being needed, between the LNA output and the analyzer's input) in place of the front-end terminator that was used earlier; put the terminator on the LNA input instead of the analyzer's input. *Keep the LNA turned off initially.*
2. With the LNA turned off, observe the spectrum analyzer's noise floor level. The same noise level should be seen as was originally observed in Step 13, above.

3. Now turn on the LNA. The observed level of the noise floor on the analyzer display should *increase* by between 3 and 10 dB; this indicates an optimal condition. *If the increase is 3–10 dB, no corrective action is needed; the LNA is ready to go.*
4. If the noise-floor rise is less than 3 dB, then the LNA gain is insufficient. Corrective action: Check the LNA power supply to make sure that it is working. Verify that the analyzer's internal RF attenuation is set to zero, and remove the intermediate RF attenuator between the LNA and the analyzer, if there is an attenuator there. If the noise floor still does not increase when the LNA is turned on, then another LNA with more gain will need to be obtained.
5. If the noise-floor rise is *more* than 10 dB, then the LNA's gain is needlessly high and the measurement system will needlessly lose available dynamic range. *Corrective action: Insert some RF attenuation between the LNA output and the analyzer's input, until the overall rise in the noise floor when the LNA is turned on is between 3 and 10 dB.*

Note: Because excessive gain levels can always be remedied by inserting an attenuator between the LNA and the analyzer, but insufficient gain can only be remedied by obtaining or buying another LNA, it is best to be conservative and estimate the gain parameter somewhat high when ordering an LNA from a vendor. This also applies if the LNA might ever need to be used with another analyzer or a receiver with a somewhat higher noise figure than the one for which the LNA was originally intended to be used.

BIBLIOGRAPHIC DATA SHEET

1. PUBLICATION NO. TR-13-490	2. Government Accession No.	3. Recipient's Accession No.
4. TITLE AND SUBTITLE Analysis and Resolution of RF Interference to Radars Operating in the Band 2700-2900 MHz from Broadband Communication Transmitters		5. Publication Date October 2012
		6. Performing Organization Code
7. AUTHOR(S) Frank H. Sanders, Robert L. Sole, John E. Carroll, Glenn S. Secrest, T. Lynn Allmon		9. Project/Task/Work Unit No. 6454000-200
8. PERFORMING ORGANIZATION NAME AND ADDRESS Institute for Telecommunication Sciences National Telecommunications & Information Administration U.S. Department of Commerce 325 Broadway Boulder, CO 80305		10. Contract/Grant Number.
11. Sponsoring Organization Name and Address National Telecommunications & Information Administration Herbert C. Hoover Building 14 th & Constitution Ave., NW Washington, DC 20230		12. Type of Report and Period Covered
14. SUPPLEMENTARY NOTES		
15. ABSTRACT (A 200-word or less factual summary of most significant information. If document includes a significant bibliography or literature survey, mention it here.) This report describes the methodology and results of an investigation into the source, mechanism and solutions for radiofrequency (RF) interference to WSR-88D Next-Generation Weather Radars (NEXRADs). It shows that the interference source is nearby base stations transmitters in the Broadband Radio Service (BRS) and the Educational Broadband Service (EBS) and that their out-of-band (OOB) emissions can cause interference on NEXRAD receiver frequencies. The methodology for determining interference power levels and mitigation solutions is described. Several technical solutions that can mitigate the problem are shown to be effective. Trade-offs between effectiveness, difficulty, and costs of various solutions are described, but it is shown that there is always at least one effective technical solution. The report shows that careful planning and coordination between communication system service providers and Federal agencies operating nearby radars is important in the implementation of these interference-mitigation techniques. A number of the report's interference mitigation options have already been implemented in several United States cities served by a BRS/EBS licensee, at licensee WiMAX stations where NEXRAD radar operations are located nearby. As of the date of this report's release, interference from the licensee's WiMAX links to NEXRAD receivers in those markets has been successfully mitigated using the techniques described herein.		
16. Key Words (Alphabetical order, separated by semicolons) airport surveillance radar (ASR); electromagnetic compatibility (EMC); interference-to-noise (I/N) ratio; NEXRAD; out-of-band (OOB) emissions; radar interference; radiofrequency (RF) interference; WiMAX; WSR-88D		
17. AVAILABILITY STATEMENT <input checked="" type="checkbox"/> UNLIMITED. <input type="checkbox"/> FOR OFFICIAL DISTRIBUTION.	18. Security Class. (This report) Unclassified	20. Number of pages 147
	19. Security Class. (This page) Unclassified	21. Price:

NTIA FORMAL PUBLICATION SERIES

NTIA MONOGRAPH (MG)

A scholarly, professionally oriented publication dealing with state-of-the-art research or an authoritative treatment of a broad area. Expected to have long-lasting value.

NTIA SPECIAL PUBLICATION (SP)

Conference proceedings, bibliographies, selected speeches, course and instructional materials, directories, and major studies mandated by Congress.

NTIA REPORT (TR)

Important contributions to existing knowledge of less breadth than a monograph, such as results of completed projects and major activities. Subsets of this series include:

NTIA RESTRICTED REPORT (RR)

Contributions that are limited in distribution because of national security classification or Departmental constraints.

NTIA CONTRACTOR REPORT (CR)

Information generated under an NTIA contract or grant, written by the contractor, and considered an important contribution to existing knowledge.

JOINT NTIA/OTHER-AGENCY REPORT (JR)

This report receives both local NTIA and other agency review. Both agencies' logos and report series numbering appear on the cover.

NTIA SOFTWARE & DATA PRODUCTS (SD)

Software such as programs, test data, and sound/video files. This series can be used to transfer technology to U.S. industry.

NTIA HANDBOOK (HB)

Information pertaining to technical procedures, reference and data guides, and formal user's manuals that are expected to be pertinent for a long time.

NTIA TECHNICAL MEMORANDUM (TM)

Technical information typically of less breadth than an NTIA Report. The series includes data, preliminary project results, and information for a specific, limited audience.

For information about NTIA publications, contact the NTIA/ITS Technical Publications Office at 325 Broadway, Boulder, CO, 80305 Tel. (303) 497-3572 or e-mail info@its.blrdoc.gov.

This report is for sale by the National Technical Information Service, 5285 Port Royal Road, Springfield, VA 22161, Tel. (800) 553-6847.